UNIVERSIDADE FEDERAL DE GOIÁS
ESCOLA DE ENGENHARIA CIVIL E AMBIENTAL
PROGRAMA DE PÓS-GRADUAÇÃO EM GEOTECNIA,
ESTRUTURAS E CONSTRUÇÃO CIVIL

SOIL STABILIZATION WITH LIME FOR RESERVOIR SHORELINE EROSION CONTROL

RICARDO MOREIRA VILHENA

D0206G19
GOIÂNIA
2019

sistema de bibliotecas ufg

PRPG
PRÓ-REITORIA DE PÓS-GRADUAÇÃO

UFG

TERMO DE CIÊNCIA E DE AUTORIZAÇÃO PARA DISPONIBILIZAR VERSÕES ELETRÔNICAS DE TESES E DISSERTAÇÕES NA BIBLIOTECA DIGITAL DA UFG

Na qualidade de titular dos direitos de autor, autorizo a Universidade Federal de Goiás (UFG) a disponibilizar, gratuitamente, por meio da Biblioteca Digital de Teses e Dissertações (BDTD/UFG), regulamentada pela Resolução CEPEC nº 832/2007, sem ressarcimento dos direitos autorais, de acordo com a Lei nº 9610/98, o documento conforme permissões assinaladas abaixo, para fins de leitura, impressão e/ou *download*, a título de divulgação da produção científica brasileira, a partir desta data.

1. Identificação do material bibliográfico: **[X] Dissertação** **[ ] Tese**

2. Identificação da Tese ou Dissertação:

Nome completo do autor: Ricardo Moreira Vilhena

Título do trabalho: Soil stabilization with lime for reservoir shoreline erosion control

3. Informações de acesso ao documento:

Concorda com a liberação total do documento [ ] SIM [X] NÃO[1]

Havendo concordância com a disponibilização eletrônica, torna-se imprescindível o envio do(s) arquivo(s) em formato digital PDF da tese ou dissertação.

Assinatura do autor[2]

Ciente e de acordo:

Assinatura da orientadora[2]

Data: 30 / 05 / 2019

[1] Neste caso o documento será embargado por até um ano a partir da data de defesa. A extensão deste prazo suscita justificativa junto à coordenação do curso. Os dados do documento não serão disponibilizados durante o período de embargo.
Casos de embargo:
- Solicitação de registro de patente;
- Submissão de artigo em revista científica;
- Publicação como capítulo de livro;
- Publicação da dissertação/tese em livro.

[2] A assinatura deve ser escaneada.

Versão atualizada em setembro de 2017.

sistema de bibliotecas ufg

UFG

TERMO DE CIÊNCIA E DE AUTORIZAÇÃO PARA DISPONIBILIZAR AS TESES E DISSERTAÇÕES ELETRÔNICAS NA BIBLIOTECA DIGITAL DA UFG

Na qualidade de titular dos direitos de autor, autorizo a Universidade Federal de Goiás (UFG) a disponibilizar, gratuitamente, por meio da Biblioteca Digital de Teses e Dissertações (BDTD/UFG), regulamentada pela Resolução CEPEC nº 832/2007, sem ressarcimento dos direitos autorais, de acordo com a Lei nº 9610/98, o documento conforme permissões assinaladas abaixo, para fins de leitura, impressão e/ou *download*, a título de divulgação da produção científica brasileira, a partir desta data.

1. Identificação do material bibliográfico: **[X] Dissertação** **[ ] Tese**

2. Identificação da Tese ou Dissertação

Nome completo do autor: Ricardo Moreira Vilhena

Título do trabalho: Soil Stabilization With Lime For Reservoir Shoreline Erosion Control

3. Informações de acesso ao documento:

Concorda com a liberação total do documento [X] SIM [ ] NÃO[1]

Havendo concordância com a disponibilização eletrônica, torna-se imprescindível o envio do(s) arquivo(s) em formato digital PDF da tese ou dissertação.

Ricardo Moreira Vilhena (5 de Setembro de 2022 16:15 ADT)

Assinatura do autor [2]

Data: 30 / 08 / 2022

[1] Neste caso o documento será embargado por até um ano a partir da data de defesa. A extensão deste prazo suscita justificativa junto à coordenação do curso. Os dados do documento não serão disponibilizados durante o período de embargo.

[2] A assinatura deve ser escaneada.

RICARDO MOREIRA VILHENA

SOIL STABILIZATION WITH LIME FOR RESERVOIR SHORELINE EROSION CONTROL

Thesis presented to the program of postgraduate studies in Geotechnics, Structures and Civil Construction of the Universidade Federal de Goiás in partial fulfillment of requirements for the degree of master of engineering.

Field of research: Geotechnics

Supervisor: Prof. Márcia Maria dos Anjos Mascarenha, Dsc.

Co-Supervisor: Prof. Renato Resende Angelim, Dsc.

D0206G19
GOIÂNIA
2019

Ficha de identificação da obra elaborada pelo autor, através do
Programa de Geração Automática do Sistema de Bibliotecas da UFG.

Vilhena, Ricardo Moreira
Soil stabilization with lime for reservoir shoreline erosion control [manuscrito] / Ricardo Moreira Vilhena. - 2019.
cxxxiv, 134 f.

Orientador: Profa. Dra. Márcia Maria dos Anjos Mascarenha; co orientador Dr. Renato Resende Angelim.
Dissertação (Mestrado) - Universidade Federal de Goiás, Escola de Engenharia Civil e Ambiental(EECA), Programa de Pós-Graduação em Engenharia Civil - Geotecnia, Estruturas e Construção Civil, Goiânia, 2019.
Bibliografia. Apêndice.
Inclui siglas, mapas, fotografias, abreviaturas, símbolos, gráfico, tabelas, lista de figuras, lista de tabelas.

1. Soil-lime stabilization. 2. Shoreline erosion. 3. Inderbitzen test. 4. Wave flume test. 5. Dam reservoirs. I. Mascarenha, Márcia Maria dos Anjos, orient. II. Título.

CDU 624.13

UNIVERSIDADE FEDERAL DE GOIÁS

ESCOLA DE ENGENHARIA CIVIL E AMBIENTAL

ATA DE DEFESA DE DISSERTAÇÃO

Ata nº **206** da sessão de Defesa de Dissertação de **Ricardo Moreira Vilhena** que confere o título de Mestre(a) em **Geotecnia, Estruturas e Construção Civil**, na área de concentração em **Geotecnia**.

Ao/s **vinte e sete dias do mês de junho do ano de dois mil e dezenove**, a partir da(s) **14:00**, no(a) **sala de reuniões do LABITECC** da **Escola de Engenharia Civil e Ambiental**, realizou-se a sessão pública de Defesa de Dissertação intitulada **"Soil stabilization with lime for reservoir shoreline erosion control"**. Os trabalhos foram instalados pelo(a) Orientador(a), Professor(a) Doutor(a) **Márcia Maria dos Anjos Mascarenha (GECON/UFG)** com a participação dos demais membros da Banca Examinadora: Professor(a) Doutor(a) **Lilian Ribeiro de Rezende (GECON/UFG)**, membro titular interno; Professor(a) Doutor(a) **José Camapum de Carvalho (UnB)**, membro titular externo, **cuja participação ocorreu através de videoconferência**. Durante a arguição os membros da banca **não fizeram** sugestão de alteração do título do **trabalho**. A Banca Examinadora reuniu-se em sessão secreta a fim de concluir o julgamento da Dissertação tendo sido(a) o(a) candidato(a) **aprovado** pelos seus membros. Proclamados os resultados pelo(a) Professor(a) Doutor(a) **Márcia Maria dos Anjos Mascarenha**, Presidente da Banca Examinadora, foram encerrados os trabalhos e, para constar, lavrou-se a presente ata que é assinada pelos Membros da Banca Examinadora, aos **vinte e sete dias do mês de junho do ano de dois mil e dezenove**.

TÍTULO SUGERIDO PELA BANCA

Documento assinado eletronicamente por **Márcia Maria Dos Anjos Mascarenha**, **Vice-Coordenadora**, em 28/06/2019, às 08:29, conforme horário oficial de Brasília, com fundamento no art. 6º, § 1º, do Decreto nº 8.539, de 8 de outubro de 2015.

Documento assinado eletronicamente por **Lilian Ribeiro De Rezende**, **Professor do Magistério Superior**, em 28/06/2019, às 10:39, conforme horário oficial de Brasília, com fundamento no art. 6º, § 1º, do Decreto nº 8.539, de 8 de outubro de 2015.

Documento assinado eletronicamente por **José Camapum de Carvalho**, **Usuário Externo**, em 02/07/2019, às 12:09, conforme horário oficial de Brasília, com fundamento no art. 6º, § 1º, do Decreto nº 8.539, de 8 de outubro de 2015.

A autenticidade deste documento pode ser conferida no site https://sei.ufg.br/sei/controlador_externo.php?acao=documento_conferir&id_orgao_acesso_externo=0, informando o código verificador **0717532** e o código CRC **B992D537**.

DEDICATION

I dedicate this work to my mother, for always encouraging my studies and especially to my beloved wife Genara, who has always contributed with her affection, patience, understanding, and support to the conclusion of another step of my life. Also, I dedicate to my daughter Laura, who brought me joys and ennobled my soul.

ACKNOWLEDGMENTS

This work would not be possible without the support of Eletrobras Furnas, not only financially, but also for encouraging the training of its employees. Thanks to the managers Renato Marques Cabral (Gerência de Serviços e Suporte Tecnológico-GST.E), Alexandre de Castro Pereira (Divisão de Tecnologia em Engenharia Civil-DTEC.E) e Carlos Antônio Reis da Silva (Divisão de Instrumentação e Suporte Tecnológico-DIST.E), as well as to Ricardo André Marques, for his unconditional support.

In particular, I thank Prof. Dr. Marta Pereira da Luz for her friendship and support, head of the research and development project entitled “Desenvolvimento e Utilização de Técnicas de Bioengenharia em Solos para Fins de Controle de Processos Erosivos no Âmbito de Empreendimentos de Usinas Hidrelétricas, em Especial em Margens de Reservatórios”. The present work is part of this main research, also called BioEngineering Project (PD-ANEEL n°.0394-1603/2016), financial supported by Agência Nacional de Energia Elétrica-ANEEL (Brazilian Electricity Regulatory Agency).

To the managers Marcos da Rocha Botelho and Alba Valéria Brandão Canellas of Divisão de Tecnologia em Engenharia Hidráulica (DTEH.E) by loan the portable 3D scanner and the Gerência de Programação Energética e Hidrometeorologia (GPH.O) meteorological data from the Itumbiara Dam.

To the coworkers from Furnas which collaborated since initial soil sampling and during laboratory tests Ademar F. Santana, Aloísio F. S, Santos, Helmar A. Cortes, Joaquim L. da Conceição, Lucinéia P. da Silva (Néia) and Silvio César Rego Braga. Also, the technician Renato Batista de Oliveira, and the chemist Leandro de Brito Silva for their amazing contributions to the microstructural and chemical analysis.

To the professors of the Program of Postgraduate Studies in Geotechnics, Structures and Civil Construction (PPG-GECON), and especially to my supervisor and co-supervisor, professors Dr. Márcia Maria dos Anjos Mascarenha and Dr. Renato Resende Angelim, respectively, who always willing and patient, contributed to my educational improvement.

To the Prof. Dr. Klebber Teodomiro Martins Formiga, of the Program of Postgraduate Studies in Environmental and Sanitary and Engineering (PPGEAS), head of the UFG Hydraulics Laboratory, for allowing the experimental tests in a wave flume.

To the technicians from the Laboratory of Soil Mechanics of the UFG João C. de Lima Júnior and Gabriel Novato, as well as the technician from the Hydraulics Laboratory, Tomás da Rosa Simões, had direct participation in the erodibility tests, besides the loans research equipment.

To the colleagues and friends of the Master, I was able to live and learn from all of them. In particular, I greatly appreciate engineer Marlon S. Schliewe for his friendship, for correcting all the flaws and leaks of the wave flume and especially for the brilliant contributions in this research. To the friends, and already masters, Jaqueline R. Ferreira, Mateus Fleury, and Roberto D. Alves, who were very important for the continuity of my academic journey.

ABSTRACT

Sedimentation issue is one of the major problems dealt with reservoir management nowadays. Large reservoirs in worldwide faces an increase of sedimentation due to climatic changes provoking shoreline erosions. The dynamics of the reservoir, for hydroelectric purposes, is related to a complex system that involves hydrological cycles, geomorphological aspects and anthropic actions that influence the erosive processes at its shores. It is still a challenge to control and reduce them, and even more so, find low-cost shore protection techniques. Soil stabilization using chemical treatment with hydrated lime is an old technique applied to constructions and slope stability. This work aims to evaluate the efficiency of the soil-lime stabilization technique for reservoir shores based on experimental erodibility research on residual soils (lateritic and non-lateritic). The sampling was realized on local site close to Itumbiara Dam, Brazilian hydropower, inside a high erosivity area for shoreline erosion, detected by GIS-based wave fetch model and satellite imagery. Soil samples were deeply analyzed by geotechnical and chemical laboratory procedures for characterization. Treatment proceeded by spraying hydrated lime in slurry form over lateritic soils by a lime solution of 1, 2 and 4% of lime solution at curing time of 1, 7, 28 and 56 days, through air-dry and moisture room storing. Also, tests with less than 1% by weight percent were carried out. The post-cured specimens were mapped first with Scanning Electron Microscopy with Energy Dispersive Spectroscopy, along with X-Ray analyzes, pH measurements and finally with erodibility tests (Inderbitzen test and wave flume test). In addition, the environmental concern of the influence of the use of lime led to the evaluation of the pH of the water in all tests. Also, it has been attempted to study the grain-size distribution of sediments of soil lost along the wave flume. Results from all lateritic and non-lateritic soils showed that the present technique produces a superficial ground crust of carbonate calcium by carbonation of lime, rather than fully stabilize the soil samples. This partial stabilization is restricted only to the efficiency and durability of this white Ca-rich layer. Lime content and curing conditions generate improvements to soils losses reduction against the erosivity of runoffs and wave impacts. Soil shrinkage increases its erodibility under air-drying curing storage. Curing time did not have a significant influence on lime treatment due to the lack of pozzolanic cementitious compounds but was verified a slight erosion reduction. Also, the formation of new cementitious minerals by pozzolanic reactions (long-term) was not verified by microstructural and chemical investigations in the lateritic and non-lateritic soils. Finally, results showed that soil-lime treatment works better on the lateritic soil than to the non-lateritic soil for effects of wave impacts and surface runoffs.

Keywords: Soil-lime stabilization. Shoreline erosion. Inderbitzen test. Wave flume test. Dam reservoirs.

LIST OF FIGURES

LIST OF TABLES

LIST OF ABBREVIATIONS

ANEEL	- Agência Nacional de Energia Elétrica
ANOVA	- Analysis of variance
ArcGIS	- Geographic Information System software
CA	- Activity Coefficient
CONAMA	- Conselho Nacional do Meio Ambiente
CTC	- Cation exchange capacity
DEM	- Digital Elevation Model
DSAS	- Digital Shoreline Analysis System
EDS	- Energy-dispersive X-ray Spectrometer
ESRI	- Environmental Systems Research Institute
FAO	- Food and Agriculture Organization
GIS	- Geographic Information System
GO	- The Brazilian state of Goiás
ICL	- Initial Consumption of Lime
INPE	- Instituto Nacional de Pesquisas Espaciais
ISSN	- International Standard Serial Number
Lm	- Lime fixation point
LDPA	- Laser Diffraction Particle Analyzer
LOI	- Lost of Ignition
Ma	- Million years
MCT	- Miniature Compacted Tropical (soil classification system)
MG	- The Brazilian state of Minas Gerais
NaHMP	- Sodium Hexametaphosphate
NASA	- National Aeronautics and Space Administration
OLC	- Optimum Lime Content

pH	- Hydrogen ion concentration
SE	- Specific surface
SEM	- Scanning Electron Microscopy
SODAR	- Sonic Detection and Ranging
SPM	- Shore Protection Manual
SWAN	- Simulating Waves Nearshore
SRTM	- Shuttle Radar Topography Mission
TOPODATA	- SRTM-based topographic data of INPE
USCS	- Unified Soil Classification System
USDA	- United States Department of Agriculture
USGS	- United States Geological Survey
XRD	- X-ray Diffractometry
XRF	- X-ray Fluorescence Spectroscopy
WRB	- World Reference Base for Soil Resources

LIST OF SYMBOLS

Al_2O_3	- Aluminum oxide
Ca^{2+}	- Calcium
CAH	- Calcium aluminate hydrate
CaO	- Calcium oxide
CL	- Lean clay
CASH	- Calcium aluminium silicate hydrate
cm	- Centimeters
cm^3	- Cubic centimeters
CSH	- Calcium silicate hydrate or calcium silicate hydrogel
CO_2	- Carbon dioxide
$Ca(OH)_2 \cdot MgO$	- Calcium-magnesium hydrated lime
$Ca(OH)_2$	- Hydrated lime
e	- Void ratio
Fe	- Iron
Fe_2O_3	- Ferric oxide
G	- Specific gravity
g	- Grams
g/cm^3	- Grams per cubic centimeters
g/g% -	- Gram per gram percent
Hz	- Frequency unit (hertz)

h	- Hour
H_2O	- Hydrogen dioxide
I_P	- Plasticity index
kg	- Kilograms
km	- Kilometers
km²	- Square kilometers
kg/m²	- Kilogram per square meters
kPa	- Kilopascals
kN/m³	- Kilonewton per cubic meters
K_2O	- Potassium oxide
LA'	- Lateritic sandy soil
LG’	- Clay lateritic soil
$L \cdot m^{-1}$	- Liter per meters
m	- Meters
meq/100g	- Millequivalents per 100 grams
mesh	- Sieve size
m_f	- Final soil mass, in grams
mL	- Mililitre
ML	- Silt
MgO	- Magnesium oxide
MJ.mm/ha.h	- Millijoule millimeters per hectare hour
mm	- Millimeters

m/s	- Meters per second
m^2/g	- Square meters per gram
MnO	- Manganese oxides
m_t	- The total mass of sediments, in grams
MW	- Megawatt
$m_{>2mm}$	- The dry mass of sediment retained in the 2 mm sieve, in grams
$m_{>75\mu m}$	- The dry mass of sediment retained in the sieve of 75 µm, in grams
$m_{<75\mu m}$	- Mass of sediments smaller than 75 µm, in grams
n	- Porosity
NA'	- Non-lateritic sandy soil
Na_2O	- Sodium oxide
NS'	- Non-lateritic silty soil
P_2O_5	- Phosphorus pentoxide
R^2	- R-squared or coefficient of determination
S	- South (wind rose)
SO_3	- Sulfur trioxide
SiO_2	- Silicon dioxide
TiO_2	- Titanium dioxide
$U(z)$	- Wind speed at height z, in m/s
$U(zr)$	- Wind speed at height zr, in m/s
V_i	- Total volume is given by the initial surface, in cm^3
Vf	- Total volume is given by the final surface, in cm^3

z	- Z-axis of the cartesian coordinate system
ZrO_2	- Zirconium dioxide
z_{1a}	- Minimum z-value
z_2	- Maximum z-value
W	- West (wind rose)
w	- Gravimetric water content
w_f	- The final moisture content of the soil ground
w_L	- Liquid limit
w_i	- The initial moisture content of the soil
w_{nat}	- Natural water content
w_P	- Plastic limit
α	- Power law exponent
γs	- Unit weight solids, in kN/m³
Δw	- Water content variation
µm	- Micrometers
ρ_d	- Dry density, in g/cm³
%	- Percent
˚C	- Degree Celsius

TABLE OF CONTENTS

CHAPTER 1

INTRODUCTION

Shoreline erosion and sedimentation are the major issues faced by reservoir managers and landowners. Sediment yield in the large reservoir has been increasing fast and almost by an uncontrolled way in worldwide due to climatic changes (De SOUZA DIAS et al., 2018) and human activities (WANG et al., 2018). This could reduce the worldwide reservoir storage capacity by nearly 25% in the next 25 to 50 years (WCD, 2000).

Sedimentation is produced by erosion processes on reservoir shorelines such as waves wind-generated (LAWSON, 1985), downhill creep (SU et al., 2017), surface runoffs (LUIZ et al., 2017), water level fluctuations (VOLKER; HENRY, 1988), and anthropization (WANG et al., 2018).

Commonly, the reservoir governance has been using high-cost methods of hard and soft structures for shorelines erosion protections, but scientists have been looking for a low-cost method of soil stabilization for over three decades (MCQUARRIE; PILKEY, 1998). Some of these methods was highlighted such as soil bioengineering techniques (SIMON; STEINEMANN, 2000) but biomineralization (VALENCIA; CAMAPUM; TORRES, 2014) and chemical treatments (GEDNEY; WEBER, 1978; SANTOS, 2011) for slope stability have not yet been used in reservoirs shores.

In Brazil, the Eletrobras Furnas, an electric power holding company (state-owned), began a research with the partnership of the School of Engineering and Environmental of Federal University of Goiás (UFG) to evaluating the soil-lime treatment for reducing shoreline erosion for hydropower reservoirs (BITTENCOURT; MARIN; LELES, 2012). In addition, this company invested on research to evaluation of soil bioengineering strategies for reservoirs shores and non-traditional low-cost techniques. Their example of engagement in the erosion control of sedimentation issues is due to need of management of 21 large hydroelectric reservoirs, also reflects on the financial support of this current work and in pioneering new techniques.

Inspired in one of the oldest (BELL, 1996) and low-cost (USGS, 2018) soil chemical stabilizers, Nascimento et al. (2019) evaluated the soil-lime treatment on lateritic soil for reducing shoreline erosion for hydropower reservoirs under surface runoffs and water level

fluctuation. Furthermore, the effects of wave erosivity potential at reservoir shoreline were studied by Menezes (2017) and Schliewe (2018), which conducted several erodibility tests (i.e. wave flume test) on compacted and undisturbed samples of lateritic soil, respectively.

The management of reservoirs from hydroelectric power plants to reduce the process of shoreline erosion and deposition of sediments is a constant concern as long as the dam exists. Therefore, universities in partnership with reservoir managers should expand their studies because each reservoir has its own characteristics that can influence the choice of treatment type and erosion control.

This paper aims to evaluate the efficiency of the soil-lime stabilization technique for reservoir shores at Itumbiara dam and the treatment performance on lateritic and non-lateritic soils.

1.1 RESEARCH OBJECTIVES AND SCOPE

The main objective of this thesis is to evaluate the soil-lime treatment on the soils of the shores of hydropower reservoirs to be applied in the reduction of shoreline erosion. The secondary objectives, needed to accomplish the main objective, are to:

- Define the local site of soil sampling by GIS-based wave fetch model;
- Track the range of influence of lime stabilization along with soil depth;
- Analyze the influence of cure conditions, lime content and time curing on lateritic and non-lateritic lime-treated soils;
- Evaluate the environmental aspect of soil-lime treatment on reservoirs;
- Compare the results of erodibility tests from different soil types.

The work focuses on the evaluation of the physical and chemical effects of adding a lime solution to lateritic and non-lateritic soil, also the influence of external conditions along a specific time. To fulfill the objectives of this study, it was necessary to realize a wide experimental program.

1.2 THESIS OUTLINE

This dissertation is organized into four chapters and three appendices. The present chapter has introduced the problems of erosions dealt by reservoir managers, a proposal of a non-traditional technique based on a line work by soil-lime treatment, and the need for new researches to reduce shoreline erosions. Finally, the objectives and scope of the dissertation

were discussed. A brief description of the contents of the remaining chapters is presented in the following paragraphs.

Chapter 2 presents the main product of this dissertation in manuscript format to be submitted to Catena (ISSN: 0341-8162), published by Elsevier. The manuscript presents the introduction and the literature review discussing the effects of erosion processes on the shores of reservoirs and uses of lime for soil stabilization. The chemical and microstructural of soil-lime reactions are studied through several types of equipment, such as X-ray fluorescence spectrometry, X-ray diffractometry, and scanning electron microscopy. The performance of the lime treatment along different time periods, curing conditions, and lime content were analyzed by the wave flume test. Finally, the discussions the results are presented.

Chapter 3 presents a comparative evaluation of the effects of lime treatment on a lateritic and non-lateritic soil from two erodibility test devices, such as the wave flume test and the Inderbitzen apparatus. In addition, discussions of the experimental results and the carbonation process are presented.

Chapter 4 presents an overview of the conclusions according to the analyses and recommendations of the results for future studies.

Appendix A presents a second product of this thesis as an article published in Water (ISSN: 2073-4441) from MDPI. This paper concerns a GIS-based analysis of the impacts of waves of the reservoir by the wind and introduced the procedure for mapping the shoreline erosion potential by wave-wind generated model around a hydropower reservoir.

Appendix B presents the summary of wave flume tests as schematic sheets, with photographs of fume and the soil sample, results of pH measurement, grain-size distribution curve, and soil losses.

Appendix C presents photographs of all stages of Inderbitzen test for lateritic and non-lateritic soils.

CHAPTER 2

MANUSCRIPT

In this chapter the main article of this research is presented, which will be submitted to Catena, an interdisciplinary journal of soil science of Elsevier with impact factor of 3.851 (Qualis CAPES A1).

EVALUATION OF LIME-TREATED SOIL FOR RESERVOIR SHORELINE STABILIZATION

Ricardo Moreira Vilhena [a], Márcia Maria dos Anjos Mascarenha [b], Renato Resende Angelim [b], Tomás da Rosa Simões [b] Renato Batista de Oliveira [c] and Marta Pereira da Luz [d]

[a] Geotechnics Postgraduate Program PPG-GECON, Federal University of Goiás, Eletrobras Furnas, BR153, km 510, Zona Rural, Aparecida de Goiânia CEP 74923-650, Goiás, Brazil; rvilhena@furnas.com.br

[b] School of Civil and Environmental Engineering, Federal University of Goiás, Universitária Ave. 1488, Setor Universitário, Goiânia CEP 74605-220, Goiás, Brazil; marciamascarenha@gmail.com; tecnoeng@gmail.com; tomas_simoes@ufg.br.

[c] Eletrobras Furnas, BR153, km 510, Zona Rural, CEP 74923-650 Aparecida de Goiânia-Goiás, Brazil; renatoba@furnas.com.br.

[d] Eletrobras Furnas, Industrial and Systems Engineering Postgraduate Program-MEPROS, Pontifical Catholic University of Goiás, BR153, km 510, Zona Rural, Aparecida de Goiânia CEP 74923-650, Goiás, Brazil; martaluz@furnas.com.br.

Abstract: Nowadays, sedimentation is one of the major problems dealt with by reservoir management. Worldwide, large reservoirs face an increase of sedimentation due to unbalance of the soil–atmosphere dynamics. Controlling and reducing it remains a challenge, and the use of low-cost shore protection techniques is an even greater challenge. This paper aims to evaluate the efficiency of the soil–lime stabilization technique for reservoir shores. Treatment proceeded by spraying hydrated lime in slurry form over lateritic soils with 1, 2, and 4% lime solution and curing times of 1, 7, 28, and 56 days with air-dry and moist-room storage. Also, a single test with less than 1% lime solution by weight percent was carried out. The post-cure specimens were mapped first with scanning electron microscopy along with X-ray analyses and finally with erodibility tests (i.e. wave flume test). Environmental concern about the influence of the use of lime led to the evaluation of the pH of the water in all tests. Also, an attempt was made to study the grain-size distribution of soil sediments lost along the wave flume. The results showed that the present technique produces a crust of carbonate calcium by carbonatation over the soil rather than stabilizing it and that the lime content and type of curing generate improvements in soil loss reduction, but the curing time does not. In addition, the technique gave relative protection against water level variation and wave impacts.

Keywords: soil stabilization; wave flume test; erodibility; microstructural analysis; lateritic soil.

1 INTRODUCTION

Shoreline erosion around reservoirs occurs due to unbalance of the soil–atmosphere dynamics and soil–water conditions triggered by wind action (Volker and Henry, 1988), gravity (Su et al., 2017), rainfall (Luiz et al., 2017), water level fluctuations (NWRPC, 2004), wave action (Lawson, 1985; Fernandez and Fulvaro, 2000; Edil, 2013), and human activities (Wang et al., 2018). Reservoir operation also plays a vital role in the intensity of the wave abrasion process that occurs on the bank slope (Volker and Henry, 1988). The sediment yield by erosion through all the natural processes and human activities increases the sedimentation rate and consequently also becomes the main issue for reservoir storage capacity, power generation, irrigation, and the environment (Lawson, 1985; Kondolf et al., 2014; Juracek, 2015; De Souza Dias, 2018). Reservoir sedimentation is a complex process that must be studied in many dam designs and hydropower plants during operation stages (Schleiss et al., 2016; Kondolf et al., 2014). Because of the lack of measures to control sediment inflow and deposition, almost 25% of the worldwide reservoir storage capacity could be lost in the next 25 to 50 years (WCD, 2000).

Soil stabilization is one of the various necessary actions taken by reservoir managers to mitigate shoreline erosion (Lawson, 1985). It could be applied at all scales of sediment yield production (far-reach, mid-reach, and in-reservoir) (Schleiss et al., 2016), and a combination of both stabilization and management actions may even be used (Edil, 2013). Hard and soft structures are traditional methods of shore protection (McQuarrie and Pilkey, 1998). Therefore, other methods are growing in popularity. Biotechnical techniques including soil bioengineering stabilization have vegetation as the main structural constituent (Simon, and Steinemann, 2000). In addition, these soil stabilization techniques aim to increase the resisting forces by mechanical improvement of the soils. Reservoirs managers and shore communities have been in search of low-cost, effective non-traditional methods of soil stabilization for over three decades (McQuarrie and Pilkey, 1998).

Chemical soil stabilization contributes to greater internal strength and durability (Krishnan, 2014) for geotechnical purposes. Its success in stabilizing compacted soils in highways, airfields, building foundations (Bell, 1996), and earthen dams is undeniable (Tran et al. 2014; Amadi and Okeiyi, 2017; Rocha and Rezende, 2017). However, there are fewer references on the use of chemical soil treatments for slope stability (Gedney and Weber, 1978; Santos, 2011), and studies on reservoir shoreline stabilization are lacking (Nascimento et al., 2019).

Lime (i.e. quicklime and hydrated lime) is one of the oldest (Bell, 1996; Jha and Sivapullaiah, 2015) and most low-cost (USGS, 2018) chemical stabilizers used nowadays for soil stabilization (Wang, 2017). Other binding agents such as cement could be used for this purpose. However, this research focused first on lime evaluation.

Lime has major environmental impacts related to its production, involving dust emissions at the mining site and even global climate change due to the emission of large quantities of CO2 (Gutiérrez et al., 2012). However, its use brings countless benefits in industrial, agricultural, construction, chemical, metallurgical, water treatment, and environmental applications (USGS, 2018, Wang, 2017; Singh and Kalamdhad, 2013; O'Donnell et al., 2016; Stimson, et al. 2017).

Soil–lime treatment causes short-term reactions (i.e. cation exchange, flocculation-agglomeration, and carbonatation) and long-term reactions (i.e. pozzolanic reactions) and depends on many variables such as the lime content, lime type, curing time, moisture, temperature, water content, and soil mineralogy (Bell, 1996; Tran et al. 2014; Wang, 2017; Eades and Grim, 1960; Diamond and Kinter, 1964; TRB, 1987; Jha and Sivapullaiah, 2016). Pozzolanic reactions provide the major improvement of the mechanical behaviour of the soil (e.g. strength, stiffness, volume changes) due to the generation of cementation compounds that may act on clay surfaces (Diamond and Kinter, 1964; Wang, 2017). Generally, studies of clay–lime–water systems (TRB, 1987) indicated that cementation could occur through a combination of solution–precipitation (physicochemical) and hydration–crystallization processes (chemical).

Researchers have reported the formation of various forms of cementitious materials depending on the soil mineralogy, of which the most common are calcium silicate hydrate (CSH) and poorly crystallized (gel) and well-crystallized calcium aluminate hydrate (CAH) and calcium alumina silicate hydrate (CASH) (Wang, 2017; Jha and Sivapullaiah, 2016).

Therefore, soil–lime stabilization also shows improvement in the geotechnical properties of unstable lateritic soil (Attoh-Okine, 1995; Latifi et al., 2017; Galvão et al., 2004). The formation of lateritic residual soil is common in tropical regions due to the intense subaerial weathering process (Herbilion and Nahon, 1988). In addition, with increased weathering, crystallization leads to a concentration of iron and/or aluminium oxide until a cementation stage around the soil particles is reached and due to this characteristic, this fine-grained type of soil could have limitations in some engineering constructions (Attoh-Okine, 1995).

The use of quicklime in the stabilization of lateritic soil was revealed to lead to better performance in terms of increasing the bearing strength and workability (e.g. plasticity and compressibility) compared to hydrated lime when both are used in the powdered form. However, hydrated lime is more applicable for soils with higher clay content (Amadi and Okeiyi, 2017), which is a common characteristic of tropical soils.

A comparison of the stabilizing effects of quicklime and hydrated lime slurries (Petry and Lee, 1988) on soil has a similar behavior with theirs dry powder forms showing that quicklime slurries produce more reduction in swelling potential and strength gain and also a higher concentration of calcium in clay soil exchange complexes than the hydrated lime slurries (i.e. milk of lime).

The slurry lime method for soil stabilization was first used in the 1950s in highway constructions. Slaked stabilizer is spread over scarified soil by a distributor truck. Furthermore, it leads to dust-free application, reducing environmental problems, and gives a better distribution of the soil–lime mixtures than dry lime (TRB, 1987). Other well-established practices that use lime in slurry form for slope stability and deep and shallow foundations are lime columns (Glendinning, 1995), lime piles (Gedney and Weber, 1978; Rogers et al., 2000), and lime slurry pressure injection (LSPI; Wilkinson et al., 2010). Therefore, a non-traditional technique called Cal-Jet has been designed for soil-treatment application based on whitewash painting (i.e. limewash) (Santos, 2011). This method has the objective of preventing detachment of soil caused by rainfall (e.g. sheet and rill erosion) through applying pulverized hydrated lime (slaked) over an excavated soil slope.

A low-cost hydrated lime slurry method also is under development in Brazilian researches on tropical soil stabilization and recent studies have already verified strength improvements of lateritic soils (Sousa and Reis, 2016; Nascimento et al., 2019) and have shown low effects on saprolitic expansive soil (Oliveira, 2018) for resisting water erosion such as sheet erosion and water level fluctuations. These works consisted of the evaluation in a laboratory of the sheet erosion on modified Inderbitzen apparatus (Aguiar, 2009) and the water level fluctuation by partial and total immersion of soil samples in a receptacle with clean water (i.e. degradation test). Both experiments are included in common Brazilian erodibility tests (Mascarenha et al., 2017) applied to studies of erosion processes.

Wind-generated waves also play an important role in the shoreline erodibility through their impact actions. Therefore, it is necessary to evaluate this erosion process, which can be done by a wave flume test. This experiment allows the determination of soil mass loss

according to the wave frequency and shore slope (Tatto, 2014; Menezes, 2017; Schliewe, 2018).

The main objective of the current work is to evaluate lime-treated soil under wave flume tests to understand the behavior against wave impacts and water level fluctuations, with the aim of mitigating the effects of reservoir shoreline erosion by a non-traditional technique. In addition, the study also aims to address the effect of varying the lime content under different curing times, the influence of curing storage (air-drying and moist room), and the influence of pH changes and to identify the depth of soil–lime microstructural and chemical reactions. The present research consists in spreading hydrated lime slurry over the surface of soil samples for shoreline stabilization, differently from many studies that test specimens of soil–lime mixtures.

2 MATERIAL AND METHODS

Samples collected from Itumbiara dam reservoir shore were treated with different cure contents, curing times, and curing conditions. The dry curing was carried out in an air conditioned laboratory room and the wet curing in a moist room with a relative humidity (RH) higher than 90% and temperature of 24 ± 3°C. Air-curing in an air-conditioned laboratory environment was adopted as the first evaluation class based on lime researches and for the safety of the samples. After the treatment with lime, with the aim of stabilizing this soil, microstructural and chemical mapping was performed abroad to evaluate the physical and chemical changes that could promote the mechanical improvement of this soil. In addition, the resistance of soil treated with lime against wave impact was evaluated by the erodibility test, also known as the wave flume test.

2.1 DESCRIPTION OF THE STUDY AREA

The study was carried out in the field and laboratory. Soil samples were collected from the site and field tests were selected based on research and realized (Vilhena et al., 2019) at the reservoir of the Itumbiara dam, which is located in Midwest Brazil in South America (Fig. 2.1).

The GIS-based fetch model tool was applied to define sites with higher potential for wave- and wind-generated erosion and a location near the dam with road access was chosen for the current study. Other researchers also reported a strong influence of rainfall

(Luiz et al., 2017; Jesus et al., 2017; Romão et al., 2017) on the watershed of Itumbiara dam reservoir. Fig. 2.1 shows the spot where a trench was opened for sampling.

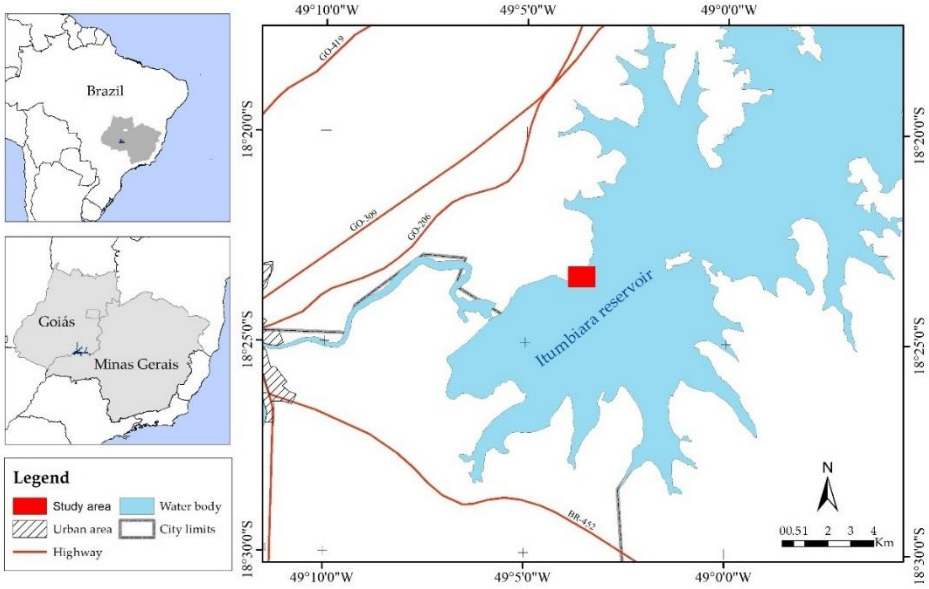

Figure 2.1 – Location map of the study area.

The average ratio of rainfall to runoff calculated by Luiz et al. (2017) was 7,708.00 MJ mm/ha.h during the rainy season (November to March). The parent rock consists of metamorphic rocks (schist-like) which produce residual erodible soils with a higher rate of soil degradation, which is increased by anthropic actions (i.e. agriculture and irregular settlements), according to Jesus et al. (2017).

The lateritic soil (i.e. oxisols) collected in the present study area is the result of intense weathering on a metamorphic parental rock and lies over a saprolitic soil (i.e. inceptisols). The morphology of shores around this reservoir is flat to gently lakeward-sloping (5°–10°) platforms that create a favourable environment for sheet and rill erosion (Vilhena et al., 2019). Figure 2.2 shows a soil profile of the lateritic soil at the local site and the soil sampling of the blocks in the trench.

Pedological characterization and soil classification of the lateritic soil profile show high amounts of organic matter (roots) on top of the pedon in the O horizon (3 cm thickness) and a transitional A horizon until 20 cm depth. In the deeper layers (20 to 120 cm) a homogeneous B horizon is found with high contents of Fe and Al.

This was classified as oxisol (USDA Soil Taxonomy) or ferralsol (FAO-UNESCO). The colours of the A and B horizons are in slightly similar ranges of hues from dark to medium

red-orange (2.5 YR 2/6–6/10). These horizons have a fine sandy loam texture with a few tubular pores and are slightly sticky; the drainage condition is well-drained.

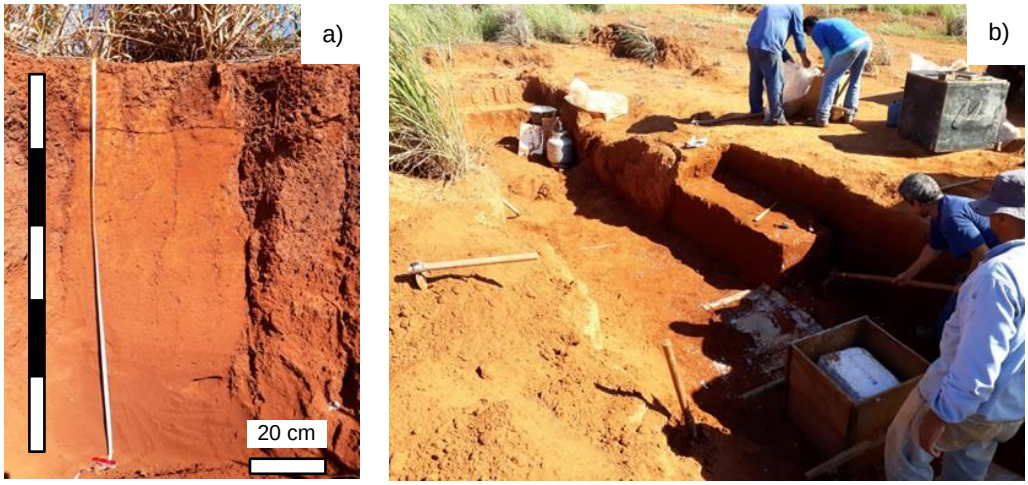

Figure 2.2 – Field photographs of: (a) profile of lateritic soil in the study area and (b) soil sampling..

Experimental testing was performed on a lateritic soil, which was classified as silty sand and characterized by a reddish-orange colour. A total of 15 undisturbed samples (30 × 30 × 30 cm blocks) and one disturbed sample were collected from a trench excavated at Area 1 on the shore of Itumbiara dam reservoir (Vilhena et al., 2019), lying between coordinates of latitude 18° 23' 12.2" S and longitude 49° 03' 25.6" W.

In addition, three exploratory drillings by hand auger were done next to the trench, each with a depth of 2 m, to perform the field gravity permeability test (ABGE, 2013) and evaluation of the subsoil profile. All field tests and investigations were realized to support soil characterization.

Soil characterization tests and specific tropical soil tests (Fabbri; 1994; Nogami and Villibor, 2009) were realized using the disturbed sample. Falling-head permeability tests (ABNT, 2000) were performed in the laboratory using three undisturbed samples.

2.1.1.1 Materials

Table 2.1 summarizes the soil physical and chemical properties, which were determined using standard soil characterization tests and specific tropical soil tests (Fabbri, 1994; Nogami and Villibor, 2009).

The coefficient of permeability found in both in situ and laboratory tests showed a value with an order of magnitude of about 10-6 m/s, which corresponds to fine sand and loose

sediments (Das, 2008) and can be considered as a semi-pervious or low permeability soil. The soil permeability estimation of the field and laboratory tests was not intended to compare them but to estimate the order of magnitude to evaluate the soil infiltration conditions. Hence, both tests simulated the soils under different conditions according to the degree of saturation, contour conditions of the water flow, and the type of flow.

Table 2.1 – Geotechnical properties of lateritic soil.

Gravel	Sand	Silt	Clay	w_L	w_P	I_P	USCS	w_{nat}	w	G	γ_s
%	%	%	%	%	%	%		%	%		kN/m³
2	34[a]/31[b]	64[a]/18[b]	0[a]/49[b]	47	29	17	ML	15.8	4.1	2.88	28.3

e	n	D	pH	CA[c]	SE[c]	CTC[c]	Soil activity class[c]	Relevant clay mineral[c]	MCT[d]	Permeability Field Test[e]	Permeability Lab Test[e]
				10^{-3} g/g%	m²/g	meq/100g				m/s	m/s
0.46	0.31	ND	6.25	10.67	17.08	1.88	Low active	Kaolinite	LG'	4.1×10^{-6}	2.2×10^{-6}

NOTE: w_L, Liquid limit; w_P, Plastic limit; I_P, Plasticity index; USCS-Unified Soil Classification System; ML, Silt; w_{nat}, Natural water content; w, water content; G, specific gravity; γ_s, Unit weight solids; e, void ratio; n, porosity; D, Dispersity; ND, Non-dispersive; CA, Activity coefficient of MCT classification; SE, Specific surface; CTC-Cation exchange capacity; Tropical soil classification - MCT (expeditious method); LG', Clay lateritic soil; pH measured in water solution.

[a] Non-addition of an agent dispersive to hydrometer analysis

[b] Addition of an agent dispersive of Sodium Hexametaphosphate (NaHMP) to hydrometer analysis

[c] Adsorption of Methylene Blue Test, from Fabbri (1994).

[d] Tablet Method, from Nogami and Villibor (2009).

[e] Average values

The commercial name of the lime used in this research is dolomitic hydrate type N (USGS, 2018), a calcium-magnesium powder hydrated lime [$Ca(OH)_2.MgO$]. Table 2.2 shows the general chemical composition of this lime and the selected lateritic soil, which was determined using X-ray fluorescence spectroscopy (XRF). As shown in Table 2.2, the dominant compounds in hydrated lime are calcium oxide (68.59%), magnesium oxide (26.59%), and silica (2.74%).

Table 2. 2 – Chemical composition of the experimental materials (percentage).

	SO_3	MgO	SiO_2	Fe_2O_3	Al_2O_3	CaO	TiO_2	P_2O_5	ZrO_2	SrO	MnO	Na_2O	K_2O	LI[a]
Lateritic soil	-	-	40.89	16.77	23.77	0.08	4.77	0.13	0.11	-	0.08	0.93	0.72	11.91
Lime	0.25	26.59	2.74	0.49	0.65	68.59	-	0.24	-	0.12	0.07	-	0.17	0.09

[a] Loss of ignition

The micro-analyses were carried on samples of natural lateritic soil and hydrated lime using X-ray diffractometry (XRD) and X-ray diagrams of both materials (Fig. 2.3). Kaolinite and quartz are the main minerals observed in the soil specimen; muscovite and iron oxides are also present. The lime samples present calcite, portlandite, brucite, and periclase.

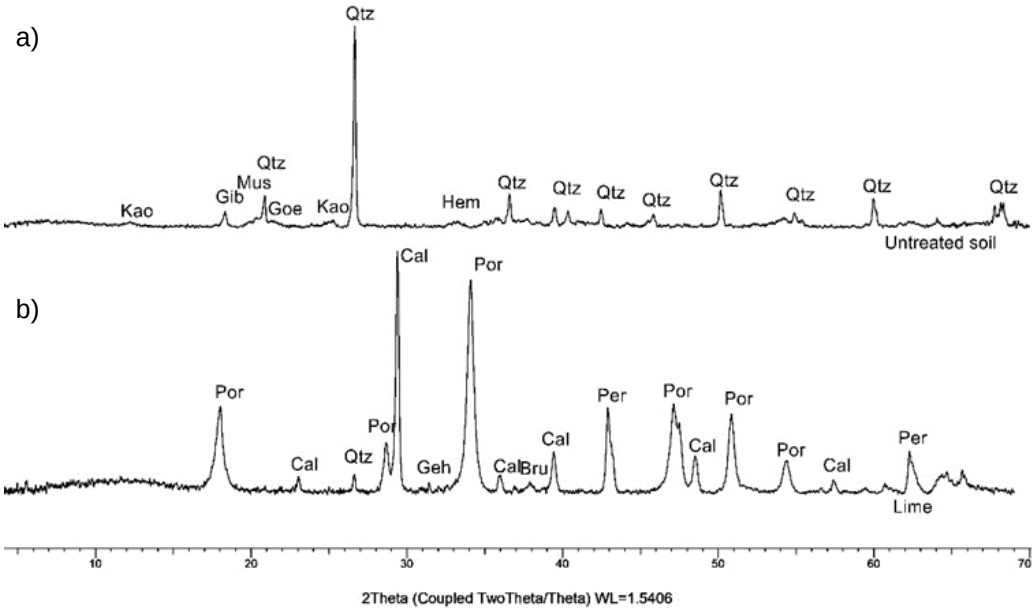

Figure 2.3 – Mineralogical analysis by XRD of (a) untreated lateritic soil and (b) lime. Bru = brucite; Cal = calcite; Gib = gibbsite; Geh = gehlenite; Goe = goethite; Hem = hematite; Kao = kaolinite; Mus = muscovite; Por = portlandite; Per = periclase; Qtz = quartz.

The microstructure of untreated soil was investigated by the scanning electron microscopy (SEM) technique and Fig. 2.4 shows photomicrographs of this sample at three different magnifications. SEM images were obtained from surface observations in parallel and perpendicular to the top of the sample. For this analysis, samples were not coated to preserve soil humidity and the SEM setups was made with low vacuum modes and backscatter imaging.

The microfabric appearance of lateritic soil is a granular particle matrix, in which the presence of micropores and macropores can be observed in an agglomeration fabric of euhedral quartz grains associated with clay minerals. This soil characteristic shows an advanced stage of weathering since the greater the degree of weathering, the greater the aggregations and the fewer the dispersed clay particles (Nogami and Villibor, 2009; Rezende, 2013). Figure 2.4b shows a larger macropore between the aggregations.

The fine particles of layered kaolinite and oxyhydroxides are assembled to quartz grains in aggregation of soil particles as presented in Fig. 2.4c. Both parallel and perpendicular observations of the surface sample showed non-typical clay crystal morphologies.

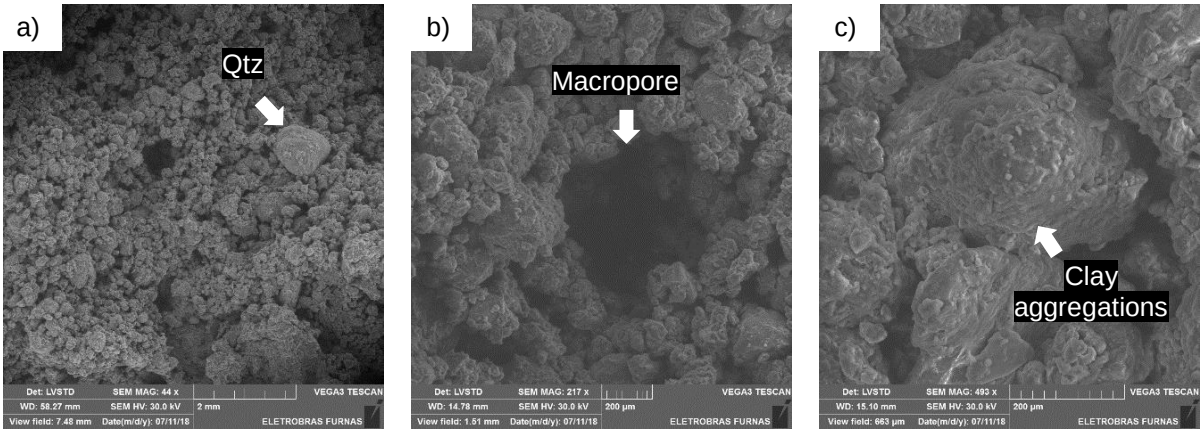

Figure 2.4 – SEM micrographs of the untreated lateritic soil: (a) a magnification of 44× shows the general aspect of the lateritic soil and a quartz grain (Qtz); (b) a macropore shown at a magnification of 217× created by biological agents; (c) aggregation of the clay minerals at a magnification of 493×.

2.1.1.2 Sample preparation for soil-lime stabilization

The tests were carried on the untreated (natural soil) and lateritic soil samples treated with 1, 2, and 4% lime by weight percent (i.e. water-lime solution). The lime content was determined by the sample volume and not by the total dry mass of the soil.

The hydrated lime powder was added to 950 ml of distilled water in a beaker in accordance with the respective lime content and was then constantly agitated with a glass rod to achieve the slurry form (i.e. milk of lime), which was carefully spread over the soil.

Also, another specimen was treated with a suspended liquid mixture of water and 1% lime content that had not been agitated. This procedure permitted the precipitation of lime and used the minimal suspended lime fraction dissolved in the water to test the reaction of the lowest stabilizer content.

The curing times employed in the present study were 1, 7, 28, and 56 days using air-drying storage. For the 56-day curing time, test storage in a moist room was included to produce uniform wetting of the sample and to compare the curing conditions.

The lime contents and curing times used in the present work were based on the same methodology as Nascimento et al. (2019) except for the curing storage and the solution with 1% lime content. Figure 2.5 illustrates the aspect of soil–lime treatment of the current work.

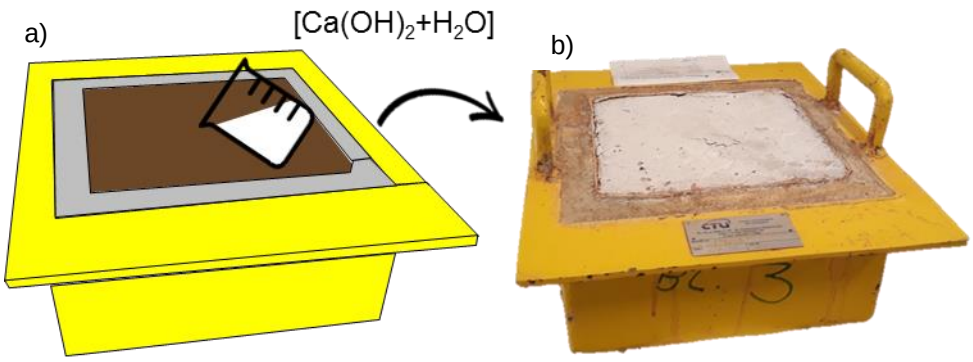

Figure 2.5 – Aspects of soil–lime treatment: (a) the hydrated lime slurry is spread over the undisturbed soil with a beaker and mixing in constant agitation; (b) treated sample (4%; 56 days) after the curing time.

2.1.2 Soil-lime stabilization mapping analysis

In most cases of soil–lime stabilization, the pozzolanic reactions improve the soil geotechnical properties (TRB, 1987) due to the formation of cementation compounds. Several works have effectively used XRD and SEM to examine the mineralogical composition and microstructure of soil treated with chemical agents (Bell, 1996; Tran et al. 2014; Diamond and Kinter, 1964; Jha and Sivapullaiah, 2015, 2016). The current study differs from the usual soil–lime mixtures preparations and thus mineralogical and microstructural characterization of the pozzolanic reactions through the soil depth is needed. In order to realize the elemental (i.e. calcium) mapping analysis of the treatment range, an energy-dispersive X-ray spectrometer (EDS) fitted on the SEM was used to scan the occurrence of calcium on the surface of treated soil before the SEM analysis.

Furthermore, the powder XRD technique was used over the areas defined by the EDS mapping analysis to identify new crystalline compounds due to long-term processes. Also, the results of the XRF analysis of the lateritic soil and lime supported the interpretation of the XRD data. In addition, the pH of lateritic soil for all sets of lime contents and time periods was examined by pH meter to verify the alkalinity condition of the soil to establish the pozzolanic reactions.

2.2 ERODIBILITY TEST

The erodibility test was performed in a wave flume or hydraulic wave channel that simulates the erosive effect of wave impacts on reservoir banks with a certain slope inclination. The wave flume used in this study was constructed by Menezes (2017), inspired by the works of Tatto (2014), and the methodology used in the current study was based on Schliewe (2018).

This wave flume has dimensions of 10.00 m in length, 1.20 m in height, and 0.47 m in width. The structure is composed of panels of tempered glass with a thickness of 10 mm at the sides and bottom, supported by metallic profiles. This device has a flap-type wave generator system, with semicircular periodic movements, controlled electronically by a frequency inverter. In addition, a metal ramp with adjustable tilt was designed to fit and attach a metal sample holder with undisturbed soil (Fig. 2.6). The sample holder with the untreated and treated lime soils is shown in Figs. 2.7a and 2.7b, respectively. Fig. 2.7c shows the soil sample holder placed in the slope at the end of the flume. A cement mortar strip was applied around the soil block inside the sample holder, due to the results that preceded the work of Menezes (2017) and Schliewe (2018), who verified significant soil losses due to the low adhesion between soil and sample holder, called the border effect.

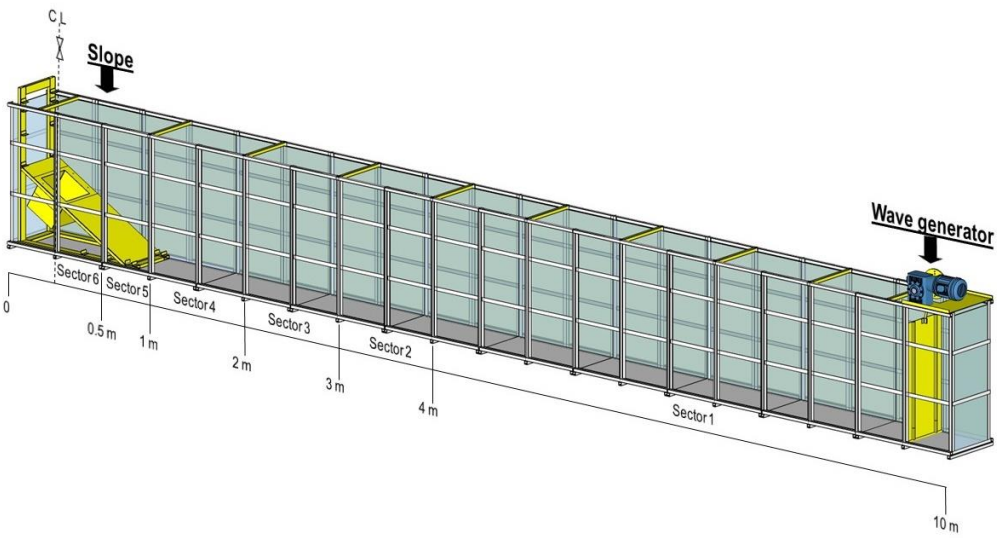

Figure 2.6 – Perspective 3D view of the wave flume.

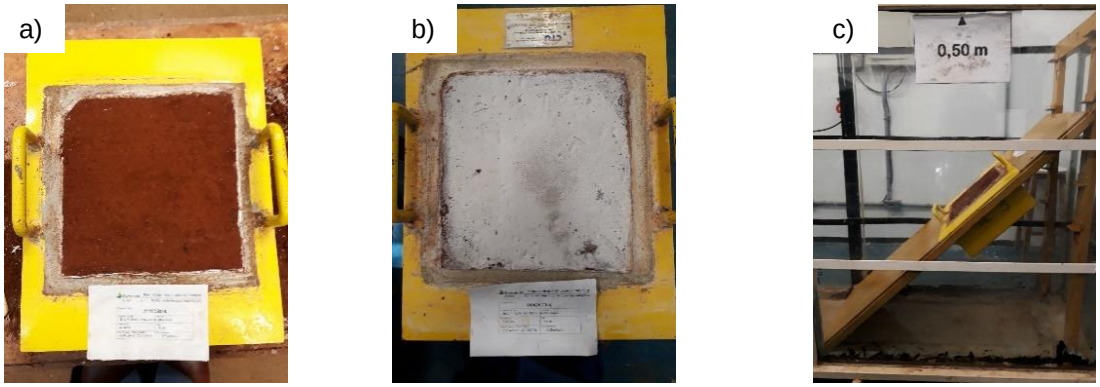

Figure 2.7 – Soil sample holders (a) Natural lateritic soil before treatment; (b) Soil treated with 4% lime; (c) Sample installed on the metal ramp (slope of 45°).

The wave flume test was divided into two main steps. The first is the simulation of the effect of the wave impact on the sample of treated and lime-treated soil, which is inside the sample holder, and the quantification of its loss of soil mass. The sample holder is inserted into a 45° inclined ramp prior to the test, and then the channel is filled until the water level coincides with the center of the sample, about 59 cm in height, and the test is started at a frequency of 0.5 Hz. Those parameters were defined by analysis of the results of the research by Schliewe (2018), from which the medium erodibility values were selected. In addition, all tests were conducted within 6 hours as established by this work. The second step is the quantification of soil mass loss by three different techniques with sediment characterization. To find the size particle distribution, a Laser Diffraction Particle Analyser (LDPA) was used, which helps in the evaluation of the extent of eroded sediment along the channel. It may also confirm a typical characteristic of sediment deposition in the reservoir such as coarse-size particles near the shores and fine sediments further away.

The soil loss analysis by the wave flume test used the formulations of Schliewe (2018) according to the following methods: weighing the initial and final soil masses within the sample holder and sieving the total dry mass of sediments collected along the channel and the difference between scanned surfaces using a handheld 3D scanner. Fig. 2.8 shows only the procedures of the second and third methods, because the first is a simpler procedure that considers only the difference between post-test and pre-test sample weighing by means of a weighing device.

The first method of determining the total mass of eroded sediments is performed by finding the difference between the initial and final masses of the soil, obtained by Equation 1:

$$m_t = \frac{m_i}{(1 + w_i)} - \frac{m_f}{(1 + w_f)} \tag{1}$$

where m_t is the total mass of sediments in grams, m_i is the initial soil mass in grams, w_i is the initial moisture content, m_f is the final soil mass in grams, and w_f is the final moisture content.

The second method begins with the collection of sediments using an industrial vacuum cleaner in six different sectors along the wave flume (1, 2, 3, 4, 5, and 6). Sector 1 is furthest from the sample and is between 10 and 4 m, Sector 2 is from 4 to 3 m, Sector 3 from 3 to 2 m, Sector 4 from 2 to 1 m, Sector 5 from 1 to 0.5 m, and Sector 6 from 0.5 m to the center of the sample (Fig. 2.6). This collected mud-like sediment is poured onto 2.00-mm and 75-µm sieves and retained in a bucket, as presented in Figures 2.8a and 2.8b. A small part of the suspended sediments (particle size smaller than 2.00 mm) was collected in the bucket

(150 mL) and dried in beakers on a hot plate, and soil particles that were retained by the sieves (particle size larger than 2.00 mm) were weighed and dried in an oven at a temperature of 105 to 110°C for 24 hours (Fig. 2.8c). The particle size distribution of all the collected sediments was found by the LDPA device. The total mass of sediments was determined by the sum of the sediments collected in the channel, expressed by Equation 2:

$$m_t = \sum_{A}^{F} \left(m_{>2mm} + m_{>75\mu m} + m_{<75\mu m} \right) \tag{2}$$

where m_t is the total mass of sediments in grams, $m > 2$ mm is the dry mass of sediment retained in the 2-mm sieve, $m > 75$ µm is the dry mass of sediment retained in the 75-µm sieve, and $m < 75$ µm is the calculated mass of sediments smaller than 75 µm, all measured in grams.

The third method, using the 3D laser scanner (Fig. 2.8d), allows the determination of the total mass of sediments based on the cubage of the volumes between scans before and after the test multiplied by the specific gravity of the soil, expressed by Equation 3:

$$m_t = \left| \sum_{z_{1a}}^{z_2} V_i - \sum_{z_{1a}}^{z_2} V_f \right| \rho_d \tag{3}$$

where m_t is the total mass of sediments in grams, z is the z-axis of the cartesian coordinate system, z_{1a} is the minimum z-value, z_2 is the maximum z-value, V_i is the total volume given by the initial surface in cm³, V_f is the total volume given by the final surface in cm³ and ρ_d is the dry density of the soil sample in g/cm³.

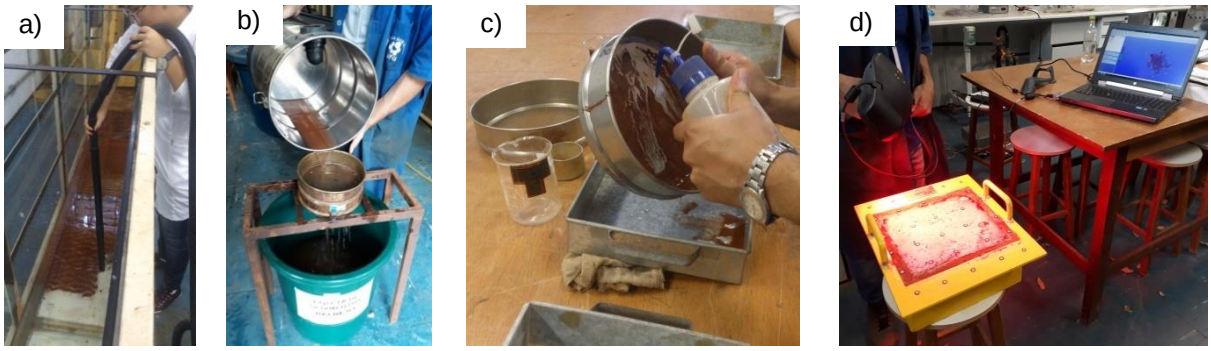

Figure 2.8 – The sieving method includes: (a) sediment collection in the flume; (b) sieving by sector; (c) selection of suspended sediments in beakers and mud soil in metallic trays for drying; (d) scanning method.

Laser scanners can record small-scale soil losses with high precision (Wu et al., 2017). This work was performed using a mesh resolution of 0.5 mm to obtain a minimum data value that gives an accurate image of the soil sample and for a better computational processing time. Fig. 2.9 shows the results of 3D scanning techniques of soil treated with lime in the sample holder before and after the wave flume test. Fig. 2.9b presents a large erosion (soil loss of 78.24%) of the soil generated by the loss of calcium carbonate crust during the erodibility experiment.

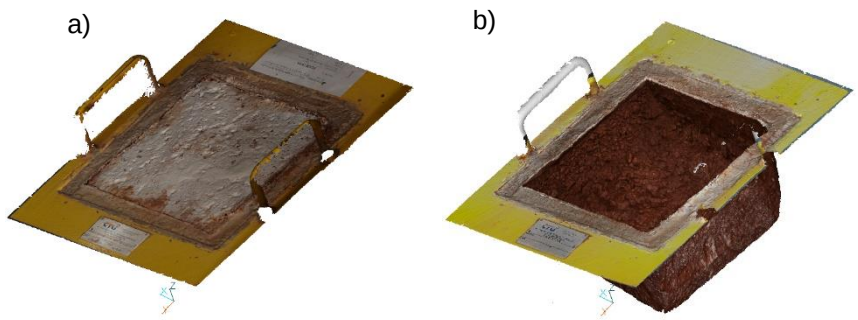

Figure 2.9 – Scan images showing 3D model data combined with photographs of soil sample treated with lime: (a) before the test and (b) after the test.

2.3 EFFECTS OF LIME INFLUENCE ON WATER PH

The objective of this work was to analyse the pH variation and to evaluate whether the soil–lime treatment could negatively influence its application in the reservoir shore, because lime applied to the soil could be washed up by fluctuation of the water level of the reservoir and could cause an increase in alkalinity of the water, even at low levels of lime application to the soil.

The effects of lime on water were analysed with a pH meter at three locations along the wave channel before and after the test. The sector near the sample was evaluated at 1 m, near the middle of the channel, at 4.5 m, and further away at 7.5 m. After obtaining the results of the measurements, the values were compared with the limits of water quality for human consumption defined by the Brazilian laws.

3 RESULTS

The results of the chemical and microstructural analysis show the investigations and mapping in order to identify the long-term pozzolanic reactions, which are important for improving the mechanical properties of the soil. Then, the results of the erodibility tests show the influences of the curing conditions, curing time, and lime content. In addition, from the tests in the wave flume, the sediment distribution pattern was observed and its similarities with the field are discussed. Finally, the results of measuring the pH of the water during the test and other environmental issues are presented with the purpose of evaluating the influence of lime on the soil–water system.

3.1 CHEMICAL AND MICROSTRUCTURAL SOIL-LIME STABILIZATION MAPPING

Microstructural mapping was performed on all samples treated with lime contents of 1, 2, and 4% lime and for time curing of 1, 7, 28 and 56 days. Therefore, twelve samples were analyzed using EDS to evaluate the presence of calcium and the extent of the treatment. In addition, SEM was used to confirm micromorphological features and soil chemical identification after the addition of lime.

The soil profile was mapped with SEM from the top of the soil to approximately 8 mm depth. The top of the soil is characterized by a calcium carbonate crust formed by the carbonatation of lime by mineral precipitation over the soil surface during application of a lime solution. The images obtained by SEM were evaluated using EDS and the bands with calcium concentrations were later analysed in greater detail in order to identify the typical characteristics of new pozzolanic formations and the characteristics of the contacts between soil particles.

Figure 2.10 shows a comparison of EDS images of treated samples with 1, 2, and 4% lime at 7 and 56 days of curing in the first 1.5 mm depth obtained by SEM inspection. The colours of each chemical element are illustrated in each micrograph image and the blue colour represents calcium. In this figure, it is observed that the higher the lime content added to the soil, the greater the thickness of the protective layer.

The treatment range does not exceed 0.5 mm for lime content up to 2%, and for the 4% content, that can settle for approximately 1 mm, suggesting that the effect of stabilization with

lime occurs only in the superficial part of the soil by quick carbonatation of lime in a Ca-rich crust. The depth of treatment range observed in the 12 samples tested did not exceed 1.5 mm.

Figure 2.11 presents SEM images of typical calcium carbonate morphologies that occurred at various curing times. The magnified SEM image in Fig. 2.11a shows the calcite mineral in a rhombohedral crystal form (1.25 µm) present in 1% lime at 7 days of curing, which indicates the occurrence of the carbonatation process of the lime, with precipitation of calcium carbonate, even from low lime contents.

Figure 2.11b shows several flower-shaped crystals as hexagonal platelets of calcium carbonate polymorph, identified in soil treated with 2% lime at 7 days of curing. SEM micrographs in Fig. 2.11c revealed a disturbing irregular aggregated matrix near the top of the soil (1 mm deep) treated with 4% lime at 56 days.

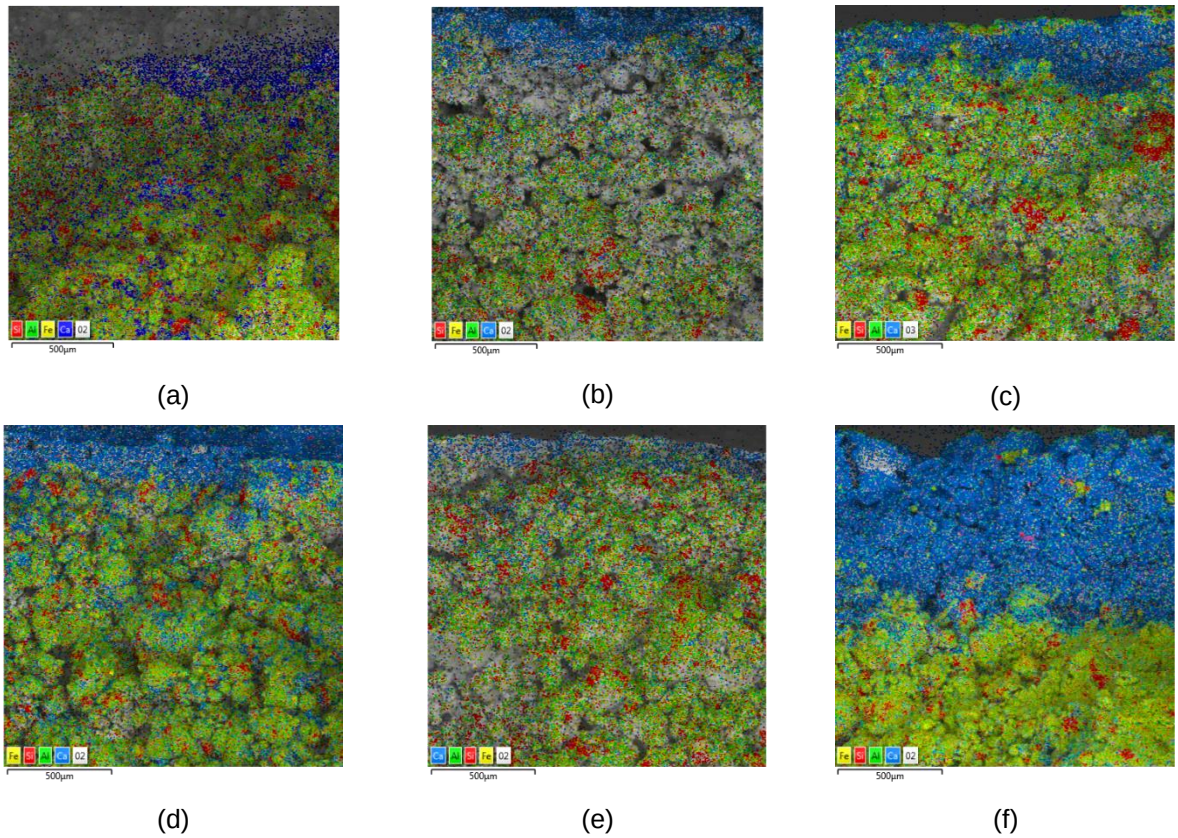

Figure 2.10 – SEM micrographs with EDS analysis of treated soil–lime: (a) soil + 1% lime, 7 days; (b) soil + 2% lime, 7 days; (c) soil + 4% lime, 7 days; (d) soil + 1% lime, 56 days; (e) soil + 2% lime, 56 days; (f) soil + 4% lime, 56 days. Meaning of colours: green = aluminium; blue = calcium; red = silicon; yellow = iron; white = no data.

This calcium carbonate crust produced by carbonatation of lime fills and coats large and small voids, causing the formation of whitish cementation compounds binding soil particles. Furthermore, this indicates a possible increase in strength with a reduction in the coefficient of permeability also observed in other researches (Jha and Sivapullaiah, 2016; Nascimento et al., 2019). The micromorphological features of pozzolanic reactions generate CSH, CAH, and CASH (C = Ca, S = SiO_2, A = Al_2O_3, and H = H_2O), which are already known for their cementitious improvement. Therefore, these new minerals have not been seen in any of the samples analysed by SEM. This indicates that the shallow stabilization of the lateritic soil is caused by a thin calcium carbonate crust, which is the only barrier against erosive forces. Without this layer, the soil does not have cementation compounds to improve the mechanical geotechnical properties of the soil.

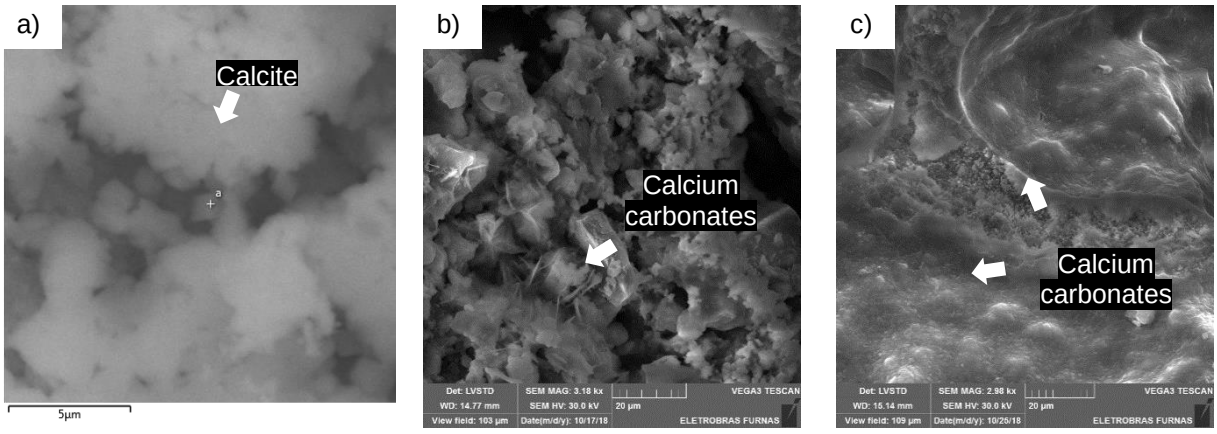

Figure 2.11 – SEM micrographs of calcium carbonate morphologies: (a) typical calcite crystal form identified in soil + 1% lime, 7 days; (b) soil + 2% lime, 7 days; (c) aspect of carbonatation of lime in a disturbed matrix in soil + 4% lime, 56 days.

The XRD analysis confirms the microstructural mapping with SEM/EDS showing that none of the treated soil evaluated presents CSH or CAH. However, for all treated soil, spreading hydrated lime produced a calcite-rich crust at the top of the soil by the carbonatation process.

Carbonatation generates insoluble calcium carbonate (i.e, calcite) from the reaction of hydrated lime [$Ca(OH)_2$] with carbon dioxide (CO_2) from the atmosphere. When the lime in slurry form is spread over the soil during the treatment, carbonatation occurs almost immediately. Soil with lime addition presents calcium carbonates, such as calcite, vaterite, and aragonite in X-ray diffraction analyzes.

Figures 2.12 to 2.14 show the XRD diagrams stacking the diffractograms for all treatment conditions except for 1% lime without agitation. The diagrams are quite similar to each other and the peaks of the untreated diffractogram also resemble the treated soils.

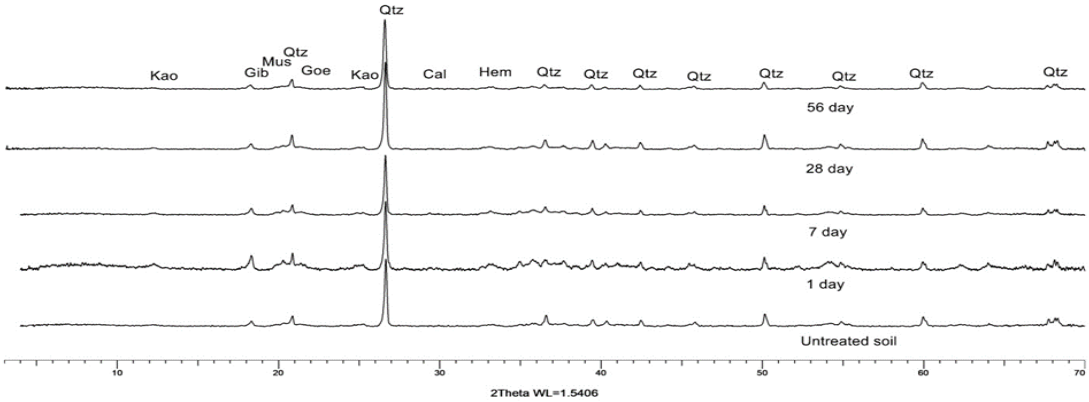

Figure 2.12 – XRD diagrams of 1% lime at 1, 7, 28, and 56 days of curing. Cal = calcite; Gib = gibbsite; Goe = goethite; Hem = hematite; Kao = kaolinite; Mus = muscovite; Qtz = quartz.

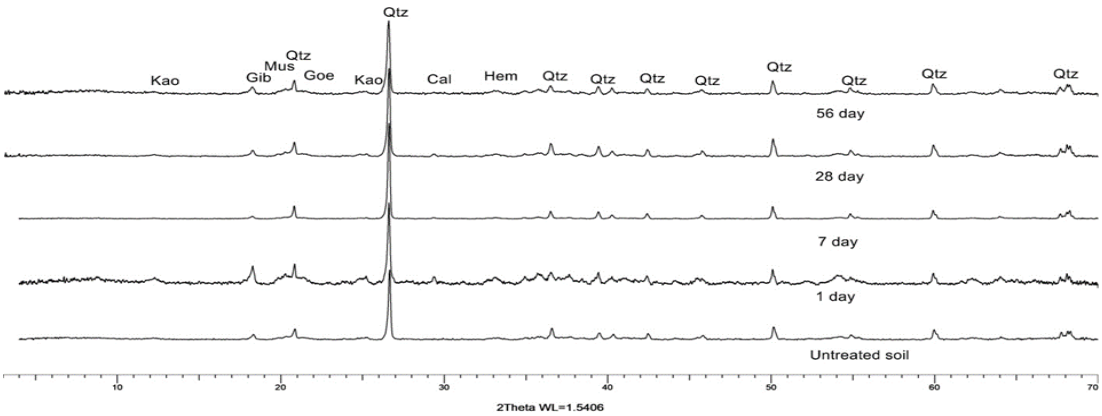

Figure 2.13 – XRD diagrams of 2% lime at 1, 7, 28, and 56 days of curing. Cal = calcite; Gib = gibbsite; Goe = goethite; Hem = hematite; Kao = kaolinite; Mus = muscovite; Qtz = quartz.

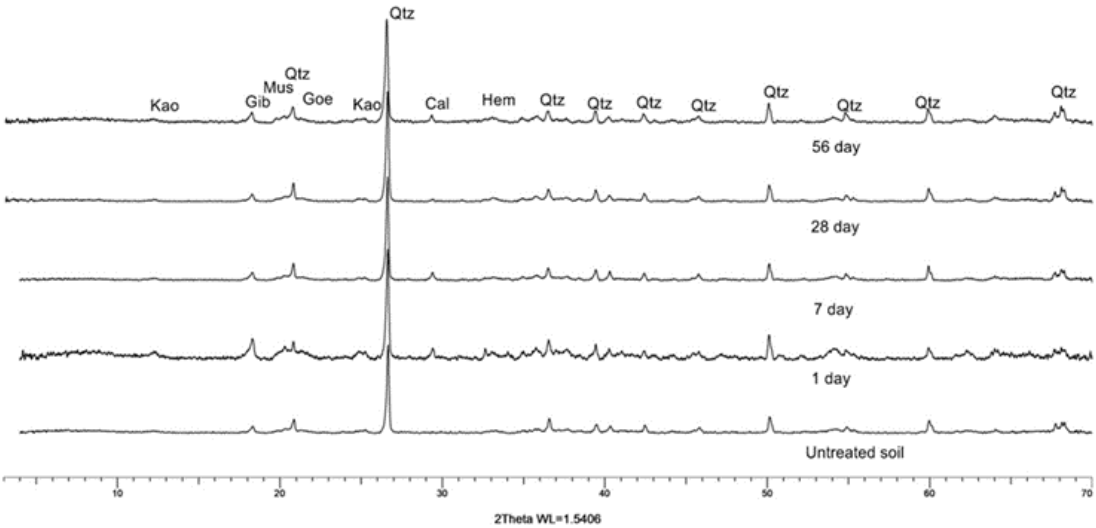

Figure 2.14 – XRD diagrams of 4% lime at 1, 7, 28, and 56 days of curing. Cal = calcite; Gib = gibbsite; Goe = goethite; Hem = hematite; Kao = kaolinite; Mus = muscovite; Qtz = quartz.

Pozzolanic reactions can be achieved depend on various factors (Diamond and Kinter, 1964) and the addition of lime to the soil leads to partial Ca^{+2} absorptions on the surfaces of clay particles that reaction between released soluble silica and alumina and the calcium ions creates cementitious materials that enhance mechanical geotechnical properties of the untreated soil (TRB, 1987).

However, the free calcium remaining after the carbonatation may not available to produce this pozzolanic reaction. Many works have observed this reaction with smaller additions of lime, that is, below 4% lime content by dry weight of soil (Bell, 1996; Jha and Sivapullaiah, 2015).

The soil stabilization researches on soil–lime treatment consider their dry or wet mixtures according to the total dry weight of soil, and in this work the lime content by volume of sample or weight percent was considered. The hydrated lime powder (weight of solute) was diluted in distilled water (weight solution) to achieve the weight percent, which is a hundred or even a thousand times lower than the lime content of the mixtures with reference to the total dry weight of soil.

Also, the lack of formation of new cementitious material can be explained by a change in pH. At high pH values (12.4), silicates and aluminates in the clay dissolve, allowing a pozzolanic reaction with the calcium (TRB, 1987; Glendinning, 1995).

In this context, pH measurements were taken from readings with a portable pH meter in a mixture of standard solution, provided by the manufacturer, and a fraction of the soil from the top of the sample.

From each sample to be treated, a small soil block was collected and the same treatment configuration was carried out. Table 2.3 shows the results for all lime contents and curing times. A long-term behaviour trend is not observed, but with a curing time of 1 day, the alkalinity increases with the increase of lime content.

Table 2.3 – Results of the pH of treated soils.

Days	1% lime	2% lime	4% lime
1	7.79	9.76	12.15
7	7.96	8.10	7.95
28	8.03	8.07	8.05
56	7.44	8.08	8.18

The results listed in Table 2.3 show low pH values, which trigger the dissolution of clay minerals (TRB, 1987; Glendinning, 1995).

However, Jha and Sivapullaiah (2015) founded pozzolanic reactions with pH above 9.76. To achieve soil stabilization by means of lime treatment, the optimum lime content (OLC) must be reached, which is dependent on various factors (Cherian and Arnepalli, 2015).

Long-term reactions could not have occurred, according to Bell (1996); the maximum modification of soil properties proceeds at an OLC of 1–3% by weight of soil, which is far above the quantities of lime applied by weight percent in this work.

In this case, the phenomenon of lime fixation may be close to the lime fixation point (Lm) or the initial consumption of lime (ICL) due to free calcium being held by the clay and thus being unavailable for further reaction (Hilt and Davidson, 1960; Cherian and Arnepalli, 2015), as well unable to increase the strength of the soil (Bell, 1996; Diamond and Kinter, 1964), and even the affinity of the soil for lime was not satisfied.

Also, the advanced degree of weathering (Attoh-Okine, 1995) may affect the amount of calcium available due to the high contents of iron and aluminium oxide-hydroxide (Galvão et al., 2004).

3.2 ERODIBILITY TEST RESULTS

In general, the erodibility tests were carried out in the wave flume and demonstrated that the carbonate crust generated by carbonation resists the effect of the impact of waves during six hours with a strong dependence on the conditions of curing, curing time, and lime content.

Table 2.4 presents the result of the soil loss of the samples treated with lime considering the three methods of evaluation of the mass of eroded soil.

The soil loss was obtained in gram units and was converted to the percentage mass loss by the division of the total dry mass by the initial dry mass and the mass loss ratio was obtained by the division of the total dry mass in kilograms per square meter area (0.25 × 0.25 m).

An attempt was made to compare the results of the soil mass loss per kilogram per square meter between these methods (Fig. 2.15) and a value of R^2 (coefficient of determination) of about 95% was achieved, showing a good correlation between them, and the weighing and sieving methods presented the best approaches.

Table 2.4 – Soil mass loss results from wave flume test.

Test condition	Weighing Method		Sieving Method	Scanning Method
	(kg/m²)	(%)	(kg/m²)	(kg/m²)
Untreated soil	23.68	15.47	22.41	19.32
Sol.1%1d[c]	25.07	14.50	27.97	2.63
1%1d	18.71	11.20	28.13	0.37
1%7d	16.78	10.35	18.09	2.43
1%28d	115.92	78.24	143.60	101.81
1%56d	109.18[a]/14.30[b]	70.66[a]/8.85[b]	120.54[a]/29.12[b]	93.13[a]/12.72[b]
2%1d	24.88	14.87	18.74	4.68
2%7d	11.78	8.08	15.17	0.61
2%28d	110.31	79.46	114.85	82.44
2%56d	68.61[a]/2.37[b]	55.20[a]/1.60[b]	95.18[a]/13.17[b]	72.73[a]/0.01[b]
4%1d	19.37	11.75	16.19	0.69
4%7d	4.09	2.71	0.00	0.06
4%28d	26.09	16.23	37.97	20.44
4%56d	84.52[a]/1.85[b]	64.04[a]/1.23[b]	110.87[a]/0.00[b]	83.35[a]/0.04[b]

NOTE: [a] Air-dry; [b] Moisture room storage; [c] Suspended lime

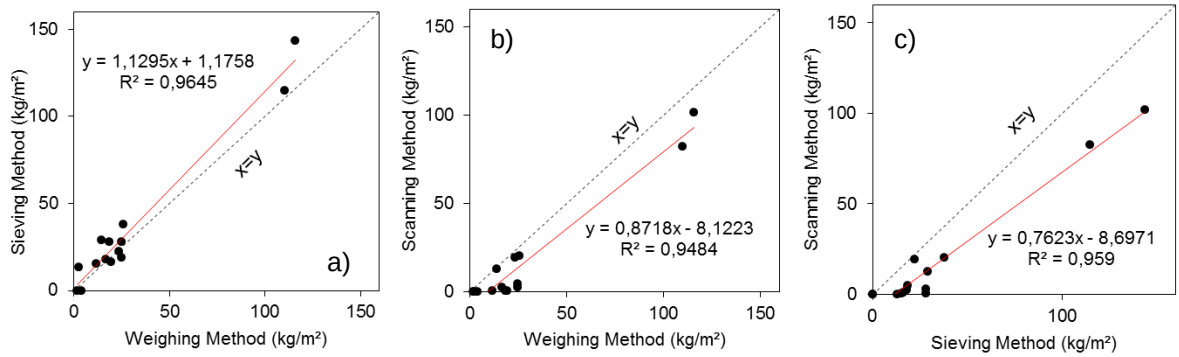

Figure 2.15 – Soil mass loss results in the following comparison: (a) sieving versus weighing, (b) scanning versus weighing and scanning versus sieving.

The scanning method takes into account only the volumetric variation obtained between the 3D meshes if there are losses below the carbonate crust that cannot be registered with the handheld scanner. The values will be smaller than the real one for negative slopes, for example. The method of weighing can be influenced by the variation of the specific weight of the soil, microstructures, and humidity. The sieving method is the closest to weighing but is strongly influenced by unwanted sediments from previous tests.

When the soil loss indicates low erosion, with values below 5 kg/m², the scanning technique tends to approximate what occurs in the visual aspect of the sample. Therefore, the scanning and weighing values are closer when the loss is above 70 kg/m² (high erosion). Medium

erosion, with results between 5 and 70 kg/m², shows a great variance within each methodology. This occurs because the dry density of the soil considered in Equation 3 was obtained from a small fraction of the undisturbed soil block and the whole sample is represented by microtubules and macropores, which could generate small density variations (Schliewe, 2018).

Also, the use of a 3D scanner creates a digital morphology of soil erosion, which is a technological advantage in comparison with other methods because it expands the possibilities of the analyses, such as the evaluation of the dynamics of the erosion process through microtopographic changes.

A one-way ANOVA model ($\alpha = 0.05$) was used to determine the interaction between the results of the three methods of evaluation of the soil loss, and no significant difference in the amount of soil erosion according to the value of $p = 0.47$ ($p > 0.05$). However, the values have a high dispersion between methods according to the coefficient of variation among groups of 119%, due to the different characteristics of the methods and the use of the specific gravity of the soil, which has great dispersion in the case of natural soil. It is assumed that the values observed in Table 2.4 are, in general, within the ranges verified by Schliewe (2018).

The natural (untreated) soil sample shows values close to that obtained by Menezes (2017), which was 22.75 kg/m², and superior to that obtained by Schliewe (2018), which was 14.76 kg/m², using the same test settings for wave frequency (0.5 Hz) and angle of slope (45°).

Based on the results obtained from the three methods of soil loss calculation along with the simplicity of the test, the weighing method was selected for the following analyses of the influence of curing conditions, curing time, and lime content.

3.2.1 Effects of curing conditions

The curing condition of air-drying storage showed a large soil mass loss (over 40%) during the erodibility test compared to curing in a moist room (below 10%) due to the excessive reduction of the water content of the sample. Figure 2.16 shows the results of comparison of samples cured for 56 days with lime contents of 1, 2, and 4% by weight percent.

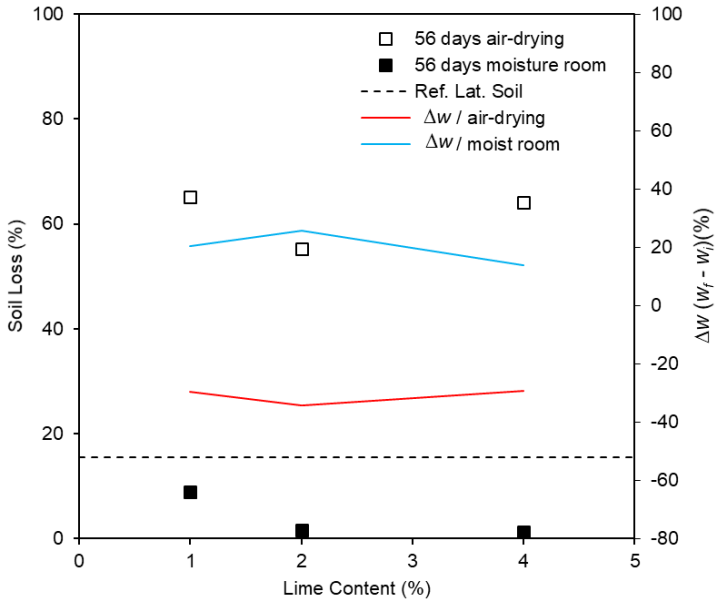

Figure 2.16 – Comparison of different curing storage conditions.

The water content of the soil is a parameter of extreme importance for its stability (Luiz et al., 2017). In addition, sandy soils with gravels are the most affected by the presence of low water content in the interstices of the particles. Dry soils present low cohesion because they have weak bonding between particles and higher soil suction, producing fragile internal structures, and therefore they can be easily destabilized by erosive agents (Nascimento et al., 2019).

Air-drying storage led to a reduction of water content because the treated sample surface was exposed to air, and even the samples stored in the laboratory with air-conditioning showed faster evaporation of water and mass loss before the test (red line in Fig. 2.16). In addition, samples which were stored in the moist room showed a positive variation or an increase of water content due to hydration of the soil in the moist room with a relative humidity (RH) of more than 90% and temperature of 24 ± 3°C (blue line in Fig. 2.16). In summary, an increase in the variation of water content (Δw = water content after applying lime minus water content before the wave flume test) lowers the soil loss and vice versa.

The behaviour of the soil in the field should be in an intermediate condition between wetting and drying cycles because the temperature and moisture below ground on the shores of the reservoir have a great influence by water table.

The air-dried samples presented high shrinkage, observed by the detachment between the soil and the paraffin used during the sampling. Besides the soil structure is more susceptible to the loss of mass by the action of the wave during the test, and the shrinkage of the soil

(Fig. 2.17) due to the reduction of the moisture content also created a gap that allowed greater damage to the sample through the entrance of water.

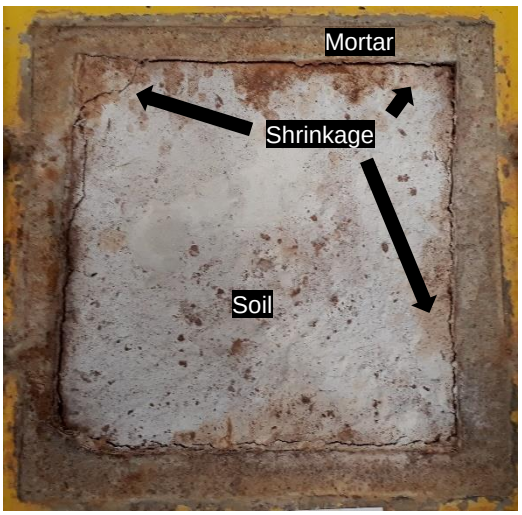

Figure 2.17 – Soil shrinkage of 1% lime after 28 days.

Also, the erodibility rates rose due to the effects of soil suction in soils with low water content, but the effects could be different in lateritic soils due to bimodal pore distribution (Almeida et al., 2015). It was verified that an increase in the soil suction increases the soil loss and reduces the influence of the lime treatment. It can be clearly seen that the curing condition strongly influenced the results of the erodibility tests, while the air-dried samples presented overall losses during a longer period of curing than those stored in the moist room.

The curing conditions of the soil (i.e., temperature and moisture) play an important role in the increase of soil strength (Nascimento et al., 2019; TRB, 1987; Cherian and Arnepalli, 2015). The results of this work show similarity to the effect of curing in concrete, where moist curing promotes a strength gain in concrete compared to air drying (Raheem et al., 2013) and a reduction in the moist-curing period results in lower strengths (Ramezanianpour and Malhotra, 1995).

3.2.2 Effects of curing time

The effect of curing time on soil–lime stabilization shows an increase of mechanical properties (mostly compressive strength) of the soil using dry soil–lime mixtures, higher quantities of lime, and dry curing, due to the formation of new cementitious compounds (Bell, 1996; Diamond and Kinter, 1964; Jha and Sivapullaiah, 2016; Attoh-Okine, 1995; Latifi et al., 2017; Wang et al., 2017).

Unlike other works on soil–lime treatment, it was verified that in this case the lime stabilization occurred only at the surface of the sample and no occurrence of new cementitious compounds was verified, and this was confirmed by XRD analysis and SEM.

In this work, Fig. 2.18 reveals a decrease in mass loss for samples stored in a moist room at a curing time of 56 days, and the behaviour of specimens in the air-drying condition was different, the mass loss has proved to be higher. Nascimento et al. (2019) also verified a slight decrease in soil loss of samples with the same preparations and curing times as this research.

Natural lateritic soil was tested as well as the other treatments and is shown in Fig. 2.18 as a soil loss baseline (dashed black line). Soil–lime treated samples showed the highest soil losses during the erodibility tests due to the loss of water content in the air-drying curing and lower soil loss due to hydration of the samples in moist curing.

Therefore, the reduction of the water content causes a more significant volume shrinkage of the soil after 7 days of curing. However, at 28 days, 4% lime treatment showed a lower soil loss of 16%, despite the results for 1 and 2% lime solutions. This can be explained by the formation of more calcium crust by carbonatation and lower soil shrinkage, compared to other samples at 28 days of curing time.

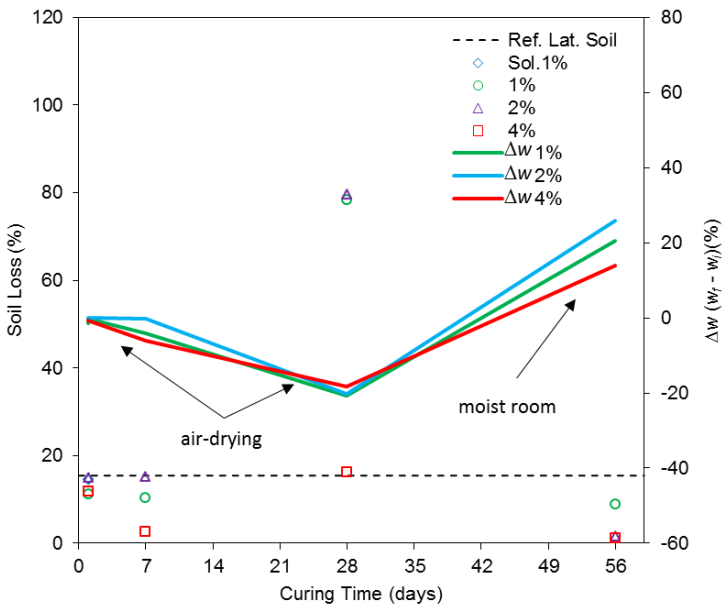

Figure 2.18 – Percentage soil mass loss based on curing time. Lateritic soil reference (Ref. Lat. Soil) = untreated soil; Δw = water content variation; Sol.1% = 1% of lime saturated solution.

In addition, this result also validated Bell's statement that the OLC of kaolinitic soils does not vary significantly with the curing period (Bell, 1996). Indeed, the increase of water evaporation creates a greater reduction of its volume by shrinkage than the soil suction itself.

3.2.3 Effects of lime content

The lime content wields a great influence on the reduction of soil mass loss as observed in Fig. 2.19. All values for 4% lime samples, except for the 56-day air-dried sample, showed soil loss below the untreated soil reference line (dashed black line).

Nascimento et al. (2019) obtained significant reductions with only 1% lime by weight percent when simulating runoff erosion. A reduction of about 72% was obtained in relation to the natural sample and in the saturated condition.

Lime solution concentrations of 2 and 4% presented soil mass losses of less than 2.5% or no losses. Another finding of these authors (Nascimento et al., 2019) was that the addition of lime favoured a greater reduction of soil mass loss in saturated samples than in unsaturated samples.

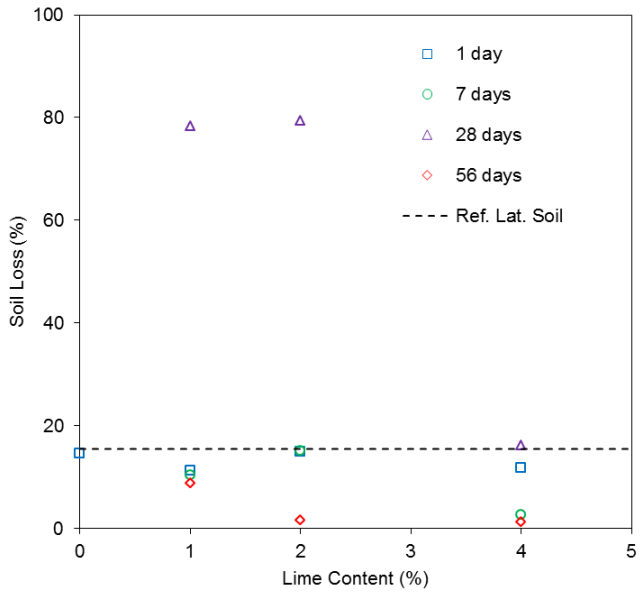

Figure 2.19 – Percentage soil mass loss based on lime content. Lateritic soil reference (Ref. Lat. Soil) = untreated soil.

As the lime content increases, the crust of calcium carbonate generated by carbonatation rises as well. The major reduction of soil loss verified in Fig. 2.19 is due to the thickness of slaked lime spread over the soil, as shown in the SEM micrographs in Fig. 2.11.

This crust gives protection to the soil surface, allowing resistance to the impact of waves and variation of the water level during the period of the test. When keeping the soil in a wet condition, an increase in the lime content can reduce the erosiveness of wave action. Furthermore, the dry soils are more vulnerable to volumetric changes and enable a breach in this protective lime layer. Once the crust is cracked, soil loss is facilitated by the flow of water and rapid saturation in porous media with low water content, allowing sediment detachment.

3.2.4 Sediment distribution patterns

Laser diffraction granulometry was used to obtain the grain-size distribution and to analyse the deposition pattern of the sedimentation. The results are shown in Fig. 2.20 and represent average values from 17 tests performed in the wave flume.

Sediments collected in the sieving method stage are mostly particles with a uniform pattern, except those observed in Sectors 5 and 6 of the fine sediments, close to the sample. In addition, the results obtained after performing the ultrasonic dispersion are not shown but it was observed that this agitation of the water led to an increase of fine particles.

Figure 2.20a shows the finer grain size (< 0.075 mm) of suspended sediments collected from the bucket by the sieving method and Fig. 2.20b shows the coarse sediments (> 0.075 mm) retained on the 200-mesh sieve. The wave flume was divided into six sectors, of which Sector 1 is the zone far from the sample holder (> 4 m) and Sector 6 (< 0.5 m) is the zone near to it. With the exception of coarse particles collected in Sector 1, the results show a decreasing particle size of sediments with increasing distance from the soil sample.

The percentage sediment deposition was calculated for all the tests (Fig. 2.21) and it was verified that the major quantity of coarse sediments lay in Sector 6 (> 0.5 m) and most of the fine sediments lay in Sector 4 (1–2 m). The grain-size distribution and sediment deposition percentage from the wave flume tests showed a classical lake deposition pattern (Lawson, 1985) of coarser grained particle deposition near to the shore and fine sediments in deep waters. The spatial distribution of reservoir sedimentation is an important issue for water management (Juracek, 2015) and aquatic life (Olson and Ventura, 2012).

The average percentage by dry weight of soil sediment deposition in the flume demonstrates that fewer coarse sediments (12%) than fine ones (88%) were deposited when the soil loss was lower than 10%. Similar results were observed when the soil loss was between 11 and 60%, with less fine sediments (25%) than coarse sediments (75%) being eroded. On the

other hand, at soil losses higher than 61%, more coarse sediments (60%) than fine ones (40%) were observed.

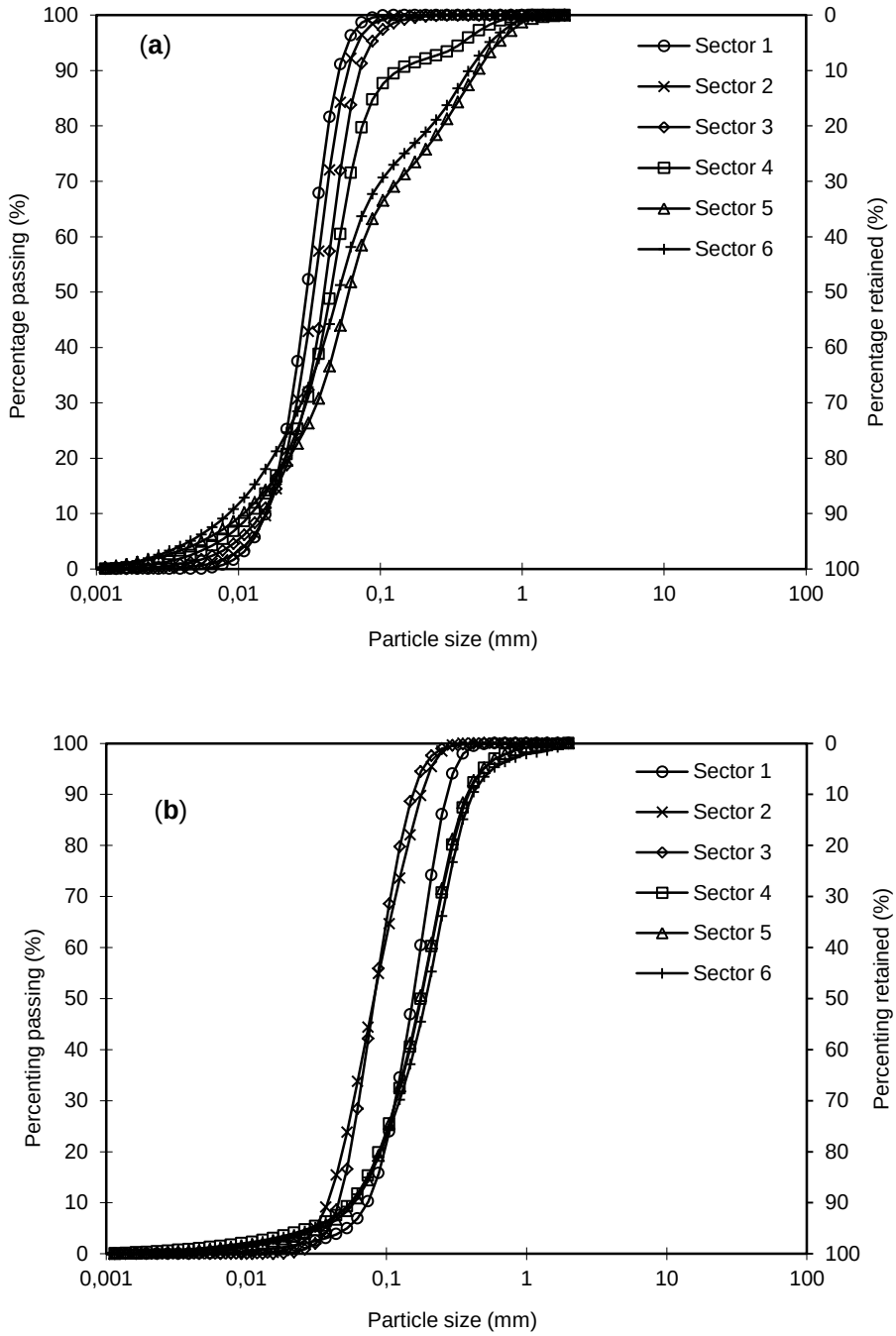

Figure 2.20 – Sieve analysis achieved by laser diffraction device in six sectors: (a) suspended sediments (fine); (b) sediments retained on 75-µm sieve (coarse). Sector 1 = far from soil; Sector 6 = near the soil.

However, sediment distribution in lakes may not apply to reservoirs due to the different river hydrodynamics, sediment types and sources, morphometric variables (Abraham et al., 1999),

water temperature, and operation system of the dam (Lawson, 1985). Indeed, the amount of deposited material at a certain locality in a lake and reservoir depends on the hydrological conditions, grain size distribution, and other factors (Sundborg, 1992).

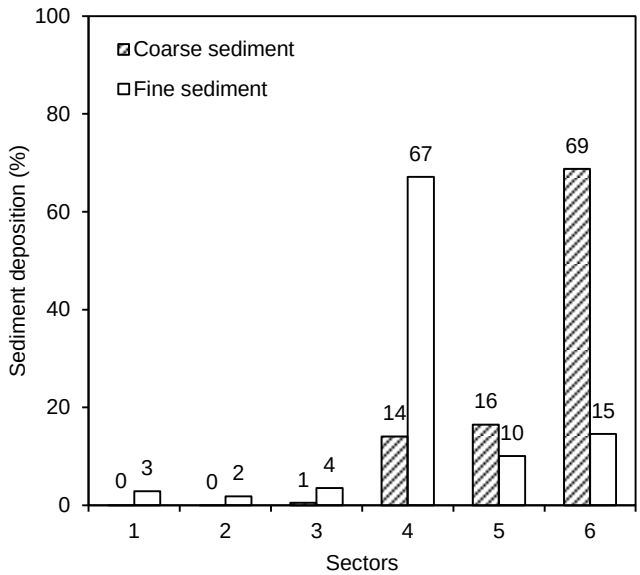

Figure 2.21 – Total sediment distribution of fine (< 0.075 mm) and coarse (> 0.075 mm) sediments.

Typically, at the reservoir shoreline, the gravel-size sediment is deposited at the beginning of the eroding bank produced by water level fluctuations, runoffs, and wave impacts, and the detached finer-grained sediment is transported by currents and wind waves to be deposited in the basinward direction (Lawson, 1985).

3.2.5 Influence of soil-lime treatment on water pH

Because lime is a chemical stabilizer, this work sought to evaluate its influence on soil and water. In the case of the pH of the water, an increase can bring environmental problems such as the demographic explosion of foreign species (fauna or flora) in the reservoir (Claudi et al., 2012), due to increases of the nutrient content, and and water quality values that do not meet the standards for human consumption (Ministry of Health, 2011).

As shown in Table 2.3, increases in the lime content with 1 and 56 days of curing time led to an increase in soil pH, which clearly reached 12.15 in the short term. There are several optimum levels of pH for the development of certain crops. An increase in the pH of the soil can provide an environment for the development of soil microorganisms that are best adapted in pH ranges close to neutrality (7.0). This occurs in the porous media of the soil due to the decomposition of organic matter by organisms that excrete cementing substances that

favour soil stability. However, a higher soil alkalinity (above 8.5) could affect the soil structure, plant growth, nutrient availability, and soil bacteria. In addition, pH levels of 6.0 to 8.5 favour correction of the soil acidity.

Figure 2.22 presents the results obtained by the direct measurement of water before and after the test in three sectors. The pH of the water supply system is 7.87. The mean values obtained before and after the test are below the natural pH value of the water, but in general, the pH values are higher after the test. In addition, the values of water pH nearest of the treated soil (<2.00 m) are higher than the values collected far away of the sample in the wave flume (>4.00 m).

According to policy and regulations under Brazilian law (Ministry of the Environment, 2005), the National Council of Environment (CONAMA, in Portuguese), which provides for the groundwater classification and environmental guidelines, it is established that fresh water for human consumption from groundwater, lakes, and rivers must have a pH value between 6.0 and 9.0. Also, the Ministry of Health recommends monitoring by sanitation companies and controls the pH of fresh water for human consumption in the range of 6.0 to 9.5 (Ministry of Health, 2011).

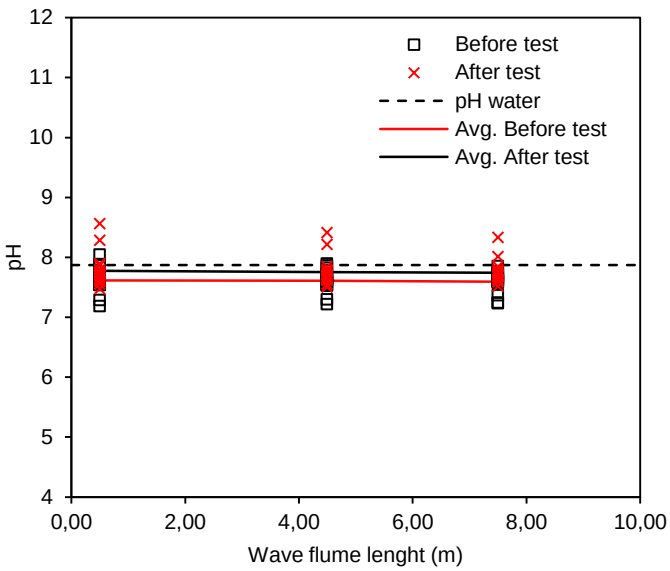

Figure 2.22 – Results of pH measurements.

Another test was conducted to verify the influence of lime on increasing the pH of the water and it was found that upon the addition of 0.003 g (1% lime) of hydrated lime in 100 mL of water, the pH increased by 3%. With 0.013 g (4% lime) of hydrated lime in the same amount of water, the pH rose by 12%.

This work was concerned with the soil–lime technique could bring more damage to the reservoir shoreline by environmental issues. However, it seems that there will be no problems with dust, since the lime is applied in liquid form directly on the ground (without vegetation), the white visual aspect can be circumvented by the use of brown color limewash pigments, the soil become less acid, and the water pH rises within the required values by the water quality control regulations.

4 DISCUSSION

The present work presents positive results for the use of hydrated lime in slurry form as a limewash for the protection of reservoir banks considering specific local conditions, but this technique does not guarantee the stabilization of the soil. It should be noted that this chemical treatment produces a calcium carbonate crust on the ground surface by carbonation of lime and the range of influence does not exceed a depth of 2 mm, as observed by SEM analysis.

According to Santos (2011), the limewash technique provides temporary protection to the soil, with reapplication being necessary, and can be used in large areas through manual or motorized application. It is a low-cost soil treatment and there is a high availability of hydrated lime. In the field, Santos used a 3:1 ratio (water:lime) by weight. A maximum pumpable content of 40% lime solution in slurry in the field was established by Bell (1988) to prevent clogging of the pump.

Moreover, the lime pile stabilization technique generates an increase in soil strength around the piles in a narrow range of 50 mm thickness due to the short distance of migration of calcium and hydroxyl ions (Rogers et al., 2000). However, it is possible that the process of carbonation of lime at the time of application of lime slurry on the soil is the main cause of the significant reduction of the range of treatment due to the availability of calcium for reaction with solubilized aluminium and silica. The curing time had no influence on the soil stabilization reactions. However, the lime content influenced the increase of the calcium carbonate crust, allowing greater protection of the soil.

In the field, soil moisture could influence the efficiency of this technique because when subjecting the soil samples to air drying for a long period of time, potential weakening of the soil structure was observed, which allowed mass loss. In periods of drought, the protective layer of lime can contract, leading to cracks that allow water infiltration and surface runoff at

shore banks, increasing the soil erodibility. Also, there should be frequent respraying of lime slurry over the soil over time, especially in dry seasons (Santos, 2011). On the other hand, the water table is shallow at reservoir shores and the temperature and moisture of the soil could be maintained during dry periods. The use of lime for soil–lime stabilization at the shoreline will not affect the chemistry of fresh water for human consumption and will probably have little influence on the reservoir's biological life, considering the values stipulated by Brazilian policy.

In future works, the soil suction process should be evaluated and field experimental programmes must be realized. Negative pore water pressures may influence the condition of the soil stability against erosive agents, including runoff and wind-generated waves. It is also necessary to find the OLC for field application because lime slurry causes clogging of the pressure pump making it difficult to pump and spray the lime (about 32% content) with an immobile slurry system. The use of lime allowed the reduction of soil loss under the effect of waves under specific conditions, and this result supports other studies of soil erosion control (Santos, 2011; Nasiri et al., 2017).

5 CONCLUSIONS

The immediate process of carbonation of the lime is the major result of spreading lime in slurry form over the soil with the aim of soil stabilization. A thin layer of calcium carbonate was produced on the surface of the sample, which prevented the formation of pozzolanic reactions and reduced the scope of treatment. Thus, the stabilization of the soil is restricted only by the efficiency and durability of this white crust of calcium carbonate.

The lime content was important for the thickening of the calcium carbonate crust together with wet curing conditions, which contributed to the improvement of the resistance of the soil against the erosivity of the waves, but the curing time did not have a significant impact. Also, no formation of cementitious compounds between the edges of the clay particles was identified and therefore the classic model of chemical and physical soil stabilization (Diamond and Kinter, 1964) through the addition of lime did not occur.

Future works are necessary to analyse the influence of soil suction on the sample in wave flume tests, the effects of soil type, and mainly the field experimentations and field models. In addition, is important to define the OLC to produce long-term reactions and to carry out

chemical tests to highlight the interaction of the Ca-rich crust and soil, including solubilization analysis of the lime, silica, iron, and amount of free aluminium.

The lime treatment proposed in this work to protect reservoir shores from erosion by waves and water table variations may be feasible considering some factors:

- Soil protection should be preserved by maintaining the carbonate layer and controlling eventual cracks. It is necessary to consider frequent application of lime, according to Santos (2011);
- The soil moisture condition should be maintained;
- The access of people, vehicles, and large animals should be restricted to avoid damaging the protective crust.

The advantages of the use of hydrated lime slurry as limewash for shoreline soil stabilization are as follows:

- The formation of a protective crust occurs, reducing the soil mass loss due to the water erosion process;
- No dust forms during its application (Lawson, 1985);
- It does not affect the pH of water for human consumption;
- The low lime content already allows the formation of a protective layer.

ACKNOWLEDGEMENTS

This paper is part of a BioEngineering Project (0394-1603/2016) and is financially supported by the Furnas Centrais Elétricas S.A., a state-owned company and subsidiary of Eletrobras, and the Agência Nacional de Energia Elétrica – ANEEL (Brazilian Electricity Regulatory Agency). The authors would like to thank the Hydraulics Laboratory of Goiás Federal University for all the support given by the installations and available team. We also thank the technicians, engineering staff, and managers of the Geotechnical Laboratory of the Civil Engineering Technology Division of Furnas.

REFERENCES

Abraham, J., Allen, P., Dunbar, J., Dworkin, S.I.,1999. Sediment type distribution in reservoirs: sediment source versus morphometry. Envr. Geol. 38, 101. https://doi.org/10.1007/s002540050406.

Aguiar, V.G., 2009. Bacia Hidrográfica do Córrego Granada – Aparecida de Goiânia-GO: Os Processos Erosivos e a Dinâmica Espacial Urbana. Masters Thesis, University of Goiás, Goiânia-GO, Brazil.

Almeida, J.G.R., Romão, P.A, Mascarenha, M.M.A., SALES, M.M., 2015. Erodibilidade de solos tropicais não saturados nos municípios de Senador Canedo e Bonfinópolis. Geociências. 34 (3), 441-451.

Amadi, A.A., Okeiyi, A.,2017. Use of quick and hydrated lime in the stabilization of lateritic soil: comparative analysis of laboratory data. Geo-Engineering. 8, 3-13. https://doi.org/10.1186/s40703-017-0041-3.

Associação Brasileira de Normas Técnicas-ABNT, 2000. NBR 14545-Solo-Determinação do coeficiente de permeabilidade de solos argilosos a carga variável. ABNT: Rio de Janeiro-RJ, Brazil. 1-12.

Associação Brasileira de Geologia de Engenharia e Ambiental-ABGE, 2013. Ensaio de permeabilidade em solos: orientações para sua execução no campo. ABGE: São Paulo-SP, Brazil. 1-80.

Attoh-Okine, N.O., 1995. Lime treatment of laterite soils and gravels — revisited. Constr. and Build. Mater. 9(5), 283–287. https://doi.org/10.1016/0950-0618(95)00030-j.

Bell, F. G., 1988. Stabilization and Treatment of Clay Soil with Lime-Part 2-Some Applications, Ground Eng. 21 (2), 22-30.

Bell, F.G., 1996. Lime stabilization of clay minerals and soils. Eng. Geol. 42, 223-237. https://doi.org/10.1016/0013-7952(96)00028-2.

Cherian, C., Arnepalli, D.N., 2015. A critical appraisal of the role of clay mineralogy in lime stabilization. Int. J. of Geosynth. and Ground Eng. 1, 1-20. https://doi.org/10.1007/s40891-015-0009-3.

Claudi, R., Graves, A., Taraborelli, A. C., Prescott, R. J., Mastitsky, S.E., 2012. Impact of pH on survival and settlement of dreissenid mussels. Aquatic Invasions. 7, 21–28. https://doi.org/10.3391/ai.2012.7.1.003.

Das, B.M., 2008. Advanced Soil Mechanics, Taylor & Francis: Oxford, UK, pp. 172-173. ISBN 0-203-93584-5.

De Souza Dias, V., Pereira da Luz, M., Medero, G.M., Tarley Ferreira Nascimento, D., 2018. An Overview of Hydropower Reservoirs in Brazil: Current Situation, Future Perspectives and Impacts of Climate Change. Water. 10, 592. https://doi.org/10.3390/w10050592.

Diamond, S., Kinter, E.B., 1964. Mechanisms of Soil-Lime Stabilization: An Interpretive Review. High. Res. Rec. 92, 83-102.

Eades, J.L., Grim, R., 1960. Reaction of hydrated lime with pure clay minerals in soil stabilization. High. Res. Board. 262, 51-53.

Edil, T.B., 2013. Erosion of Coastal Slopes and Landslides. Proceedings of the 2013 Geo-Congress. San Diego, California, USA, ASCE: Reston, USA. https://doi.org/10.1061/9780784412787.133.

Fabbri, G.T.P., 1994. Caracterização da fração fina de solos tropicais através da adsorção de azul de metileno. Doctoral Thesis, Escola de Engenharia de São Carlos-USP, São Carlos-SP, Brazil.

Fernandez, O.V.Q., Fulvaro, V. J.,2000. Rates and processes of bank erosion. Itaipu Reservoir. Paraguay-Brazil border. South America. Proceedings of the 5th International Symposium on Environmental Geotechnology and Global Sustainable Development. Belo Horizonte-MG, Brazil

Galvão, T.C.B., Elsharief, A., Simões, G.F., 2004. Effects of lime on permeability and compressibility of two tropical residual soil. J. Environ. Eng. 130, 881-885. https://doi.org/10.1061/0733-9372(2004)130:8(881).

Gedney, D.S., Weber Jr, W.G., 1978. Design and construction of soil slopes. In TRB Special Report 176: Landslides - Analysis and Control. Schuster, R.L., Krizek, R.J. Eds., TRB: Washinton DC, USA, pp. 188-189.

Glendinning, S., 1995. Deep Stabilisation of Slopes Using Lime Piles. Doctoral Thesis. Loughborough University of Technology, Loughborough, UK.

Gutiérrez, A.S., Caneghem, J.V., Martínez, J.B.C., Vandecasteele, C., 2012. Evaluation of the environmental performance of lime production in Cuba. J. Clean. Prod. 31, 126-136. https://doi.org/10.1016/j.jclepro.2012.02.035.

Herbilion, A.J., Nahon, D., 1988. Laterites and laterization processes. In Iron in Soils and Clay Minerals, Stucki, J.W., Goodman, B.A., Schwertmann U., Eds., Springer: Dordrecht, NL, 217, pp. 779-796. ISBN 978-94-009-4007-9.

Hilt, G.H., Davidson, D.T., 1960. Lime fixation on clayey soils. High. Res. Rec. 262, 20-32.

Ibrahim, A., Abdullah, M.S., Jamalludin, D., Apo, M., 2007. Comparison between hydrated lime dry powder and slurry on peat soil stabilization. Esteem Academic Journal, 3.87-100. ISSN 1675-7939.

Jesus, A.S., Sousa, M.S., Nascimento, D.T.F., Romão, P.A., Camapum de Carvalho, J., 2017. A influência de aspectos geomorfológicos, de cobertura do solo e climáticos no surgimento e evolução de processos erosivos no entorno de reservatório. In Erosão em Bordas de Reservatório, first ed., Sales, M.M., Camapum de Carvalho, J., Mascarenha, M.M., Luz, M.P., Angelim, R.R., Souza, N.M., Eds., Gráfica UFG: Goiânia, Brazil, pp. 172–192. ISBN 978-85-495-0118-9.

Jha, A.K., Sivapullaiah, P.V., 2015. Mechanism of improvement in the strength and volume change behavior of lime stabilizes soil. Eng. Geol. 198, 53-64. https://doi.org/10.1016/j.enggeo.2015.08.020

Jha, A.K., Sivapullaiah, P.V., 2016. Volume change behavior of lime treated gypseous soil - influence of mineralogy and microstructure. Appl. Clay Sci. 119, 202-212. https://doi.org/10.1016/j.clay.2015.09.017

Juracek, K.E., 2015. The aging of America's reservoirs in reservoir and downstream physical changes and habitat implications. J Am Water Resour Assoc. 51(1), 1-18, https://doi.org/10.1111/jawr.12238.

Kondolf, G.M., Gao, Y., Annandale, G.W., Morris, G.L., Jiang, E., Zhang, J., Cao, Y., Carling, P., Fu, K., Guo, Q., et al., 2014. Sustainable sediment management in reservoirs and regulated rivers: Experiences from five continents. Earth's Future. 2, 256–280. https://doi.org/10.1002/2013EF000184.

Krishnan, D.K., Janani, V., Ravichandran, P.T., Annadurai, R., Gunturi, M., 2014. Soil stabilization using phosphogypsum and flyash. Int. J. of Eng. Trends and Tech. 9 (14), 736-739. https://doi.org/10.14445/22315381/IJETT-V9P339

Latifi, N, Eisazadeh, A, Marto, A., Meehan, C.L., 2017. Tropical residual soil stabilization: A powder form material for increasing soil strength. Constr. and Build. Mater. 147, 827-836. https://doi.org/10.1016/j.conbuildmat.2017.04.115

Lawson, D.E., 1985. Erosion of Northern Reservoir Shores. and Analysis at Application of Pertinent Literature, CRREL. Monograph 85-1, USACE: Hanover, NH, USA, pp. 35-37.

Luiz, G.C., Gitirana Júnior, G.F.N., Romão, P.A.. Almeida, F.P., 2017. Interação solo-atmosfera e a sua relação com erosão em borda de reservatórios. In Erosão em bordas de reservatório, Sales, M. M., Camapum de Carvalho, J., Mascarenha, M.M., Luz, M.P., Angelim, R.R., Souza. N.M. Eds., Gráfica-UFG: Goiânia-GO, Brazil, pp. 127-151.

Mascarenha, M.M.A., Vasco, J.R.G., Matamoros Sevilha, T.M., Vargas, C.A.L., Schliewe, M.S., Menezes, A.V., Tatto, J., 2017. Ensaios aplicados ao estudo de erosões nas bordas e áreas do entorno de reservatórios. In Erosão em bordas de reservatório, Sales. M. M.. Camapum de Carvalho. J., Mascarenha, M. M., Luz, M. P., Angelim, R. R., Souza, N. M. Eds.,. Gráfica-UFG: Goiânia-GO, Brazil, pp. 229-259.

McQuarrie, M., Pilkey, O., 1998. Evaluation of alternative or non-traditional shoreline stabilization devices. J. Coastal Res. 26, 269-272.

Menezes, A. V., 2017. Proposta Metodológica Para Estudo de Perda de Massa de Solos Situados em Bordas de Reservatório Devido ao Efeito de Ondas Por Meio de um Canal Hidráulico. Masters Thesis, University of Goiás, Goiânia-GO, Brazil.

Ministry of Health, Ordinance nº 2,914, 12 December 2011 Available online: http: // bvsms.saude.gov.br/bvs/saudelegis/gm/2011/prt2914_12_12_2011.html (accessed 20 March 2019).

Ministry of the Environment, Normative Resolution of CONAMA n°. 357, 17 March 2005. Available online: http: // www2.mma.gov.br/port/conama/legiabre.cfm?codlegi=459 (accessed 20 March 2019).

Nascimento, R.O., Oliveira L.M., Mascarenha M.M.A., Angelim R.R., Oliveira R.B., Sales M.M., Luz M.P., 2019. Uso de Solução de Cal para Mitigação de Processos Erosivos em um Solo da UHE Itumbiara. Revista Geociências. 38, 279-295.

Nasiri, M., Lotfalian, M., Modarres, A., Wu, W., 2017. Use of rice husk ash as a stabilizer to reduce soil loss and runoff rates on sub-base materials of forest roads from rainfall simulation tests. Catena. 150, 116-123. https://doi.org/10.1016/j.catena.2016.11.010.

Nogami, J.S., Villibor, D.F., 2009. Pavimentos Econômicos. Arte & Ciência: São Paulo-SP, Brazil, pp. 1-291.

Northwest Regional Planning Commission-NWRPC, 2004. Shoreline Stabilization Handbook for Lake Champlain and Other Inland Lakes, Lake Champlain Basin Program and US Environmental Protection Agency: St. Albans, VT, USA, pp. 1-49. ISBN 0-9754546-0-9.

O'Donnell, A.J., Lytle, D.A., Harmon, S., Vu, K., Chait, H., Dionysiou, D.D., 2016. Removal of strontium from drinking water by conventional treatment and lime softening in bench-scale studies. Water Res. 103, 319-333. https://doi.org/10.1016/j.watres.2016.06.036.

Oliveira, L.M., 2018. Estudo experimental de uso de solução de cal para estabilização de um solo saprolítico de talude de erosão. Bachelors Thesis, University of Goiás, Goiânia-GO, Brazil.

Olson, E.R., Ventura, S.J., 2012. Geospatial methods to examine shoreline erosion in the Chippewa Flowage: A case study. Lake Reserv. Manag. 28, 170–175. https://doi.org/10.1080/07438141.2012.689798.

Petry, T.M., Lee, T.W., 1988. Comparison of quicklime and hydrated lime slurries for stabilization of highly active clay soils. Transportation Research Record, No. 1190. pp. 31-37. ISBN 0309047587

Raheem, A.A., Soyingbe, A.A., Emenike, A.J., 2013. Effect of curing methods on density and compressive strength of concrete. Int. J. Appl. Sci. and Technol. 3(4).

Ramezanianpour, A.A., Malhotra, V.M., 1995. Effect of curing on the compressive strength, resistance to chloride-ion penetration and porosity of concretes incorporating slag, fly ash or silica fume. Cem. Concr. Compos. 17, 125-133. https://doi.org/10.1016/0958-9465(95)00005-W

Rezende, L.R., 2013. Estudo do Comportamento de Materiais Alternativos Utilizados em Estruturas de Pavimentos Flexíveis. Doctoral Thesis, University of Brasília, Brasília-DF, Brazil.

Rocha, M.T, Rezende, L.R., 2017. Laboratory study of a granular tropical soil chemically stabilized for pavement purposes. Revista Matéria. 22 (4), 1-25.

Rogers, C.D.F., Glendinning, S., Holt, C.C., 2000. Slope stabilization using lime piles—a case study. Proc. Inst. Civ. Eng. Ground Improv. 4(4), 165–176. https://doi.org/10.1680/grim.2000.4.4.165.

Romão, P.A., Souza, N.M., 2017. Aspectos geológicos e hidrogeológicos na deflagração e evolução da erosão hídrica em margens de reservatórios. In Erosão em Bordas de Reservatório, first ed., Sales, M.M., Camapum de Carvalho, J., Mascarenha, M.M., Luz, M.P., Angelim, R.R., Souza, N.M., Eds., Gráfica UFG: Goiânia, Brazil, pp. 153–170. ISBN 978-85-495-0118-9.

Santos. A.R., 2011. Técnica Cal-Jet – Manual de Execução. Independent consultant, São Paulo-SP, Brazil.

Schleiss, A.J., Franca, M.J., Juez, C., De Cesare, G., 2016. Reservoir Sedimentation. J. Hydraul. Res. 1-17. https://doi.org/10.1080/00221686.2016.1225320.

Schliewe, M.S., 2018. Estudo experimental da erosão pela ação de ondas de um solo laterítico situado nas margens do reservatório de Itumbiara. Masters Thesis, Universidade Federal de Goiás, Goiânia.

Simon, K., Steinemann, A., 2000 Soil bioengineering: challenges for planning and engineering. J. of Urban Plan. Devet. 126(2), 89–102. https://doi.org/10.1061/(ASCE)0733-9488(2000)126:2(89)

Singh, J., Kalamdhad, A.S., 2013. Effects of lime on bioavailability and leachability of heavy metals during agitated pile composting of water hyacinth. Bioresource Tech. 138, 148-155. https://doi.org/10.1016/j.biortech.2013.03.151.

Sousa, A.C.L., Reis, G.C., 2016. Aplicação de Cal Hidratada em Suspensão em um Solo Laterítico para Mitigação de Processos Erosivos. Bachelors Thesis. Univertisy of Goiás, Goiânia-GO, Brazil.

Stimson, A.G., Allott, T.E.H., Boult, S., Evans, M.G., Pilkington, M., Holland, N., 2017. Water quality impacts of bare peat revegetation with lime and fertiliser application, Appl Geochem. 85, 97-105. https://doi.org/ 10.1016/j.apgeochem.2017.09.003.

Su, X., Nilsson, C., Pilotto, F., Liu, S., Shi, S., Zenga, B., 2017. Soil erosion and deposition in the new shorelines of the Three Gorges Reservoir. Sci. Total Environ. 599-600, 1485-1492. https://doi.org/ 10.1016/j.scitotenv.2017.05.001.

Tatto, J., 2014. Comportamento de filtros geotêxteis em taludes sujeitos a impactos de ondas. Doctoral Thesis, Univertisy of Brasília, Brasília-DF, Brazil.

Tran, T.D., Cui, Y., Tang, A.M., Audiguier, M., Cojean, R., 2014. Effects of lime treatment on the microstructure and hydraulic conductivity of Héricourt clay. J. Rock Mech. Geotech. Eng. 6, 399-404. https://doi.org/ 10.1016/j.jrmge.2014.07.001

Transportation Research Board-TRB, 1987. State of the Art Report 5: Lime Stabilization – Reactions, Properties, Design and Construction, TRB: Washinton DC, USA, pp. 3-53.

U.S. Geological Survey - USGS, 2018. Mineral commodity summaries 2018, U.S. Geological Survey: Washington DC. USA, pp. 96-97. ISBN 978-1-4113-4199-9.

Vilhena, R.M., Mascarenha, M.M.A., Sales, M.M., Romão, P.A., Luz, M.P., 2019. Estimating the Wind-Generated Wave Erosivity Potential: The Case of the Itumbiara Dam Reservoir. Water. 11, 342. https://doi.org/ 10.3390/w11020342.

Volker, A., Henry. J.C., 1988. Influence of wind waves on the erosion of reservoirs banks in Slovakia. In Side Effects of Water Resources Management: Overviews and Case Studies. IAHS: Oxford, UK, 172 (Redbook), pp. 51-78. ISBN 0-947571-46-9.

Wang, Y., Duc, M., Cui, Y., Tang, A.M., Benahmed, N., Sun, W.J., Ye, W.M., 2017. Aggregate size effect on the development of cementitious compounds in a lime-treated soil during curing. Appl. Clay Sci. 136, 58-66. https://doi.org/10.1016/j.clay.2016.11.003.

Wang, Y., You, W., Fan, J., Jin, M., Wei, X., Wang, Q., 2018. Effects of subsequent rainfall events with different intensities on runoff and erosion in a coarse soil. Catena 170, 100-107. https://doi.org/10.1016/j.catena.2018.06.008.

Wilkinson, A., Haque, A., Kodikara, J., Adamson, J., Christie, D., 2010. Improvement of problematic soils by lime slurry pressure injection: case study. J. Geotech. Geoenviron. Eng. 136(10), 1459–1468. https://doi.org/10.1061/(ASCE)gt.1943-5606.0000359.

World Commission on Dam–WCD, 2000. The report of the world commission on dams - Dams and Development, Earthscan Publications Ltd: London, UK, pp. 15-16. ISBN 1-85383-798-9.

Wu, L.Z., Zhoua, Y, Sunb, P, Shi, J.S., Liu, G.G, Bai, L.Y., 2017. Laboratory characterization of rainfall-induced loess slope failure. Catena. 150, 1-8. https://doi.org/10.1016/j.catena.2016.11.002.

CHAPTER 3

EFFECTS OF RESIDUAL SOIL TYPE

Tropical soils have clay minerals which contribute to the pozzolanic reactions, for example, kaolinite, halloysite, and crystallized aluminum hydroxides, but iron compounds can be disadvantageous to stabilization (GALVÃO; ELSHARIEF, SIMÕES, 2004). In addition, free silica has been leached during laterite genesis, reducing the availability of silica (ATTOH-OKINE, 1995). Indeed, with the increase of weathering higher the clays coverage by iron and aluminum sesquioxides, and lower is the soil-lime stabilization (ATTOH-OKINE, 1995). In addition, laterization could promote agreggation of clay particles and impose more difficult to dissolves the clay mineral, which in turn liberated Si and Al. Although, the role of iron oxides in lime-soil reaction is not yet fully clear or understood (QUEIROZ DE CARVALHO, 1981).

The soil strength improvement from lateritic soil and non-lateritic soil (e.g. saprolitic soil) treated with lime may differ from each other or not provided any significant changes (CAMPOS; NOGUEIRA; SOUZA, 2016). Silva (2016) concluded that lateritic soil showed higher mechanical improvement than non-lateritic soil. This statement also confirms the conclusions of several other researchers who verified minimal soil mass losses due to rises of laterization cited by Almeida et al. (2015). However, the tropical weathering (i.e. laterization) results on a complex structure of macro and microporous and could have different suction effects (ALMEIDA et al., 2015), with an increase of soil cementation and the soil erodibility by surface runoff (CAMAPUM DE CARVALHO et al., 2006).

In recent Brazilian studies, for evaluation of effects of stabilization of reservoir shores with this chemical method, a lime solution with low lime content have produced a strength improvements of lateritic soils (SOUSA;REIS, 2016; NASCIMENTO et al., 2019) and no gain was observed for non-lateritic soil (OLIVEIRA, 2018), due to the small amount of macropores generated by aggregation due and low degree of weathering. The laboratory experimental apparatus used for soil erodibility evaluation includes a modified Inderbitzen apparatus (AGUIAR, 2009) for sheet erosions simulation; wave flume test for wave impact (TATTO, 2014; MENEZES, 2017; SCHLIEWE, 2018), and degradation test for water level fluctuation by partial and total soil sample immersion (SANTOS, 1997).

In this chapter, the comparison of the effects of lime treatment on lateritic and non-lateritic soils was realized under two erodibility tests for wave impacts (wave flume test) and surface runoff (Inderbitzen test). In addition, the effect of different lime contents under different curing periods and curing conditions were investigated. The microstructural and chemical changes were analyzed through SEM analysis and pH measurements. Finally, the performance of lime-treated soils was evaluated in these soil erodibility tests with the removal of the calcium carbonate crust.

3.1 SOIL SAMPLING

The present work collected two types of soils to proceed with laboratory analyses from the right side at reservoir shores of the Itumbiara dam at the site called Area 1 from the work of Vilhena et al (2019). Therefore, the geotechnical classifications from both soils collected on the trenches at local site are lateritic soil (i.e. oxisols) and saprolitic or non-lateritic soil (i.e. inceptisols), in Trench 1 and Trench 2, respectively. Figure 3.1 shows the location spots from soil sampling at the shore of the Itumbiara dam reservoir. Soil drillings realized closer to Trench 1 (lateritic soil) showed that non-lateritic soil layer appears to 1 m to 1.50 m depth and the ground elevation is about 521 m, based on Google Earth's model elevation data. In trench 2 at the elevation of 519 m, the non-lateritic soil is outcropping. The blocks from both soils were excavated at 0.3 m depth below the surface.

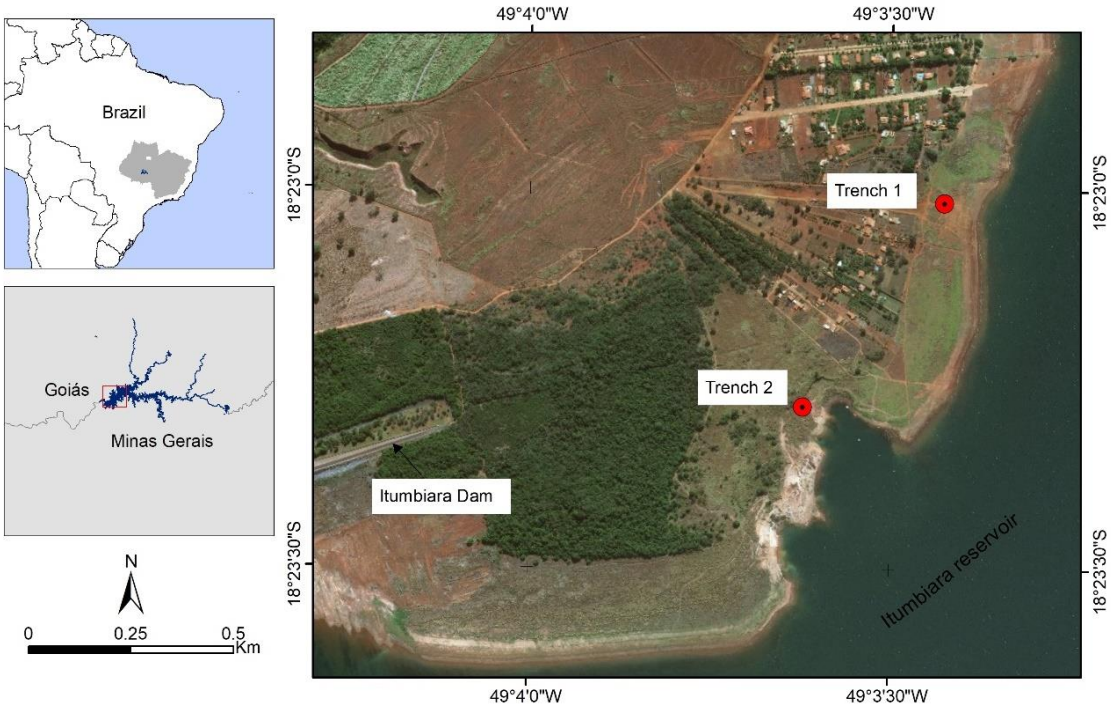

Figure 3.1 - Study area and trench point's location.

There were collected 6 samples from each of lateritic and non-lateritic soils were tested on the wave flume. Inderbitzen test evaluated a total of 24 samples, 12 for each soil type. In addition, the permeability field test and hand auger drilling were also carried out.

The soil physical characterization was defined by sieving, hydrometer analysis with adding sodium hexametaphosphate and without this agent dispersive, Atterberg limits, determination of moisture content and specific mass. In order to characterize the classification of tropical soils, it was necessary to perform specific experimental analysis as the Table Method and Adsorption of Methylene Blue Test according to the methodology of Nogami and Villibor (1995) and Fabbri (1994), respectively.

Lime added to the non-lateritic soil samples was a hydrated lime [Ca(OH)2·MgO] following the same procedure presented in Chapter 2. Although, for each of erodibility test type were considered specific ratios of solute and water by the sample volume. In wave flume test setup of treatment was of 1, 2, and 4% lime solution for 7-day curing time, and with 1 and 4% lime solution at 56 days due to lack of samples.

The specimens for Inderbitzen test were treated with 1, 2 and 4% of lime solution for 1, 7, 28, 56 days of curing. In addition, these samples tested in the surface runoff simulation device based on the procedures from Nascimento et al. (2019). Furthermore, a comparison between lateritic and non-lateritic soils was realized with the set-up present in Table 3.1.

Table 3.1 - Lime treatment configurations of the experimental program

Erodibility Test	Lateritic soil				Non-Lateritic soil			
	1 day	7 days	28 days	56 days	1 day	7 days	28 days	56 days
Wave flume test	Natural soil	1,2, 4%	-	1, 4%	Natural soil	1,2, 4%	-	1, 4%
Inderbitzen test	1,2, 4% and Natural soil	1,2, 4%	1,2, 4%	1,2, 4%	1,2, 4% and Natural soil,	1,2, 4%	1,2, 4%	1,2, 4%,

NOTE: Volumes of water solution part for wave flume test was from 950 mL and for Inderbitzen test was 50 mL

These authors state that the treatment with a lime solution was efficient with increasing the lime content, even after performing partial removal of the layer of lime. Analyzing their results and the aspect of the calcium carbonate layer formed at the top of the soil sample, it was decided to carry out the same procedures and methodology of these authors, but with the removal of the total Ca-rich crust after saturation of the sample.

Samples that were prepared for Inderbitzen test was cured in air-drying conditions, and also the specimens for wave flume test of 7 days curing period. However, samples with a curing time of 56 days for wave flume test was storage differently. These lime-treated soils were storage in moisture room with relative humidity (RH) of more than 90% and temperature of 24±3 °C to evaluate the moisture content variation of the soil.

This storing procedure is based on the methodology presented in Chapter 2 due to results of higher soil loss of lateritic soil due to the shrinkage capacity during air-drying conditions. This shrinkage property could be related to the clay mineralogy (TESTONI et al., 2017) of Fe-rich soils (oxisols).

3.2 COMPARATIVE SOIL ASSESSMENTS

Lateritic soil samples analyzed in this work was from the right shore of the Itumbiara reservoir, which has been collected on the same excavated trench of the researches from this work, Nascimento et al. (2019), and Schliewe (2018), at following dates respectively April 2018, September 2016 and October 2017.

It was identified as a red oxisols, consisting of silty clays and silty sands. All geotechnical characterization of lateritic soils samples of the present work and from other researches that collected in the same location and non-lateritic soil are summarized in Table 3.2 and Table 3.3.

Table 3.2 - Soil physical and chemical parameters, and geotechnical characteristics.

Soil Parameters	Lateritic Soil		Lateritic Soil (Adapted from Nascimento et al., 2019)		Lateritic Soil (Adapted from Schliewe, 2018)		Non-lateritic Soil	
	NAD(1)	AD(2)	NAD	AD	NAD	AD	NAD	AD
Gravel (%)	2	2	3	3	4	8	1	1
Sand (%)	34	31	62	48	33	15	34	38
Silt (%)	64	18	35	26	63	39	65	37
Clay (%)	0	49	0	23	0	38	0	24
Liquid Limit - w_L (%)	47		39		49		45	
Plastic Limit - w_P (%)	29		27		31		25	
Plasticity Index - I_p (%)	17		12		18		20	
Unified Soil Classification System - USCS	ML		ML		ML		CL	
Field water content w_F (%)	15.8		19.5		22.3		13.4	
Water content - w (%)	4.1		7.47		19.75		1.47	

Soil Parameters	Lateritic Soil	Lateritic Soil (Adapted from Nascimento et al., 2019)	Lateritic Soil (Adapted from Schliewe, 2018)	Non-lateritic Soil
Specific gravity – *G*	2.88	2.76	2.87	2.71
Unit Weight Solids - γ_s (kN/m³)	28.3	27.1	28.1	26.6
Void ratio – *e*	0.46	0.54	0.64	0.36
Porosity – *n*	0.31	0.35	0.39	0.27
pH	6.25	-	-	6.04
Permeability field tests (m/s)	4.1×10^{-6}	-	-	2.7×10^{-6}
Falling-head permeability tests (m/s)	2.2×10^{-6}	-	-	2.9×10^{-6}

NOTE: (1) Hydrometer analysis with Non-Agent Dispersive – NAD; (2) Agent Dispersive – AD with Sodium Hexametaphosphate – NaHMP; ML=Silt; CL= Lean clay; pH measured in water solution.

Table 3.3 – Tropical soil characterization.

Soil Parameters	Lateritic Soil	Lateritic Soil (Adapted from Schliewe, 2018)	Non-lateritic Soil
Activity coefficient – CA (10^{-3} g/g%) (1)	10.67	7.43	12.27
Specific surface – SE (m^2/g) (1)	17.08	9.76	9.76
Cation exchange capacity - CTC (meq/100g) (1)	1.88	1.07	1.07
Soil activity classification (1)	Low Active	Low Active	Active
Key-clay mineral (1)	Kaolinite	Kaolinite	Kaolinite
Tropical soil classification - MCT (expeditious method) (2)	LG'	LA' - LA'-LG'	NS' / NA'

NOTE:(1) Adsorption of Methylene Blue Test (Fabbri, 1994); (2) Tablet Method Test (Nogami and Villibor, 1994); MCT=Tropical Soil Classification System; LG'=Lateritic clayed soil; LA'=Lateritic sandy soil; NS'=Non-lateritic silty soil; NA'=Non-lateritic sandy soil.

Table 3.4 shows the chemical composition the materials of this study, which were determined using X-ray fluorescence (XRF) spectroscopy and a comparison with the work of Schliewe (2018). Non-lateritic soil shows a higher percentage of silica (68%), and lower iron (4%) and aluminum oxides (19%) than lateritic soil.

The micro-analyses used X-ray diffractometry (XRD) to reveal the chemical composition of the untreated non-lateritic sample. Figure 3.2 present X-ray diagrams that compare with lateritic soil sample and lime.

Kaolinite and quartz are the main minerals observed in soil specimens, and to a lesser amount, gibbsite, goethite, and muscovite. Illite is a clay mineral identified only in non-lateritic soil, which represents a lower degree of weathering. Results from Nascimento et al. (2019),

Schliewe (2018), presented in Chapter 2 showed for the lateritic soil mineralogy peaks of muscovite, vermiculite, and hematite, besides quartz and kaolinite.

Table 3.4 - Chemical composition of lateritic and non-lateritic soil.

Chemical Composition	Lateritic Soil (%)	Lateritic Soil - Adapted from Schliewe, 2018 (%)	Non-lateritic Soil (%)	Lime (%)
Sulfur trioxide - SO_3	-	-	-	0.25
Magnesium oxide - MgO	-	-	-	26.59
Silicon dioxide - SiO_2	40.89	44.64	68.24	2.74
Ferric oxide - Fe_2O_3	16.77	16.14	3.68	0.49
Aluminium oxide - Al_2O_3	23.82	16.14	19.40	0.65
Calcium oxide - CaO	0.08	-	0.07	68.59
Titanium dioxide - TiO_2	4.77	4.21	0.53	-
Phosphorus pentoxide - P_2O_5	0.13	0.14	-	0.24
Zirconium dioxide - ZrO_2	0.11	0.11	0.06	-
Strontium oxide - SrO	-	-	-	0.12
Manganese oxide - MnO	0.08	0.08	-	0.07
Sodium oxide - Na_2O	0.93	0.00	-	-
Potassium oxide - K_2O	0.72	0.69	1.00	0.17
Lost of Ignition - LOI	11.91	17.85	7.02	0,09

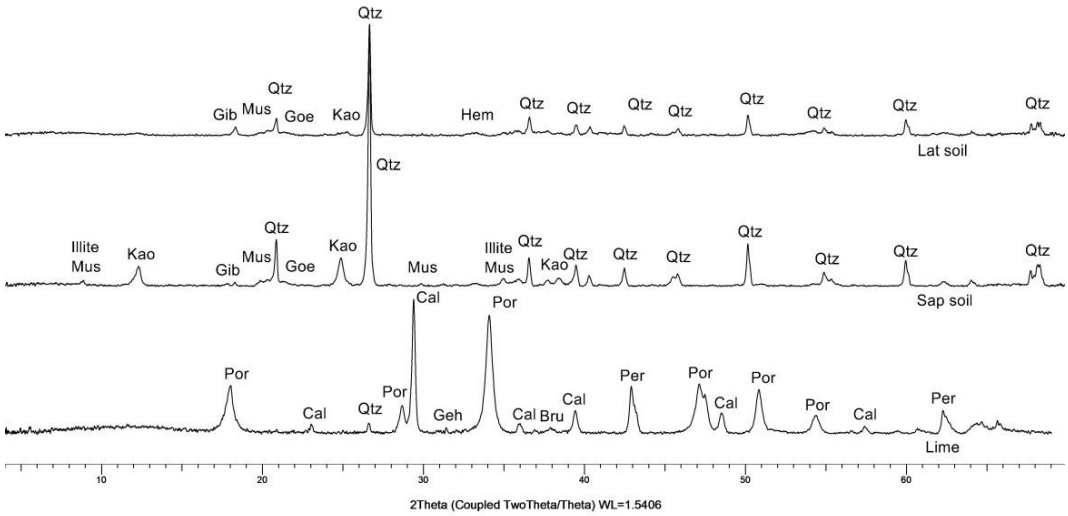

Figure 3.2 - Comparison of the XRD analysis of materials. Lat soil=lateritic soil; Sap soil=non-lateritic soil; Bru=brucite; Cal=calcite; Geh= gehlenite; Gib=gibbsite; Goe=goethite; Hem=hematite; Kao = kaolinite; Mus=muscovite; Por=porlandite; Per=pertlandite; Qtz=quartz.

The microstructure was analyzed by Scanning Electron Microscopy (SEM) technique with low vacuum modes and backscatter imaging to preserve humidity of the sample. In Figure 3.3 shows photomicrographs different aspects of non-lateritic soil from the parallel

and perpendicular profile of the sample. The microfabric appearance of non-lateritic soil is an irregular matrix with macropores (Figure 3.3a) and micropores (Figure 3.3b), similar to the lateritic soil showed in Chapter 2 (Figure 2.4) Furthermore, kaolinite is the major clay mineral observed on micrographs and occurs as aggregates of platelets and booklets crystals (Figure 3.3b). The degree of weathering of this soil is in a lesser stage in comparison with the lateritic soil, as seen by the quartz vein-like microstructure from the parent rock (Figure 3.3c).

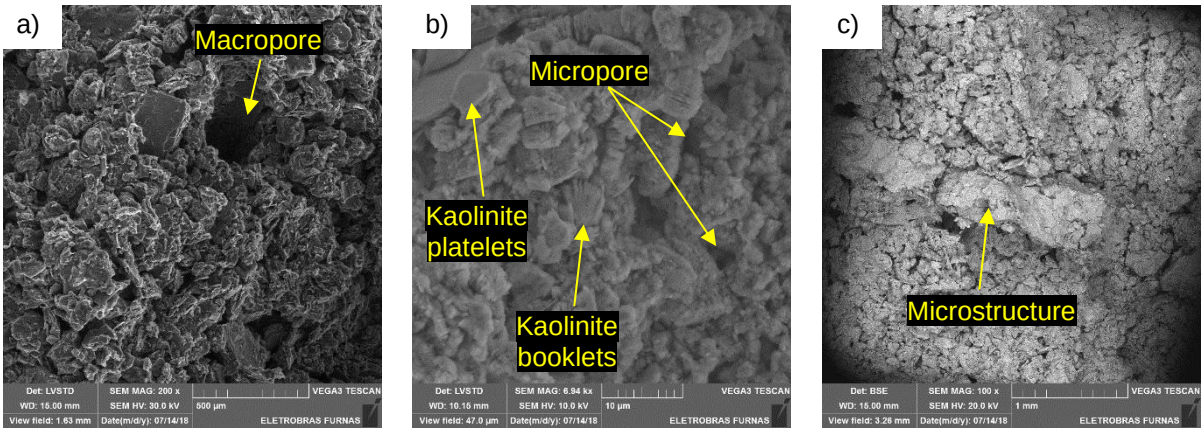

Figure 3.3 - SEM micrographs of the natural non-lateritic soil: (a) A magnification of 200 x shows general aspect of soil, clay minerals, and macropore; (b) Micropore showed in amplification of 6.94 kx and typical kaolinite morphology; (c) Microstructure represented by a diagonal transverse quartz vein along the perpendicular profile at 100 x magnification.

The results presented in this section analyze the effects of carbonation, curing time and lime content on lateritic soils and non-lateritic (i.e. saprolitic soil). Carbonation was analyzed not only visually but also through microstructural and chemical mapping. The effects of curing time and lime content were evaluated from the erodibility tests, which in this work are the wave flume test and the Inderbitzen test.

3.2.1 MICROSTRUCTURAL AND CHEMICAL ANALYSIS

The influence below the surface of the lime treatment was analyzed first by SEM with Energy Dispersive Spectroscopy (EDS) system to scan the sample looking for any trace calcium. The next procedure was to identify by SEM micrographs the presence of pozzolanic materials from the morphology of this new cementitious compounds, as such calcium silicate hydrate (CSH), calcium aluminate hydrate (CAH), and calcium aluminate silicate hydrate (CASH). For the last, an XRD analysis was conducted to confirms these minerals.

In addition, the pH measurements were conducted in all the non-lateritic soil samples due to the pH of soil plays a fundamental role in the process of pozzolanic reactions

(GLENDINNING, 1995). Adding lime to the soil generates two reactions as such short-term and long-term. Long-term reactions (Pozzolanic reactions) are considered the most important for soil stabilization and therefore the research sought to verify the presence of new cement compounds to justify the results observed in the erodibility tests.

The mapping of the pozzolanic minerals was performed by EDS analysis in SEM with the following settings of cure time and file content: untreated saprolitic soil for 1%-7 days, 1%-56 days, 4%-7 days, and 4%-56 days. Figure 3.4 presents micrographs mapping and each color corresponds to the respective identified chemical elements in the image. In these SEM micrographs is possible to verify that the accumulation of file occurs only in the first 500 µm of 3 mm of the soil profile. This influence is lower than observed in lateritic soil, in which the carbonation of lime was observed at 1 mm depth, according to Chapter 2 (Figure 2.10). It occurs because aggregation of the lateritic soil contributes to promoting more lime infiltration, but does not necessarily reflect in strength increase, as will be discussed in the next section.

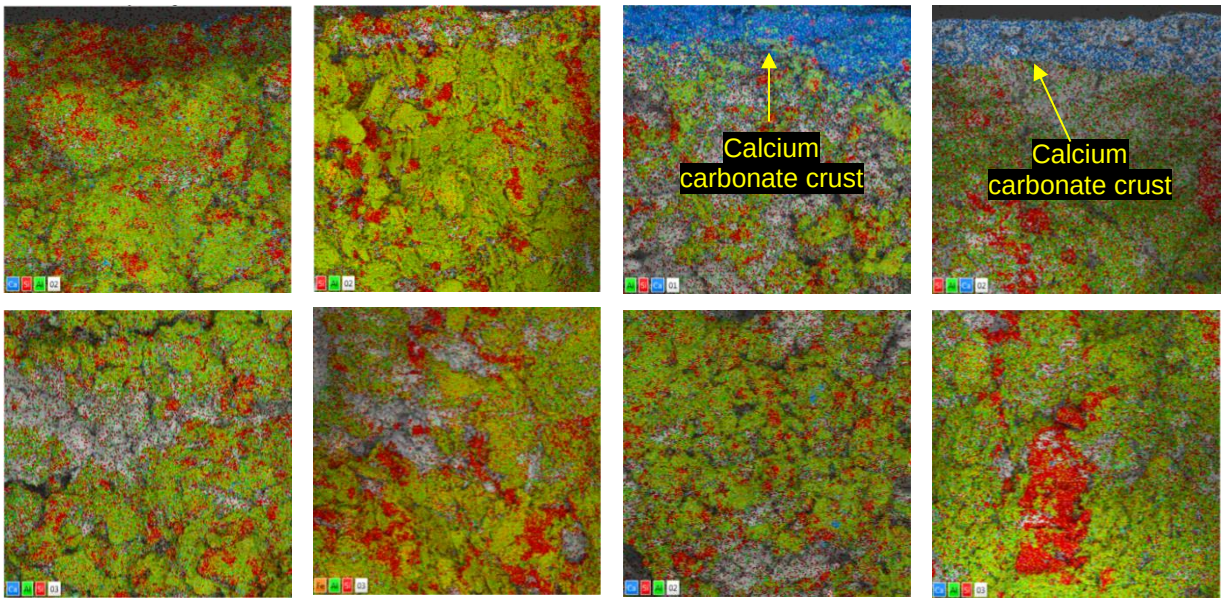

(a) (b) (c) (d)

Figure 3.4 - EDS analyzes of lime treated soil in magnification of 500 µm for (a) 1%-7 days, (b) 1%-56 days, (c) 4%-7 days and (d) 4%-56 days. The soil profile is considered 3 mm depth. EDS chemical colors are Ca=blue, Si=red, Al=green, Fe=orange.

X-ray analysis for non-lateritic soil was performed to confirm the presence of aluminates and hydrated calcium silicates but was not observed in Figures 3.5 to 3.7. However, the dominant presence of calcite is noted on 4% of a lime solution even in 7 and 56 days. Similar results were observed in lateritic soil presented in Chapter 2 (Figures 2.12-14).

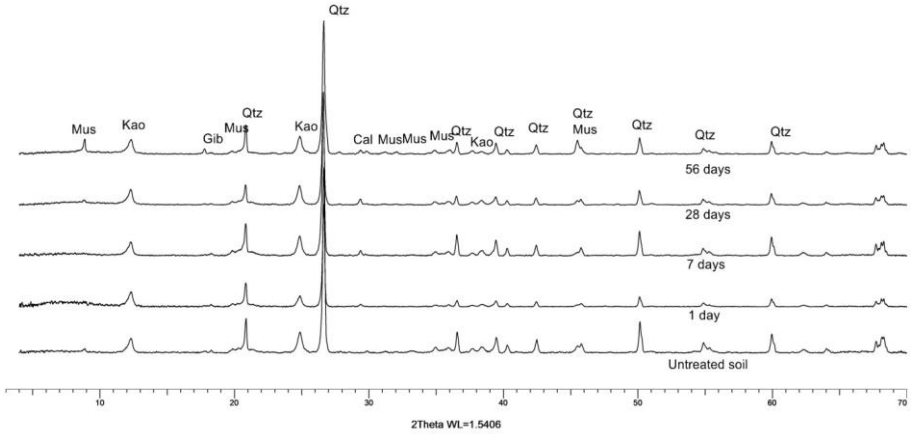

Figure 3.5 - XRD diagrams of 1% lime at 1, 7, 28 and 56 days curing time. Cal=calcite; Gib=gibbsite; Goe=goethite; Kao = kaolinite; Mus=muscovite; Qtz=quartz.

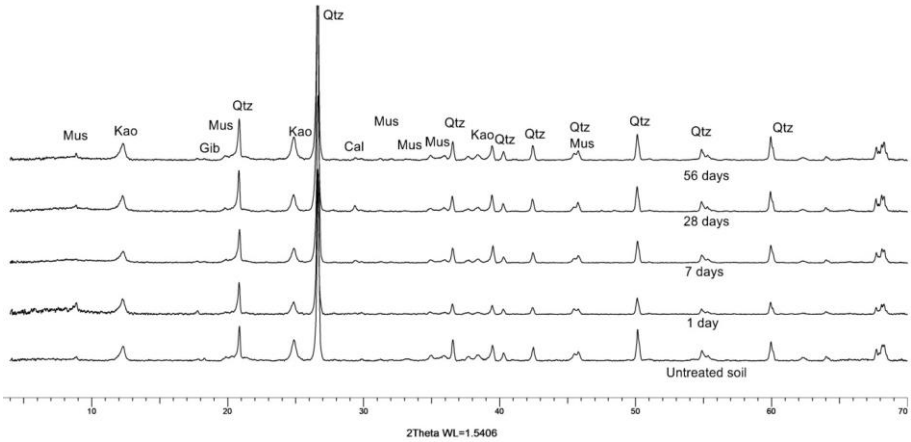

Figure 3.6 - XRD diagrams of 2% lime at 1, 7, 28 and 56 days curing time. Cal=calcite; Gib=gibbsite; Goe=goethite; Kao = kaolinite; Mus=muscovite; Qtz=quartz.

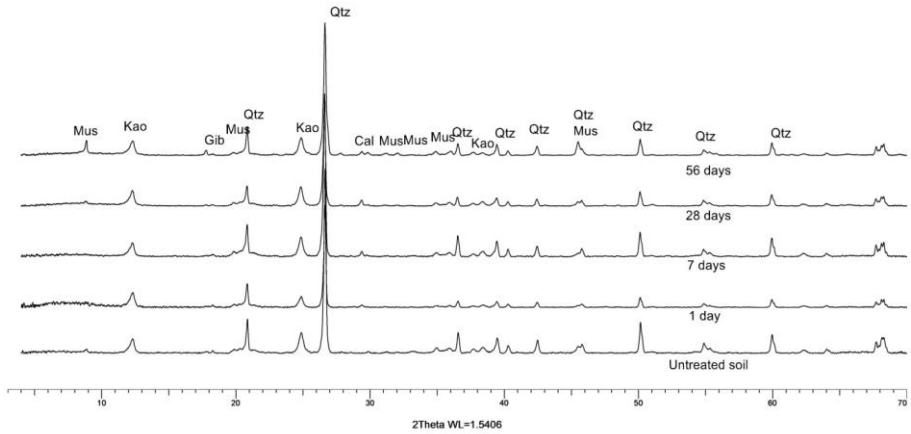

Figure 3.7 - XRD diagrams of 4% lime at 1, 7, 28 and 56 days curing time. Cal=calcite; Gib=gibbsite; Goe=goethite; Kao = kaolinite; Mus=muscovite; Qtz=quartz.

Another analysis to evaluate the affinity of soil to pozzolanic reactions is the measurement of soil pH. As shown in Table 3.5, both lateritic and saprolitic soils did not present high pH values above 12.4 (GLENDINNING, 1995), which should favor the stabilization of soil chemistry for generating cementitious compounds.

Table 3.5 - Results from the pH of treated soils.

Days	Non-Lateritic soil			Lateritic soil		
	1% lime	2% lime	4% lime	1% lime	2% lime	4% lime
1	7.42	7.38	12.54	7.79	9.76	12.15
7	8.49	8.90	8.61	7.96	8.10	7.95
28	8.78	9.11	9.00	8.03	8.07	8.05
56	7.86	9.14	9.17	7.44	8.08	8.18

From these microstructural and chemical analyzes, it can be verified that there was no formation of pozzolanic minerals, but rather the formation of a Ca-rich crust on top of the soil sample, formed from the short-term carbonation reaction of the lime.

Thus, the influence of the lime treatment is superficial, corroborating with results showed in Chapter 2 for lateritic soil and visually checked. In Figure 3.8 it is possible to verify the appearance of the sample before and after the application of the lime, as the white crust produced by carbonation of lime.

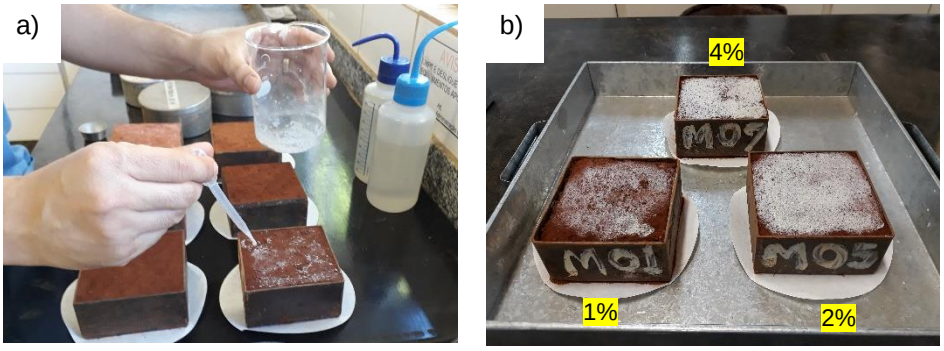

Figure 3.8 - Soil-lime treatment of samples for Inderbitzen test under (a) preparation; and (b) treated samples of lateritic soil after curing time.

Bell (1996) observed that pozzolanic reactions can be achieved lower than 4% of lime by dry weight of soil by the formation of new cementitious minerals, which could be related to the optimum lime content (OLC). This concept establishes the minimum amount of lime by weight of soil necessary to produce pozzolanic reactions.

However, in the present work, the amount of lime by the solution of lime is a hundred or even a thousand times lower than lime content by weight of soil. For this reason, the soil stabilization could not be established by a lower amount of lime and because the carbonation of the lime consumed the most amount of free Ca^{2+}.

3.2.2 Erodibility tests

The soil erodibility tests were performed to evaluate the impact of waves and water level variation with the wave flume test and the superficial runoff with the Inderbitzen device.

Soil erodibility behavior of lateritic and non-lateritic soils differs from wave flume and Inderbitzen tests because the lime-treated samples for surface runoff evaluation have a Ca-rich crust removal. In contrast, the specimens analyzed by wave impact have kept this crust. The explanation for distinct results of soil loss will shortly be brought in the sections that follow.

3.2.2.1 Wave flume test

The wave flume test simulates the impact of wave wind-generated that reaches soils at the banks of reservoirs (TATTO, 2014). This device consists of a hydraulic channel, a wave generation system and a slope with the soil sample or sample holder, allowing to quantify the loss of soil mass by the action of the impact of waves. The methodology and test procedures used in this work followed the studies of Menezes (2017), Schliewe (2018) and that already was described in Chapter 2 (in Section 2.2). All samples were tested based on average erodibility values of slope angle of 45° and a wave frequency of 0.5 Hz from Schliewe (2018). In addition, the soil loss was calculated by weighing method and converted to a percentage by dividing the total dry mass by the initial dry mass.

The saprolitic soils were treated in the following sets: untreated soil 1%-7 days, 1%-56 days, 2%-7 days, 4%-7 days, and 4%-56 days. Figure 3.9 presents a comparison between these values and the results of lateritic soil presented in Chapter 2 (Table 2.4). In addition, these authors also verified that the curing condition plays an important role in a long-term cure and have higher effects on soil erodibility. For this reason, it was adopted for samples of 56 days curing time the storing in moisture room.

It is also observed, that the non-lateritic (saprolitic) soil has lower soil loss than lateritic soils, about half to the untreated soil. Non-lateritic soil has generally are resistant to wave impacts

than lateritic soil, which is corroborated by statements of Camapum de Carvalho et al. (2006) due to the low degree of weathering and the greater cohesion of the particles.

All soil types have better performances with increase of curing time, hydration storage condition and lime content as observed at 56 days. While the lateritic soil showed a dispersion between 1% and 4% of lime solution, the non-lateritic soil present similar results, considering the same lime contents. This may have the influence of the laterization of the soil due to aggregations.

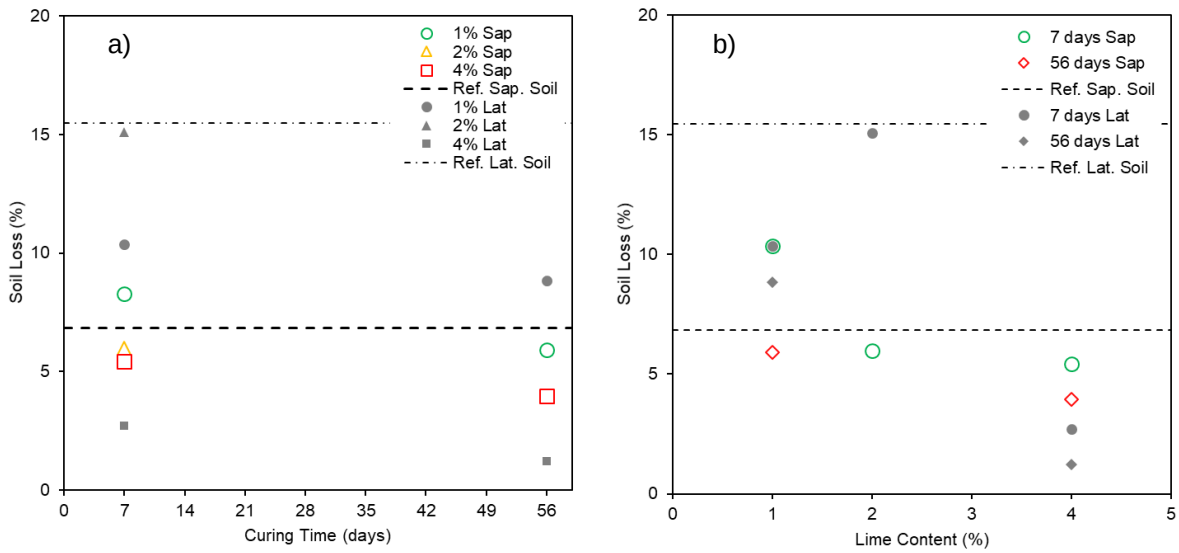

Figure 3.9 - Comparison from soil loss of wave flume tests of non-lateritic and lateritic soils by (a) Curing time and (b) Lime content.

However, the addition of lime solution to these soils produces a slight reduction of erodibility due to the thickening of the calcium carbonate crust than increase the free calcium for soil stabilization. In lateritic soil, this Ca-rich crust is thicker than non-lateritic soil, as verified in the previous chapter (Figure 2.10) and in Figure 3.4. It gives a good insight into the behavior of soil loss of the lateritic soil with 4% of lime solution (Figure 3.9b). The lateritic soil samples of 7-days curing present different soil losses than non-lateritic soil. These specimens were storage in air-drying condition and could promote the increase of shrinkage by reduction of moisture content of these soils, also a decrease of soil cohesion of clay particles (ALMEIDA et al., 2015). Again, non-lateritic soil seems to have similar values of soil loss unrelated to curing conditions. Its seems that the addition of lime solution to the lateritic soil improve mechanical soil parameters than to the non-lateritic soil. Lime-treated saprolitic soil samples showed values of soil losses much similar to each other and to the natural soil.

Sediment deposition percent of non-lateritic soil is present in Figure 3.10 and was verified the similar pattern of lateritic soil showed in Chapter 2 (Figure 2.21), that is, coarse sediments lays near the sample (Sector 6) and fine particles were carried out farthest (Sector 4). The discussion about the sediment disposition along the flume was given in the preceding chapter.

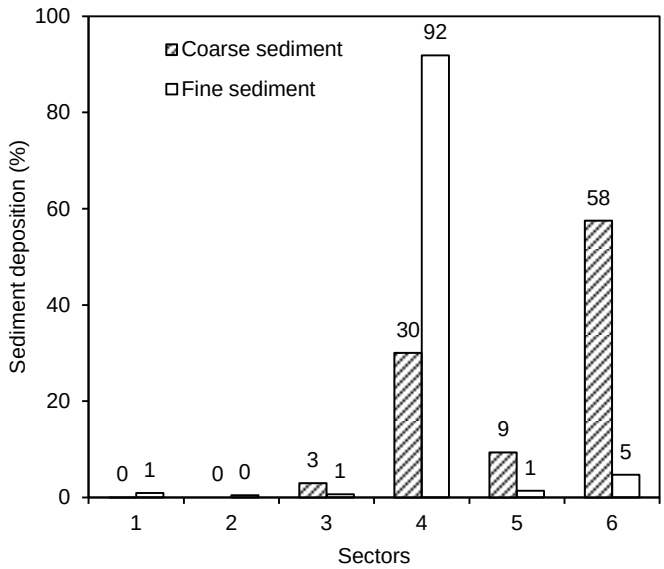

Figure 3.10 - Sediment deposition of fine (<0.075 mm) and coarse (>0.075 mm) sediments of saprolitic soil.

The amount of fine sediments deposition has varied from 82% to 100% by dry weight in comparison with 0% to 18% of coarse sediments from all the 6 samples of non-lateritic soil. The sediment distribution of the lateritic soil present in Chapter 2 (Figure 2.21) showed more quantity of coarse particles and less fine grains than non-lateritic soil, which contradicts the results from sieve analysis present in Table 3.2. Lateritic soil has more clay particles than non-lateritic soil, however, this has a lower silt content. Hence, the soil aggregates may relatively weaken when exposed to water and the clay particles easily detached by the erosive process according to Almeida et al. (2015).

3.2.2.2 Inderbitzen test

The Inderbitzen test allows the quantification in the laboratory of the volume of soil mass loss, influenced by the surface runoff, simulating the effect of sheet erosion. Its a widely used device in soil erodibility research and was utilized an equipment build by Aguiar (2009). This apparatus can also be used to evaluate the influence of soil suction on the loss of soil mass estimation of hydraulic parameters of erodibility (BASTOS, 1999) and slope influence on soil

erodibility (MASCARENHA et al., 2015). This apparatus has an acrylic flume with an adjustable inclination of 1 m in length and 10 cm in width. The sample is set in square shape sized metal mold of dimensions of 10x10 cm and thickness of 5 cm, at the end of the flume.

The methodology used in this study used a proposal by Aguiar (2009), observing some adaptations of procedures suggested by Almeida et al. (2013), as such the continuous flow of water, longer time period and new mass loss formulation, and Nascimento et al. (2019), which included analysis in Laser Diffraction Particle Analyzer (LDPA). Lime-treated soils were saturated by capillarity 24 h before the tests to simulate the real field conditions, the slope angle was set to 10° and water flow rate of 50 $L.min^{-1}$.

The test begins with the opening of the continuous water supply that flows over the flume, with a hydraulic shear tension of 0.007 kPa, and the soil. Sediment retained in 200 mesh (0,075 mm) sieve was collected by time intervals of 1, 2 and 30 s, 5, 7 and 30 s, 10; 15; 20; 30; 40; 50 and 60 min. After 1 h the soil sediments were dried in an oven for 24 h. The evaluation of soil loss (in grams) is calculated by a ratio of soil dry mass restrained in 200 mesh sieve (>0.075 mm) to the percentage of fine sediments (<0.075 mm), based on LDPA with ultrasound. The use of this value rather than the data of particle size distribution curve from sieving analysis with NaHMP is a modification on the formulation of the Almeida et al. (2013).

In order to evaluate the performance of soil-lime treatment was removed the calcium carbonate crust after curing time due to a reduction of erodibility observed by Nascimento et al. (2019), because of the same carbonation of lime that produces Ca-rich crust.

This layer as analyzed in the present work by EDS is superficial and as confirmed with the X -ray analysis the soil does not form pozzolanic minerals. The stabilization of the soil is based on the permanence of this carbonaceous crust and its thickness as a function of the increase of the quantity of lime added to the soil.

In Figure 3.11 the results of the Inderbitzen test of lateritic and saprolitic soils having the carbonate crust removed can be observed. Thus, this layer has an important role in the stabilization of the soil and in general, the values of the soils treated with lime and having this superficial layer removed presented high erodibility and above the values of the respective soils without treatment.

The lime treatment to the lateritic soil, considering the removal of the crust formed by the carbonation, does not result in the reduction of soil loss against the surface runoff. However, some lime-treated non-lateritic soil samples achieved results of soil loss below untreated soil

reference value. In addition, this behavior occurred only in one of the lateritic soil sample treated with 4% lime at 56-days, which are influenced by the thickening of carbonate calcium crust.

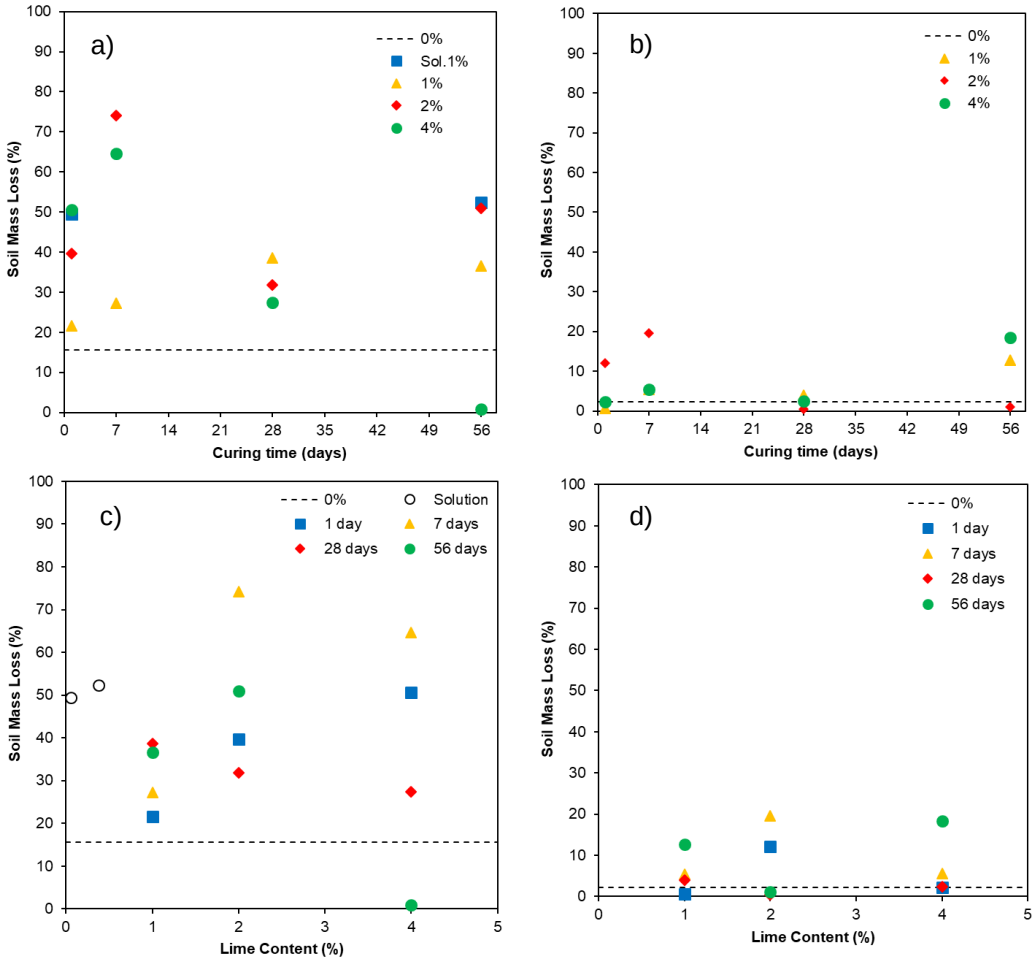

Figure 3.11 – Effects of curing time (days) and lime content (%) on soil mass loss for the Lateritic Soil (a) (c); and Non-lateritic Soil (b) (d).

In fact, the carbonation of lime is deeper in lateritic soil (Figure 2.10) than non-lateritic soil (Figure 3.4) and should be able to withstand erosion, although it was observed that the lateritic soil was more vulnerable and this could be explained by the weakening of the soil aggregation structure by saturation before the test.

It was expected for the lateritic soil that curing time has no significant influence on soil stabilization and the lime content by 2% of the lime solution produced an increase of strength against surface runoff (NASCIMENTO et al., 2019). However, with the increase of lime content lateritic soil samples showed more volumetric shrinkage due to air-drying and those who have low lime content, produced higher soil mass loss than those with 4% of lime solution. The moisture content loss hundermined the effects of curing time and lime content

to the soil erodibility, making it difficult to evaluation them. to Non-lateritic soil not showed a direct relationship between the influence of curing time or lime content on soil erodibility due the low soil loss values.

Almeida et al. (2015) and Camapum de Carvalho et al. (2006) showed that lateritic soil has higher erodibility than non-lateritic soil, submitted to sheet erosion simulation. However, this statement contradicts the conclusions of other researchers (Marques et al., 1997; Bastos, GEHLING, MILITITSKY, 2001; SILVA et al., 2009). The soil erodibility depends on many variables such as grain size, bulk density, water content, cementation, aggregation, mineralogy, texture, and soil chemistry. According to Bastos, Gehling, and Milititsky (2001), soils whose cohesion are lost by surface runoff and the increase of water content are those most susceptible to erosion.

Also, the low erodibility of the saprolitic soil can be explained by the low degree of weathering (ALMEIDA et al., 2015) it has undergone and its structure differs from lateritic, with less aggregation. Lateritic soil has a complex porous media (macro and micropores) which permits different behavior of soil suction. However, this characteristic of lateritic soil associated with the presence of the iron and aluminum oxides and hydroxides (CAMAPUM DE CARVALHO et al., 2006) may also have the inverse effect and explain the lower erodibility values found in the wave flume test.

3.3 DISCUSSIONS

The effects of soil type in the soil stabilization proved to be an important role for lime treatment. Although a greater amount of curing times and lime contents were not tested, it was observed that both soils presented a reduction in soil loss against erosive actions of wave impact and runoff (NASCIMENTO et al., 2019) by reactions of carbonation of lime on the surface of the sample and production of the calcite rich layer.

However, without this calcium crust, the soil does not show an effective stabilization, as observed in the Inderbitzen tests (Figure 3.11). Finally, the lateritic soil as a function of the laterization has a bimodal structure and a fragile bond between the clay particles presenting greater erodibility compared to the non-lateritic soil, even if the carbonation range depth was greater.

Soil-lime treatment to the lateritic soil showed a higher performance than non-lateritic soil against erosivity of surface runoffs and wave impacts, because the non-lateritic soil has an inherent strength behavior to this erosion processes.

CHAPTER 4
FINAL CONSIDERATIONS

This chapter presents the conclusions and suggestions for future work.

4.1 CONCLUSIONS

The geospatial method used to highlight the higher erosivity wave potential areas supported the soil sampling campaign, and coincide with large erosions sites detected by satellite imagery. However, the analysis of wind behavior requires several years of the dataset for set up more reliable values.

The research presented the depth of influence of the addition of lime solution (low lime content) in lateritic and non-lateritic soil, in which it was considered short, up to 2 mm. No formations of new cementitious compounds were observed from the pozzolanic reactions. The hydrated lime solution generated a calcium carbonate crust on the surface by the carbonation process, which could lower the amount of lime available for long-term reactions. Carbonation occurs in a similar way in both types of soil and has been found to be fundamental for reducing soil mass loss from erodibility tests.

The non-lateritic soil samples presented lower soil erodibility than lateritic soil specimens on both Inderbitzen and wave flume tests due to less degree of weathering. The influence of soil type associated with mineralogy type, cementation and microstructure were noted on the mechanical behavior of these lime-treated soils.

The analysis revealed from the wave flume test and the Inderbitzen test that the higher the lime content the lower the soil erodibility as a function of carbonatic crust thickening, and the greater the shrinkage caused by the loss of moisture, the greater the erodibility. The effect of curing condition plays an important role in soil erodibility, it was realized that storage in moisture room causes soil hydration and avoids extreme moisture reduction observed in the air-drying storage. The effect of the curing time does not have a significant capability in the lime-soil treatment in a hydrated lime slurry form.

Therefore, it is concluded that the methodology adopted in this work using a lime solution in very low amounts, compared with to common soil-lime mixture applications, produces an improvement of soil resistance against erosion caused by waves impact, water level

variations, and surface runoffs. However, soil stabilization is more physical than chemical and thus any damage to the protective layer (calcium carbonate crust) exposes the soil to its initial conditions. Drying and wetting cycles in shores reservoirs due to water level operation and climate might breach this layer and for this reason, is necessary reapplication the lime slurry or limewash paint.

The particle-size distribution curve and sediment deposition percentage from wave flume tests showed deposits of coarse-grained particles (sandy fraction) near the sample and fine sediments (silty clay fractions) were carried farther away in a typical lake deposition pattern.

The uses of lime for shoreline stabilization will not affect the chemical of fresh water for human consumption and will probably have little influence on the reservoir's biological life, considering the values stipulated by the Brazilian policy. Finally, we can state that the soil-lime treatment was more efficient for the analyzed samples of lateritic soil than the non-lateritic soil because the saprolitic soil itself showed the lowest soil losses against the erosive processes.

4.2 RECOMMENDATIONS FOR FUTURE RESEARCH STUDIES

From this thesis, the following recommendations for future research emerge:

- Investigate the role of soil suction due to the effects on the hydromechanical behavior of unsaturated soils along the shoreline of the reservoir under wetting-drying cycles;
- Direct measurements by the tensiometer-type suction probe for measurements of any changes of soil state during the tests;
- Evaluate in the field the behavior of soil-lime treatment with lime solution method;
- Proceed wet curing analysis to lime-treated samples on Inderbitzen test;
- Cover the lime-treated soils analysis in wet curing condition between 1 and 56 days curing;
- Find the optimum lime content for field applications;
- Analyze the interaction soil-calcium carbonate crust;;
- Investigate chemical reactions of free calcium and iron, and amorphous form of silica and aluminium;
- Evaluate the effects of water flow in soil-lime treatment;
- Comparison with field experimentations the role of chemical lime treatment and biomineralization.

REFERENCES

ALMEIDA, J.G.R.; ROMÃO, P.A.; MASCARENHA, M.M.A.; SALES, M.M. Erodibilidade de Solos Tropicais não Saturados nos Municípios de Senador Canedo e Bonfinópolis - GO. **Geociências**, v 34, p. 441-451, 2015.

AGUIAR, A.A. **Análise do Comportamento Mecânico de Solos Compactados e Estabilizados Quimicamente para uso em Barragens**. 2014. 281 f. Doctoral thesis - Faculdade de Tecnologia. Departamento de Engenharia Civil e Ambiental, UNB – Universidade de Brasília, Distrito Federal, DF, 2014.

AGUIAR, V.G. **Bacia Hidrográfica do Córrego Granada – Aparecida de Goiânia-GO: Os Processos Erosivos e a Dinâmica Espacial Urbana**. 2009. Master thesis – Escola de Engenharia Civil e Ambiental Universidade Federal de Goiás, Goiânia-GO, 2009.

ATTOH-OKINE, N.O. Lime treatment of laterite soils and gravels — revisited. **Construction and Building Material**, v 9(5), p. 283–287, 1995. DOI: 10.1016/0950-0618(95)00030-J.

BASTOS, C. A. B. **Estudo geotécnico sobre a erodibilidade de solos residuais não saturados**. Porto Alegre/RS, 1999, 269 f. Doctoral thesis, Programa de Pós-Graduação em Engenharia Civil, Universidade Federal do Rio Grande do Sul, Porto Alegre, 1999.

BASTOS, C.A.B.; GEHLING, W.Y.Y; MILITITSKY, J. Estudo sobre a erodibilidade de solos residuais não saturados a partir de propriedades geomecânicas. **Teoria e Prática na Engenharia Civil**, n. 2, p.9-18, 2001.

BELL, F.G. Lime stabilization of clay minerals and soils. **Engineering Geology**, v 42, p. 223-237, 1996. DOI: 10.1016/0013-7952(96)00028-2.

BITTENCOURT, R.M.; MARIN, E.F. B.; LELES, C.R., Monitoramento de Processos Erosivos e Estudo de Técnicas Alternativas para Estabilização de Processos Erosivos em Reservatórios de Usinas Hidrelétricas: FURNAS Centrais Elétricas S.A.. Rio de Janeiro, RJ, 2012, 12 p.

CAMAPUM DE CARVALHO, J.; SALES, M.M.; MORTARI, D.; FÁZIO, J.A.; MOTTA da, N.O.; FRANCISCO, R.A. Processos erosivos. *In*: Camapum de Carvalho, J.; Sales, M.M.; Souza, N.M.; Melo, M.T.S. (Org.). Processos Erosivos no Centro-Oeste Brasileiro, Brasília: FINATEC; 2006. p. 39-88.

CAMPOS, D.J.F.; NOGUEIRA, J.F.; SOUZA, A.T., Análise experimental de solos característicos do Distrito Federal estabilizados com cal. *In*: **CONGRESSO BRASILEIRO DE MECÂNICA DOS SOLOS E ENGENHARIA GEOTÉCNICA**, n. 18., 2016, Belo Horizonte.

FABBRI, G. T. P. **Caracterização da fração fina de solos tropicais através da adsorção de azul de metileno**. 1994. 176 f. Doctoral thesis – Escola de Engenharia de São Carlos - USP, São Carlos-SP.

DE SOUZA DIAS, V.; PEREIRA DA LUZ, M.; MEDERO, G.M.; TARLEY FERREIRA NASCIMENTO, D. An Overview of Hydropower Reservoirs in Brazil: Current Situation, Future Perspectives and Impacts of Climate Change. **Water,** v 10, 592, 2018.DOI: 10.3390/w10050592.

GALVÃO, T.C.B.; ELSHARIEF, A.; SIMÕES, G.F. Effects of lime on permeability and compressibility of two tropical residual soil. **Journal of Environmental Engineering**, v 130, p. 881-885, 2004. DOI: 10.1061/(ASCE)0733-9372(2004)130:8(881).

GLENDINNING, S. **Deep Stabilisation of Slopes Using Lime Piles**. 1995. Tese (Doutorado) - Loughborough University of Technology, Loughborough, UK, 1995.

GEDNEY, D.S., WEBER JR, W.G. **Design and construction of soil slopes**. In: Schuster, R.L., Krizek, R.J. (Org) **TRB Special Report 176**: Landslides - Analysis and Control. Washinton DC, EUA: TRB, p. 188-189, 1978.

LAWSON, D.E. 1985. **Erosion of Northern Reservoir Shores. and Analysis at Application of Pertinent Literature**, CRREL. Monograph 85-1, USACE: Hanover, NH, USA, pp. 35-37, 1985.

LUIZ, G.C., GITIRANA JÚNIOR, G.F.N., ROMÃO, P.A. ALMEIDA, F.P. **Interação solo-atmosfera e a sua relação com erosão em borda de reservatórios**. *In* Sales, M. M., Camapum de Carvalho, J., Mascarenha, M.M., Luz, M.P., Angelim, R.R., Souza. N.M. (Org.). **Erosão em bordas de reservatório**, Goiânia-GO: Gráfica-UFG, p. 127-151, 2017.

MARQUES, J.J.G.S.M.; ALVARENGA, R.C.; CURI, N.; SANTANA, D.P. SANTANA; SILVA, M.L.N. Índices de erosividade da chuva, perdas de solo e fator erodibilidade para dois solos da região dos cerrados - primeira aproximação. **Revista Brasileira de Ciência do Solo**, n 21, p. 427-434, 1997.

MASCARENHA, M.M.A.; MAHLER, C.F.; LAFAYETTE, K.P.V.; ALMEIDA, J. G. R.; NACINOVIC, M. G. G.; BANDEIRA, A. P. N. **Erosão**. *In*: Camapum de Carvalho, J.; Gitirana Jr., G. F. N.; Machado, S. L.; Mascarenha, M. M.; Silva Filho, F. C. (Org.). **Solos não saturados no contexto geotécnico**. São Paulo: ABMS, p. 581-612, 2015.

MASCARENHA, M.M.A.; VASCO, J.R.G.; MATAMOROS SEVILHA, T.M.; VARGAS, C.A. L.; SCHLIEWE, M.S.; MENEZES, A.V.; TATTO, J. **Ensaios aplicados ao estudo de erosões nas bordas e áreas do entorno de reservatórios**. *In:* Sales, M. M.; Camapum de Carvalho, J.; Mascarenha, M. M.; Luz, M. P.; Angelim, R. R; Souza, N. M. (Org.). **Erosão em bordas de reservatório**. Goiânia-GO: Gráfica-UFG, p. 229-259, 2017.

MCQUARRIE, M.; PILKEY, O. Evaluation of alternative or non-traditional shoreline stabilization devices. **Journal of Coastal Resources**, v 26, p. 269-272, 1998.

MENEZES, A. V. Proposta Metodológica Para Estudo de Perda de Massa de Solos Situados em Bordas de Reservatório Devido ao Efeito de Ondas Por Meio de um Canal Hidráulico. 2017. Master thesis – Escola de Engenharia Civil e Ambiental Universidade Federal de Goiás, Goiânia-GO, 2017.

MOURA, F. D.; COELHO, A. T.; **Projeto de Pesquisa e Desenvolvimento - FURNAS Centrais Elétricas S.A. n°.TC 8000009024.** Desenvolvimento e Utilização de Técnicas de Bioengenharia em Solos para fins de Controle de Processos Erosivos no Âmbito de Empreendimentos de Usinas Hidrelétricas, em especial em Margens de Reservatórios. Rio de Janeiro-RJ, 2016. 22 p.

NASCIMENTO, R.O.; OLIVEIRA, L.M.; MASCARENHA, M.M.A.; ANGELIM, R.R.; OLIVEIRA R.B.; SALES, M.M.; LUZ, M.P. Uso de Solução de Cal para Mitigação de Processos Erosivos em um Solo da UHE Itumbiara. **Geociências**. v 38, p. 279-295, 2019.

NOGAMI, J. S.; VILLIBOR, D. F. **Pavimentos Econômicos**. São Paulo (SP): Arte & Ciência, 2009. 291 p.

OLIVEIRA, L.M. **Estudo experimental de uso de solução de cal para estabilização de um solo saprolítico de talude de erosão**. 2018. Bachelors thesis – Escola Ambiental e Sanitária da Universidade Federal de Goiás, Goiânia-GO, 2018.

QUEIROZ, DE CARVALHO, J.B. Amorphous materials and lime stabilized soils. *In*: 10th ICSMFE. **Proceedings of the 10th International Conference on Soil Mechanics and Foundation Engineering**, v. 3, 1981, Stockholm.

SANTOS, A.R. **Técnica Cal-Jet**: Manual de Execução, São Paulo-SP, 2011, 24 p.

SANTOS, R.M.M. **Caracterização geotécnica e análise do processo evolutivo das erosões no município de Goiânia**. Brasília, 1997, 138 p. Master thesis, Departamento de Engenharia Civil e Ambiental, Universidade de Brasília, 1997.

SCHLIEWE, M.S. **Estudo experimental da erosão pela ação de ondas de um solo laterítico situado nas margens do reservatório de Itumbiara**. 2018. Dissertação (Mestrado em Engenharia Civil) – Escola de Engenharia Civil e Ambiental Universidade Federal de Goiás, Goiânia-GO, 2018.

SILVA, A.M.; SILVA, M.L.N.; CURI, N.; AVANZI, J.C.; FERREIRA, M.M. Erosividade da chuva e erodibilidade de cambissolo e latossolo na região de Lavras, sul de Minas Gerais. **Revista Brasileira de Ciência do Solo**, n 33, p. 1811-1820, 2009.

SILVA, M. F. **Estudo da estabilização com cal de um solo laterítico e um solo não laterítico**. 2016, 152 f. Master thesis - Programa de Pós-Graduação em Engenharia de Transportes e Área de Concentração em Infra-Estrutura de Transporte - Escola de Engenharia de São Carlos da Universidade de São Paulo.

SIMON, K., STEINEMANN, A. Soil bioengineering: challenges for planning and engineering. **Journal of Urban Planning and Development**. v 126, n.2, p. 89–102, 2000. DOI: 10.1061/(ASCE)0733-9488(2000)126:2(89).

SOUSA, A.C.L.; REIS, G.C. **Aplicação de Cal Hidratada em Suspensão em um Solo Laterítico para Mitigação de Processos Erosivos**. 2016. Bachelor thesis – Escola de Engenharia Civil e Ambiental Universidade Federal de Goiás, Goiânia-GO, 2016.

SU, X., NILSSON, C., PILOTTO, F., LIU, S., SHI, S., ZENGA, B. Soil erosion and deposition in the new shorelines of the Three Gorges Reservoir. **Science of the Total Environment**, v 599-600, p. 1485-1492, 2017. DOI:10.1016/j.scitotenv.2017.05.001.

TATTO, J. **Comportamento de filtros geotêxteis em taludes sujeitos a impactos de ondas**, 2014 123f. Doctoral thesis – Departamento de Egenharia Civil e Ambiental, Universidade de Brasília, Brasília-DF.

TESTONI, S.A.; ALMEIDA, J.A.; SILVA, L.; ANDRADE, G.R.P. Clay Mineralogy of Brazilian Oxisols with Shrinkage Properties. **Revista Brasileira de Ciência do Solo**, v 41, p.1-16, 2017.

USGS: U.S. GEOLOGICAL SURVEY. **Mineral commodity summaries 2018**. Washington DC. USA, 2018, p. 96-97.

VALENCIA, Y., CAMAPUM, J., TORRES, F.A. Influence of biomineralization on the physico-mechanical profile of a tropical soil affected by erosive processes. **Soil Biology & Biochemistry**, v 74, p. 98-99, 2014. DOI: 10.1016/j.soilbio.2014.03.002.

VILHENA, R.M., MASCARENHA, M.M.A, SALES, M.M., ROMÃO, P.A., LUZ, M.P. Estimating the Wind-Generated Wave Erosivity Potential: The Case of the Itumbiara Dam Reservoir. **Water**, v 11, p. 342, 2019. DOI: 10.3390/w11020342.

VOLKER, A., HENRY. J.C. **Influence of wind waves on the erosion of reservoirs banks in Slovakia**. *In* Side Effects of Water Resources Management: Overviews and Case Studies. IAHS: Oxford, UK, 172 (Redbook), pp. 51-78, 1988.

WANG, Y., YOU, W., FAN, J., JIN, M., WEI, X., WANG, Q Effects of subsequent rainfall events with different intensities on runoff and erosion in a coarse soil. **Catena**, v 170, p. 100-107, 2018. DOI: 10.1016/j.catena.2018.06.008.

WCD: WORLD COMMISSION ON DAM. The report of the world commission on dams - Dams and Development. London, UK, 2000, 356 p.

APPENDIX A

PUBLISHED ARTICLE

This appendix presents a published manuscript on Water, an MDPI Journal, on 18 February 2019 (*Qualis* Capes A2).

Citation:

Vilhena, R.M.; Mascarenha, M.M.A.; Sales, M.M.; Romão, P.A.; Luz, M.P., 2019. Estimating the Wind-Generated Wave Erosivity Potential: The Case of the Itumbiara Dam Reservoir. Water, 11, 342. https://doi.org/10.3390/w11020342.

ESTIMATING THE WIND-GENERATED WAVE EROSIVITY POTENTIAL: THE CASE OF THE ITUMBIARA DAM RESERVOIR

Ricardo Moreira Vilhena [1], **Márcia Maria dos Anjos Mascarenha** [2], **Maurício Martines Sales** [2], **Patrícia de Araújo Romão** [3] and **Marta Pereira da Luz** [4]

[1] Geotechnics Postgraduate Program PPG-GECON, Federal University of Goiás, Eletrobras Furnas, BR153, km 510, Zona Rural, Aparecida de Goiânia CEP 74923-650, Goiás, Brazil; rvilhena@furnas.com.br

[2] School of Civil and Environmental Engineering, Federal University of Goiás, Universitária Ave. 1488, Setor Universitário, Goiânia CEP 74605-220, Goiás, Brazil; marciamascarenha@gmail.com (M.M.d.A.M.); sales.mauricio@gmail.com (M.M.S.)

[3] Institute of Socio-environmental Studies of the Federal University of Goiás, Esperança Ave., Samambaia Campus, Goiânia CEP 74690-900, Goiás, Brazil; patricia_romao@ufg.br

[4] Eletrobras Furnas, Industrial and Systems Engineering Postgraduate Program-MEPROS, Pontifical Catholic University of Goiás, BR153, km 510, Zona Rural, Aparecida de Goiânia CEP 74923-650, Goiás, Brazil; martaluz@furnas.com.br.

Abstract: The impact of wind waves is a process that affects reservoir shorelines, causing economic and environmental damage. The objective of this paper is to analyze the erosive potential of waves generated by winds at the shoreline of a large tropical reservoir of the Itumbiara Dam that stands along the Paranaiba River in the Midwest of Brazil. A GIS-based analysis was carried out using a wave fetch model tool (WAVE) developed by the US Geological Survey with wind data from a Doppler sensor (SODAR—SOnic Detection and Ranging) and an ultrasonic anemometer. A wave erosivity potential map was generated combining 16 fetch rasters from every 22.5° wind directions and was weighted according to its corresponding wind frequency over the rainy season. This result showed the critical areas which may have a high wave potential to increase sediment detachment along the reservoir shoreline. Finally, some of these high erosivity potential areas coincide with large erosions sites, which are detected by satellite imagery. This technique was capable of identifying the wave potential which can cause shoreline erosions and also contribute to reservoir management and support future works, including field experimental programs and shoreline erosion treatments.

Keywords: GIS; wind erosivity; reservoir shoreline

1 INTRODUCTION

Dam reservoirs are responsible for changes in the hydrodynamic characteristics of their ecosystems by increasing the erosive processes on the shorelines. In addition, there is a direct correlation between these factors and long-term reservoir deposition [1].

Erosive processes that affect the shoreline of dam reservoirs are related to the susceptibility of different shoreline erosion sources such as wave action [2] and surface runoff [3]. Rainfall is the main source of shoreline erosion, which is represented by sheet and rill erosions, as well as wave action generated by the wind or wakes of boats.

Another type of natural force acting in reservoirs is the gravity force causing slumping and soil creep. The geotechnical properties, characteristics, and dynamics of the material from the shores (i.e. the soil or rock) make the comprehension of shoreline erosion more complex due to the interactions between the geology, topography, and climate [4–6].

Sedimentation is a global issue that comes from natural and man-made erosions that influence the strategies of water managers to resolve economic and environmental problems [7–14]. This problem causes a reduction of the effective reservoir storage capacity, decreases the effective lifespan of dams and lessens various reservoir functionalities [8]. Many researchers studied the effects of erosion by rainfall [15–19] and waves [2,20–22] to predict or examine sediment yield in the reservoir.

Wave energy is the most important parameter in predicting erosion rates of water bodies and is influenced by the wave height, speed, and frequency of the wind [23,24]. Furthermore, the effects of wave erosivity depend on several factors, such as the wind direction and speed at the shoreline and vegetation cover, as well as geometric characteristics of the shoreline profile (e.g. the shape, size, and slope).

Also, the physical and chemical properties of the soil [25], through wet-dry cycles, contribute to the intensity of its degradation. However, wave energy mensuration requires wind data, bathymetry data, and offshore/onshore measurement systems, which are not always available for consultation.

The wind erosion agents can be analyzed from a low-cost perspective using a geographic information system (GIS) or a combination of geospatial model tools supported by remote sensing. Some authors applied geospatial analysis and numerical models to estimate the erosive potential of wind-generated waves in natural lakes, reservoirs, and estuaries: Mattosinho [26] and Sandford and Gao [23] used SWAN (Simulating Waves Nearshore);

Kaliraj et al. [27] and Bheeroo et al. [28] used the DSAS (Digital Shoreline Analysis System); Olson and Ventura [29] used the WAVES tool; and OndisCAD was applied by Hernández [30].

Larger lakes usually provide longer distances of open water, producing wind-generated waves with higher wave heights across a body of water, resulting in high energy waves along the shoreline, causing erosion and environmental problems.

This concept is called fetch, the distance the wind travels over water in a constant direction. In lakes (i.e. inland water), the fetch is smaller than on the coast (i.e. open water) because ocean waves have more energy and longer distances to grow. The geometry of man-made reservoirs also contributes to small fetches because they are more irregular and often present dendritic forms.

GIS techniques provide an important platform that can assist in reservoir management for the monitoring of dam reservoirs [9,20]. The WAVES tool (v.2012) has proven to be able to provide reliable results in the study of shoreline erosion in a large inland lake [29]. This tool was developed by Finlayson [20] on behalf of the U. S. Geological Survey (USGS) to estimate the erosive potential of waves from the measurements of wind and geospatial correlations. In this study, this numerical approach overestimated the erosion of the lake shoreline, but the final result was adequate to identify potential areas for erosive processes by waves.

The WAVES tool also allows the elaboration of wind fetch and wave models. In addition, the bathymetry of the reservoir is not necessary to estimate the wave potential. This geospatial tool calculates effective fetches using the recommended procedure of the Shore Protection Manual (SPM) [20].

The analysis of wind fetch with a geospatial tool allows the identification of the buffer strip of a reservoir affected by the wave impact, thus helping to make better decisions regarding the monitoring and intervention in shorelines, as well as the definition of the local sites that will probably require shoreline erosion treatment and assist in laboratory tests, including erodibility tests (i.e. wave flume tests).

Therefore, the objectives of this study are (i) to investigate the erosive potential of wind-generated waves using a GIS fetch model tool applied to an inland lake, (ii) compare wind data from two different anemometer devices, and (iii) determine the wave erosivity potential due to the action of local winds on the shoreline of the Itumbiara Dam reservoir.

2 MATERIALS AND METHODS

2.1 Study area

The study area covers the large tropical reservoir of the Itumbiara Dam (with a water surface area of 778 km^2), a South American earth-filled dam that is located between two Brazilian cities, Itumbiara-GO and Araporã-MG (Figure 1), standing along the Paranaíba River. This embankment dam lies between latitude 18°24’27” S and longitude 49°5’53” W and is the 14th largest hydroelectric power plant reservoir in a water surface area and 12th in installed capacity (i.e. 2082 MW) [31] in Brazil.

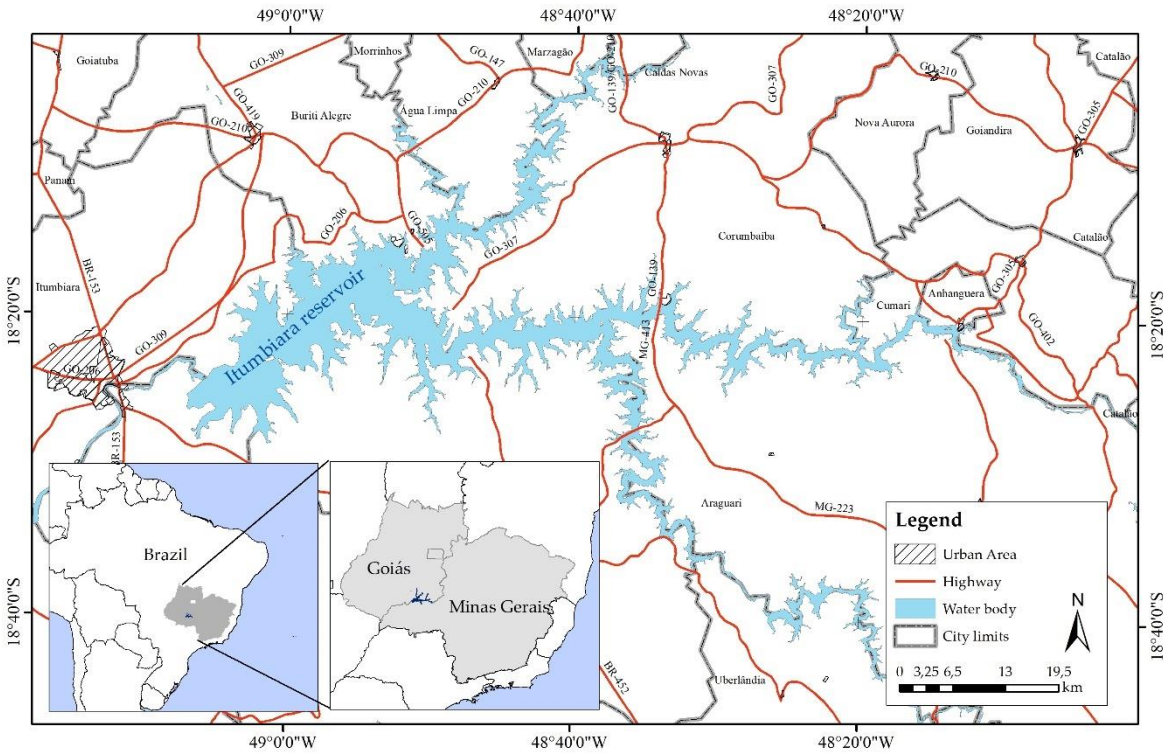

Figure 1. The study area of the Itumbiara Dam reservoir.

The bedrock geology of the Itumbiara Dam reservoir includes metamorphic rocks of pre-Cambrian age (older than 570 Ma) lying beneath the volcanic flood basalts of the Serra Geral Formation.

These rocks underwent intense tectonism, identified by various regional structural lineaments.

The lithological sequences of metamorphic rocks, from the base to the top of the bedrock, are amphibole-gneiss, biotite-gneiss, amphibolite, muscovite-gneiss, and quartzites.

Furthermore, the soil of this region is a detrital laterite cover of quaternary age (1.6 Ma). Based on the geotechnical soil classification, the residual soils and colluvium are normally deposited on the land surface and the alluvium on the riverbeds [32].

According to the soil taxonomy, the soil orders found in the study area are inceptisols, oxisols, and Entisols (or cambisols, ferralsols, and leptosols in the FAO/WRB soil system). They are related to the weathering process of soil formation from an intensely schistous metamorphic rock that shows a high erodibility potential for shoreline erosion [33].

Geomorphic features can also be observed along the shore, from nearly flat to gently lakeward-sloping (5–10°) platforms; this condition allows for higher sheet flows producing an increase in hillslope evolution. Locally, the shore zone is more predisposed to the sheet than to rill erosion [34] and the action of wave erosion.

2.2 Wave erosivity potential

The shoreline erosive potential was evaluated based on the previous work of Olson and Ventura [29] that used a wave fetch model to estimate the wave potential generated by the wind. This GIS-based model produces a wave potential raster of the combined effects of the fetch and that were weighted to produce a fetch raster.

The wave potential of the Itumbiara Dam reservoir was obtained following three main procedures, as follows: input data, preprocessing and geospatial analyses (overlay analysis and output data). Input data includes wind data from two different anemometers, precipitation data, and the land raster.

Preprocessing involves the statistical analysis of the wind behavior and suitability of the digital terrain model.

All the geospatial data were analyzed using the geoprocessing tools in ArcGIS 10.3 (v.10.3, ESRI, Redlands, CA, USA). Finally, the overlay analysis and output of data used tools in a GIS platform to elaborate the final model of wave erosivity. Figure 2 shows the flowchart of the main procedures of this study that determined the Shoreline Erosivity Potential map.

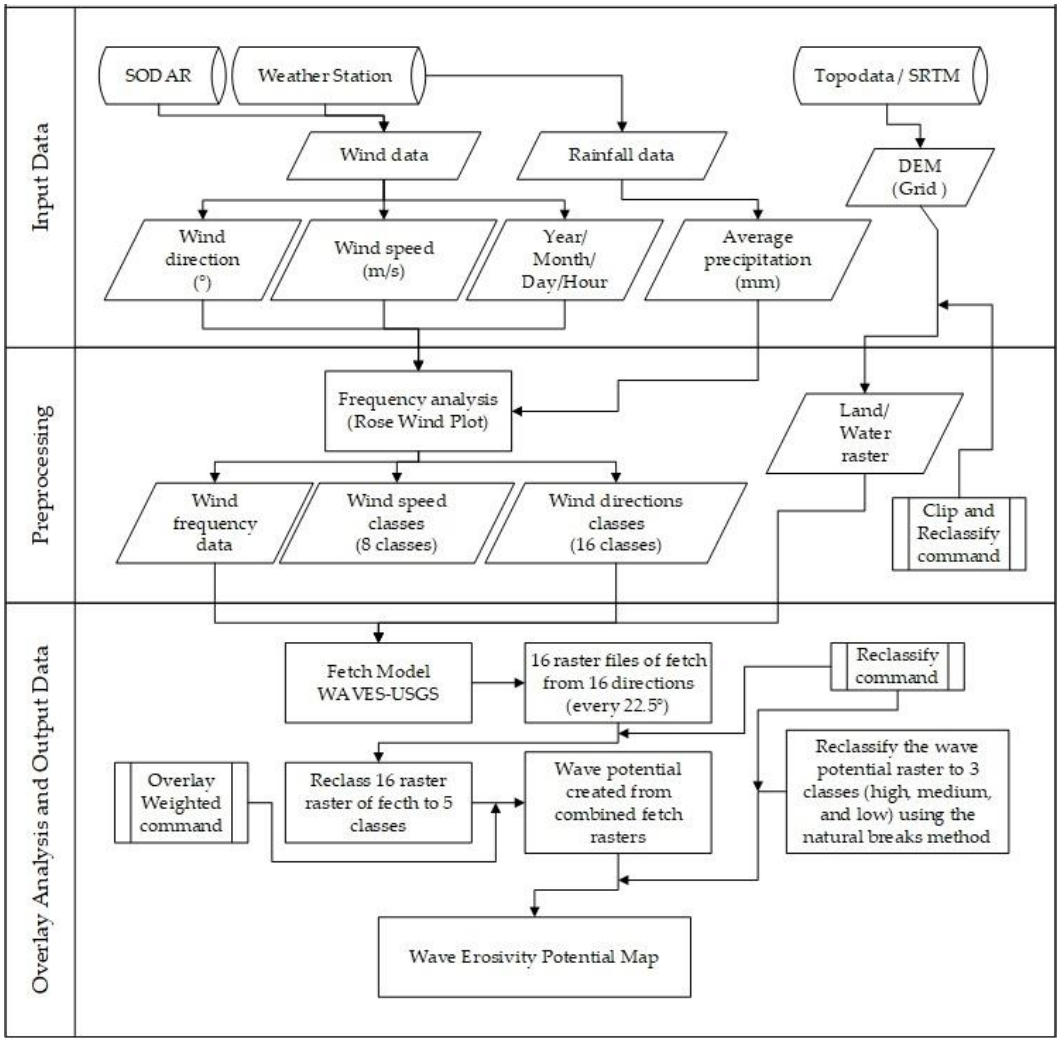

Figure 2. Shoreline Wave Erosivity Potential flowchart.

The determination wave erosivity from actual wave energy is a complex analysis that requires several input parameters, such as soil properties, shoreline geomorphology and wave characteristics (e.g. wave height, wave length, shallow, and deep-water effects). The wind-fetch model of WAVES tool ignores nearshore processes and does not consider deep water effects. This study focused on estimating wave erosive potential from the wind fetch model and qualitative analysis of the local natural characteristics (geology and geomorphology), allied with satellite imagery.

2.2.1 Input data

Wind speed and direction measurements were used in different systems as follows: an acoustic Doppler sensor, also called a SODAR (SOnic Detection And Ranging) sensor and an ultrasonic anemometer, installed at a height of 10 meters on a meteorological tower (i.e. a weather station). The acoustic sensor performs readings every 10 minutes at various

heights: 40, 50, 60, 80, 100, 120, 140, 160, 180, and 200 m. The ultrasonic device measures the wind every hour only at a height of 10 m. Both sensors were installed in different locations of the Itumbiara Dam. Furthermore, the wind data were acquired from 23 September 2014 to 23 December 2015 to coincide with the time period in which SODAR remained in that area.

The meteorological tower is located downstream of the dam, lying between latitude 18°24’27.67” S and 49°06’37.1” W longitude, and the SODAR sensor remained on the left abutment of the embankment of the Itumbiara Dam for 1 year after the removal of the tower. The SODAR sensor was located at the geographic coordinates of 18°25’38” S latitude and 49°07’06” W longitude.

The SODAR sensor is an acoustic sensor (i.e. Doppler), classified as a remote sensing system capable of measuring wind characteristics at different heights (40–200 m) without the need to install an active sensor at each reading point [35]. The models used in this research are a sonic wind profiler, Triton, and ultrasonic wind sensor, WS425, both from manufacturer Vaisala. This study does not have the aim of addressing the acquisition techniques and data accuracy between the SODAR sensor and the meteorological tower. A comparison was made to evaluate the influence of the dam barrier on the meteorological tower.

Both wind datasets must be analyzed at the same height to compare the results; also, the fetch model from WAVES tool only considers a wind data at 10-meter elevation measurements to calculate wave potential. The wind speeds from the SODAR sensor, from a reference height of 40 m (zr), were converted to a height of 10 m (z) using the equation of the wind energy profile or power-law profile, as presented in Equation (1) [35]. Furthermore, the SODAR wind data measurements were modified from the minutes format to the hours format. The vectors (the direction and intensity of the wind) were defined as a classic arithmetic measure, preserving itself as an original measure.

The power law is a mathematical relationship for the vertical wind speed profile, which can be expressed as follows:

$$U(z) = U(z_r)\left(\frac{z}{z_r}\right)^{\alpha} \tag{1}$$

where U(z) is the wind speed at height z, U(zr) is the reference wind speed at height zr, and α is the power law exponent.

The power law exponent is dependent on many parameters. However, for a theoretical reservoir surface model, a value equal to 1/7 (0.143) was defined because this ratio indicates the correspondence between wind profiles and flow over flat plates [35].

Wind data were organized into spreadsheets that necessarily include the following information: the year, month, hour, wind direction (°) and wind speed (m/s). In addition, rainfall values in millimeters were also included in the wind data spreadsheets. It was possible to divide the analysis of the winds for the dry and rainy periods, in addition to a more comprehensive climatological analysis.

The Fetch model function of the WAVES tool features the following input data: the wind direction, wind frequency, and land raster (i.e. the digital elevation model (DEM)). The land raster contains information on both terrain surfaces on the shoreline and the water mass of the reservoir. A raster image is defined as a dot matrix data structure that represents a rectangular grid of pixels with a certain value, and each pixel has a vertical elevation value (i.e. altitude). The land raster was acquired from the TOPODATA Project database [36] of the Brazilian National Institute of Space Research (INPE), and its topographic data is generated from NASA's Shuttle Radar Topography Mission (SRTM) and is resampled from 3 arc-seconds to 1 arc-second, or approximately 30 m of spatial resolution. It should be emphasized that a higher spatial resolution of the land raster produces a longer processing time and a larger amount of stored data due to the higher level of perceptible details and classes of wind directions. Thus, it is important to establish an appropriate spatial resolution and number of classes before preprocessing.

2.2.2 Preprocessing

The wind patterns acquired from the SODAR sensor and ultrasonic anemometer are examined with WRPlot View (v.8.0.0, Lake Environmental, Waterloo, ON, Canada), and then generates wind rose plots and wind rose statistics (i.e. the frequency of wind directions and wind speed for a specific time period). The wind speeds (in m/s) were grouped into eight classes according to the Beaufort Scale (Table 1). The wind directions (in degrees) were grouped into 16 classes of wind directions, determined by dividing 360 degrees into 16 wind directions (of 22.5° each), to allow the analysis of the effective fetch, as follows: 0°, 22.5°, 45°, 67.5°, 90°, 112.5°, 135°, 157.5°, 180°, 202.5°, 225°, 247.5°, 270°, 292.5°, 315°, and 337.5°.

The results were analyzed to determine which climate period (i.e. the dry and rainy season) is more severe in the Itumbiara reservoir. Olson and Ventura [29] showed an increase in the

wind speed during the rainy season, leading to higher wave height and wave energy on the shorelines. The wind data were separated by the acquisition source (i.e. the SODAR sensor and the weather station).

Table 1. Beaufort Wind Scale [1].

Force	Wind Speed (m/s)	Wind Descriptive Terms
0	<0.3	Calm
1	0.3 to 1.5	Light air
2	1.6 to 3.3	Light breeze
3	3.4 to 5.4	Gentle breeze
4	5.5 to 7.9	Moderate breeze
5	8.0 to 10.7	Fresh breeze
6	10.8 to 13.8	Strong breeze
7	13.9 to 17.1	High wind
8	≥ 17.1	Gale

Notes: [1] Winds on the Beaufort scale [37].

2.2.3 Overlay analysis and output data

The original DEM raster data cover the watershed of the reservoir. Due to the processing time, the terrain raster format was limited by the shape of an input polygon feature at EL 520 m (the Maximorum water level), using the raster processing function (i.e. the Clip command) of ArcGIS. Before using the wind fetch model, it is necessary to reclassify the DEM using the ArcGIS Reclassify tool.

This geospatial tool changes the raster values based on criteria producing specific intervals; and for applying the model, it was necessary to group the raster values into two separated classes: land, with values above 1; and water, for values equal to zero.

Overlays analysis merge several rasters using a common measurement scale and weights each according to its importance. Therefore, the resolution of the DEM will have high or low relevance because of the scale of the reservoir.

The fetches are estimated for 16 wind directions from the wind data and the reclassified land raster. This analysis was performed according to the method of the Shore Protection Manual (SPM), which calculates the arithmetic mean of the fetch lengths for each raster cell, spreading nine radials around the principal wind direction at 3° increments, forming a 24°-arc. In general, this larger arc represents a more realistic condition for shoreline evaluation. The wind-fetch model ignores any near-shore processes [20]. Figure 3 shows the SPM schematic.

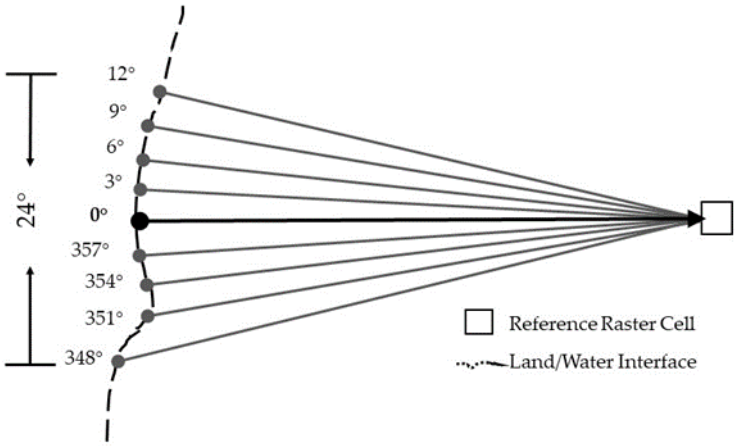

Figure 3. Schematic SPM method to evaluate the wind fetch model.

This process produces 16 fetch raster files from each individual direction and wind class, previously analyzed by the wind rose plot. These files were reclassified into five classes to allow fetch values to be processed and combined.

These rasters were combined with the Weighted Overlay tool, generating a single file with all the fetches weighted by the frequency of the winds in a certain period of time. This combination allowed us to estimate the energy potential of the waves, considering that strong winds on long fetches develop high waves. Thus, the action of the waves in the margin with greater energy will cause an erosive action of greater intensity.

A wave erosivity potential map was created by a new reclassified image of the wave potential using the natural breaks classification method in three classes: low, medium and high. In addition, the shoreline wave erosivity potential was compared with the Itumbiara soil erosion susceptibility (i.e. the sheet and rill erosions) from the work of Romão and Souza [33] and Jesus et al. [38].

3. RESULTS

The wind data from the SODAR sensor and weather station were submitted to statistical climate analysis using a WRPlot View. This software generated wind rose plots, which allowed us to observe the behavior of the wind speed and frequency of occurrence in a range of directions. Figure 4 presents a comparison between the wind rose plots of the statistical evaluations of the wind data from 23 September 2014 to 23 December 2015 of the SODAR sensor and the weather station. In addition, the wind rose plots were separated by dry (April 2014 to October 2015) and rainy (November 2014 to March 2015) seasons to determine the worst-case scenario for high wave generation.

It is also observed that the speeds obtained by the SODAR sensor (Figure 4a,b) are higher than those obtained by the weather station (Figure 4c,d), reaching speeds above 13.80 m/s. This is probably due to an attenuation in the wind speed caused by the position of the weather station downstream of the Itumbiara Dam.

However, the wind direction distributions were consistent. Differences between wind speeds measured by the SODAR sensor and the tower sonic anemometer were verified [39] and justified by the methodology of device acquisition.

Statistical analysis shows that a preferred wind direction in the northeastern sector lies in the range of 67.5° to 90°. The wind speeds during the rainy season, as expected, show higher intensities, on average approximately 3%, in comparison to the dry season, independent of the measuring device. However, strong winds from the southwest (azimuth from 225° to 247.5°) were recorded.

The most frequent wind speed values lie in the range of 3.30 to 5.40 m/s. Therefore, the wind data from the rainy season were selected to produce the wind fetch maps and wave erosivity potential maps.

This is because the analyses have shown that rainstorms have a clear influence on the erosiveness and wave intensity [29,40]. Shoreline erosions are stronger in the tropical South American summer (i.e. the high water season) than in the winter (i.e. the low water season).

Previous work on the Itumbiara reservoir [41-43] shows that the wind mainly blows from the northeast and east and that the wind speeds range between 3.0 and 8.0 m/s, thereby confirming the findings and conclusions presented in this study.

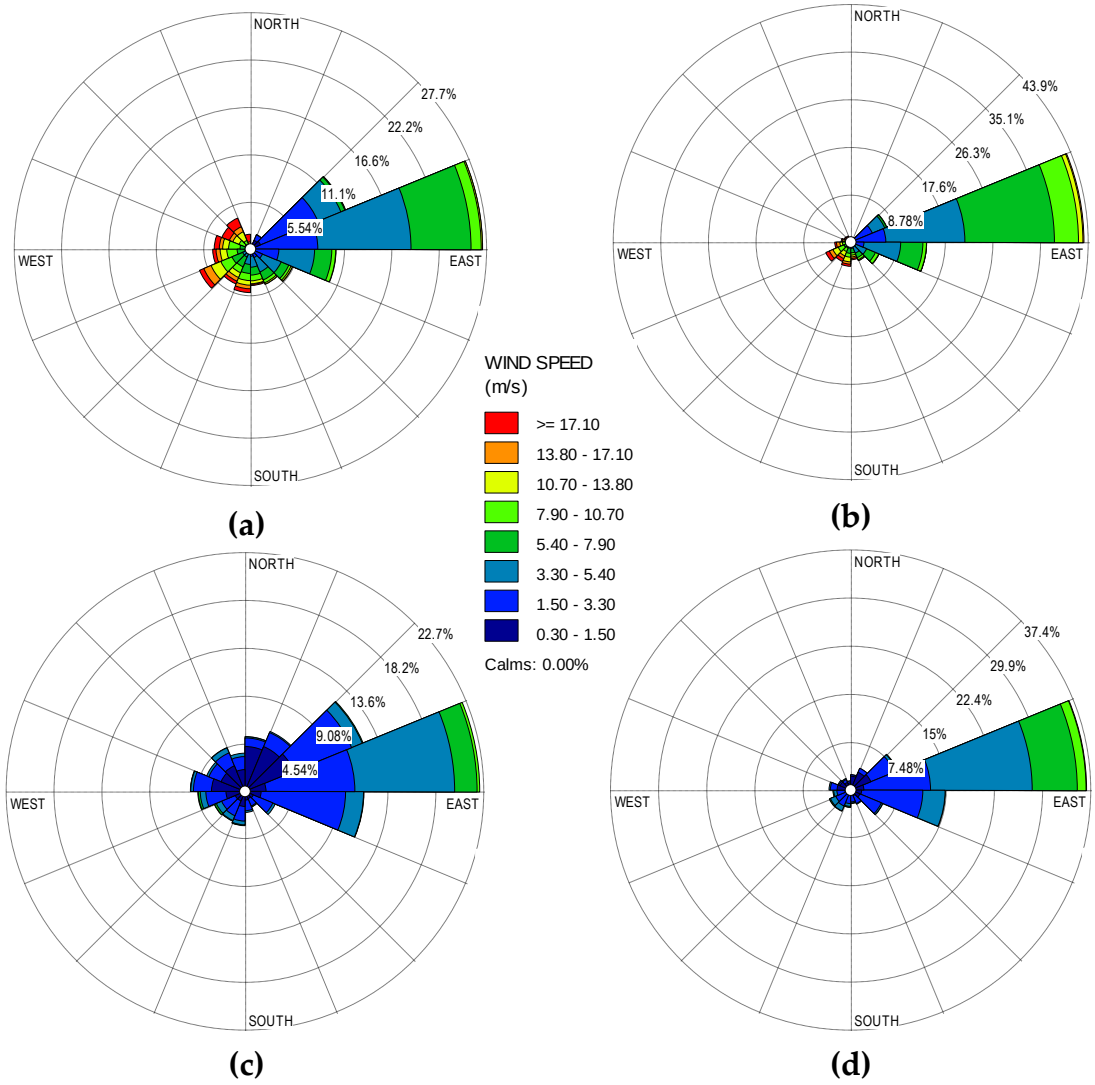

Figure 4. The wind rose plots, separated by rainy (a) and dry (b) seasons of SODAR, and rainy (c) and dry (d) seasons for the weather station.

The shoreline that is affected by waves depends on the wind conditions (i.e. speed, duration, direction, and fetch) and the shape of the land. In most situations, the inland reservoir has small fetch lengths because the fetches are limited by the landforms surrounding the waterbody.

In general, the Itumbiara reservoir has an irregular (i.e. not uniform) fetch length path, but this parameter, ranging from 45° to 70°, has a straight path showing longer fetches, allowing the wind to blow for a greater distance before reaching the shoreline reservoir. The main wind direction for the erosive process in the Itumbiara reservoir is 67.5°.

In general, the characteristics of the wind waves that approach the shoreline include wind speed and direction, storm/wind duration, fetch length, and reservoir bathymetry [40]. The wave heights and wave periods are also lower if the waves are generated in shallow rather than deep water [40].

Thus, during periods of rainfall, the wave energies have different intensities in the swallow and in deep water. The wave actions are more severe on the shore profile toe [40]. The longest fetch length, wind frequency, and wind speed result in greater shoreline erosion.

After the wind rose plot analyses, the original land raster (DEM) was modified with a new single file including a water body and shoreline at an elevation of 520 m. This raster file only has the objective of representing the interface between the land and water.

Therefore, after preprocessing the input data, this study proceeds with the WAVES tool applications. A high-resolution land raster dataset allows a better definition of islands and shore boundaries.

However, increasing the spatial resolution of land rasters requires more processing time. In the case of the Itumbiara reservoir, at least 12 hours were needed to calculate 16 fetches from the data with the 30-m spatial resolution.

The fetches were compiled for 16 azimuthal directions, including four cardinal directions shown in Figure 5. Wind speeds below 0.3 m/s were not observed in the rose plots. In addition, the Doppler sensor had difficulties acquiring speeds below 4 m/s and above 18 m/s [35].

It was observed that the wind directions of 45° and 67.5° are the main fetch lengths that affected the shoreline, especially in the right margin. The wind directions of 90° to 337.5° have the lowest fetch lengths compared with those of 0° to 67.5°.

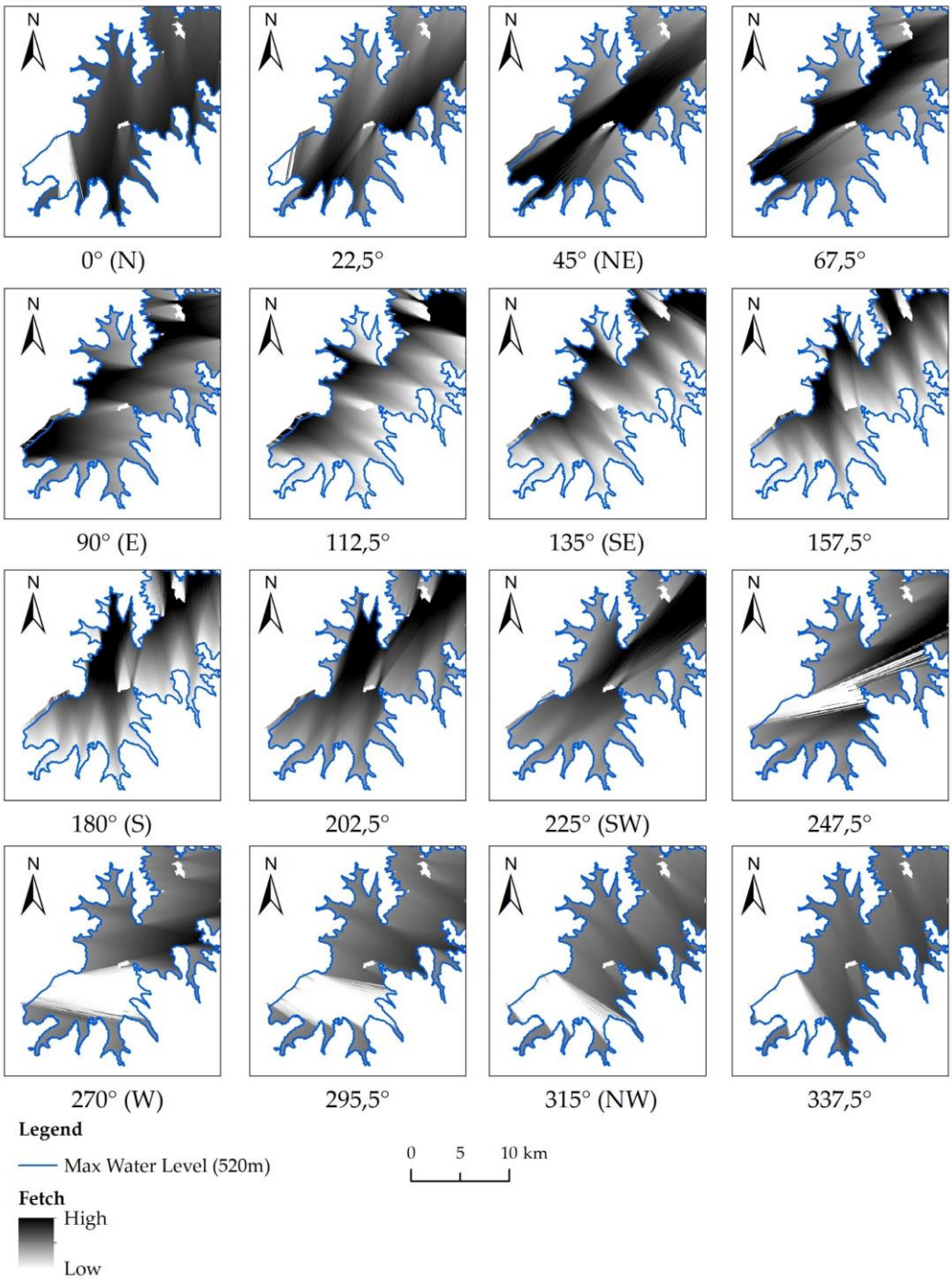

Figure 5. The fetches of the 16 normal wind directions.

Figure 6 illustrates the raster image of the input data to the WAVES tool, such as the original DEM raster and land / water raster. Additionally, the preprocessed fetch model data and reclassified fetches were used to produce the wave potential. The DEM and reclassified land / water raster are shown in Figure 6a, b, respectively. Figure 6c presents the main fetch that affects the shoreline of the Itumbiara reservoir, and Figure 6d illustrates the reclassified main fetch.

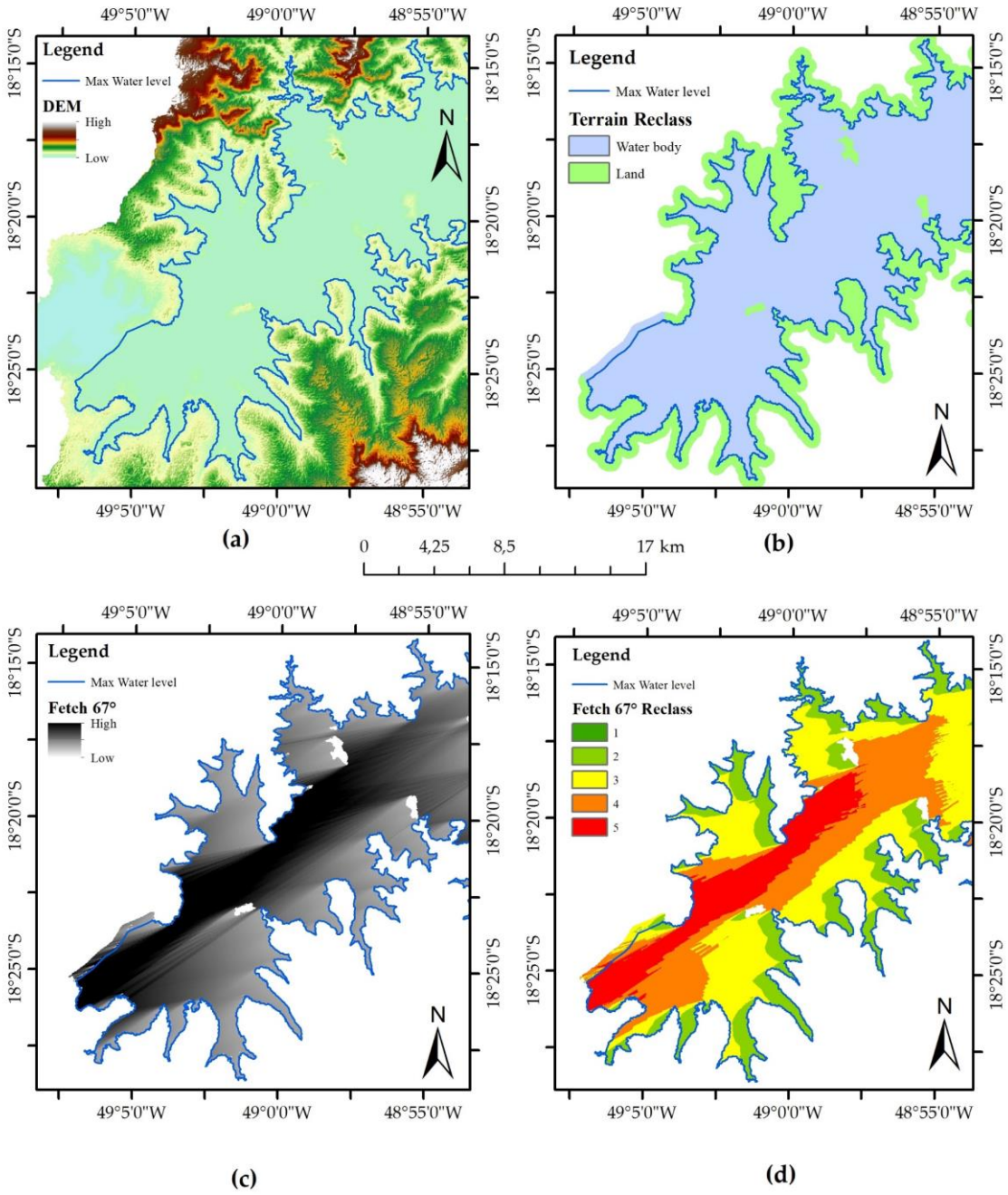

Figure 6. (a) Digital Elevation Model, (b) reclassified Land/Water raster, (c) fetch of 67.5° wind direction, and (d) reclassified raster of the fetch of 67.5°.

The WAVES tool produce 16 fetch raster files, and each individual raster was reclassified by the manual method of classification into five classes to remove the negative data and reduce the processing time. These rasters were combined with the weighted overlay tool according to the corresponding wind frequency during a specific time period. Once again, the Reclassify tool was used on this single weighted file to generate three new classes of raster

with the Natural Breaks classification method producing the wave erosivity potential of the Itumbiara reservoir.

This method of classification (or Jenks method) is a GIS common criterion for dividing a significantly different dataset for a suitable arrangement of values into a certain number of homogenous classes reducing the variance within classes and maximizing the variance between each class.

The shoreline of the land/water raster buffer strip is 200 m wide, which represents the boundary of the reservoir limited to the left by the elevation of 520 m (the Maximorum water level) and to the right by the elevation of 510 m. This range was chosen because it corresponds to the maximum water level variations.

In addition, this wave erosivity potential was generated for both wind data obtained from the SODAR sensor and the weather station. The comparison between these maps presented very similar values.

Only the map generated by the wind sound profiler data (i.e. the Doppler sensor) is illustrated in this paper and presented in Figure 7, which covers almost the entire Itumbiara reservoir. It is a small-scale map (i.e. 1:250.000) and indicates the area with the highest occurrence of highly erosive wave potential.

This map also presents the occurrences of water erosion processes, mapped by field visits and satellite image analysis, according to Jesus et al. [37]. The erosion occurrence illustrated in Figure 7 includes sheet erosion, rill erosion and the association of those erosions, and mass movement. Some sheet erosion-mapped sites coincide with high shoreline wave erosion.

Table 2 presents the wave erosivity potential perimeter calculated in values of meters, kilometers, and percent in ArcGIS. According to this estimation, the high impact of waves affects the shoreline of Itumbiara reservoir only along 2% of its perimeter.

Table 2. Wave Erosivity Potential of the Itumbiara-GO reservoir perimeter.

Class	**m**	**km**	**(%)**
Low	1,088,811	1089	64%
Medium	590,483	590	34%
High	33,820	34	2%

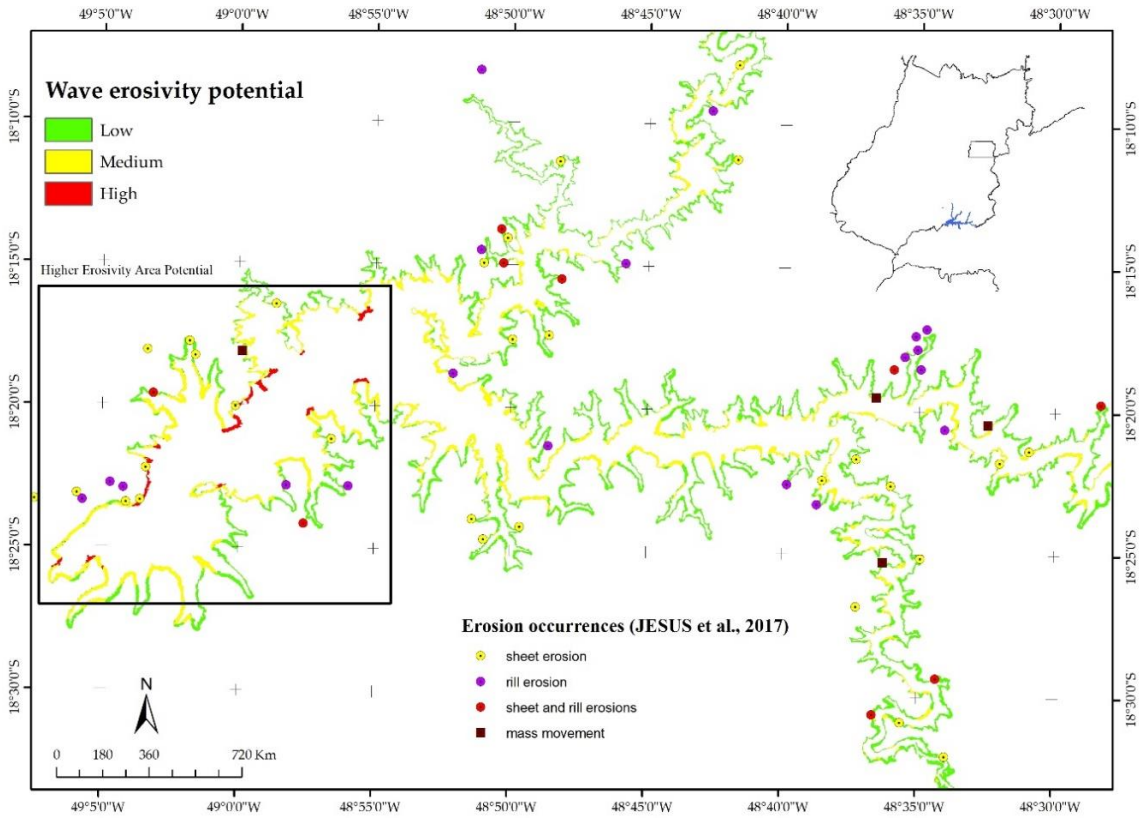

Figure 7. Wave erosivity potential map of the Itumbiara Dam reservoir

DISCUSSION

It was observed that the high values of shoreline wave erosion are concentrated near the Itumbiara Dam. Due to this, an area of high wave erosivity potential was delimited in Figure 7, and a large-scale map is illustrated in Figure 8. It was verified that the greatest influence of the waves occurs mainly in the right margin of the Itumbiara reservoir and is caused by the winds from the northeast. In addition, 14 buffer strips of high values are numbered and indicated in this figure for further analyses.

Figure 9 presents the sheet (inter-rill) erosion susceptibility to surface runoff [33,37]. High to moderately high values of susceptibility were observed along the shores. The shoreline of the Itumbiara-GO reservoir has medium to low wave erosivity along most of its perimeter and coincides with medium values of sheet erosion susceptibility from the comparison of Figures 9 and 10. Additionally, the higher values of susceptibility to sheet erosion match the high values of wave erosivity potential. However, there is no direct correlation between erosion processes due to the complexity of the soil properties and the erosion agents. The correct correlation requires determination of the wave erosion susceptibility, which was not the object of this study and requires both fieldwork and laboratory experiments.

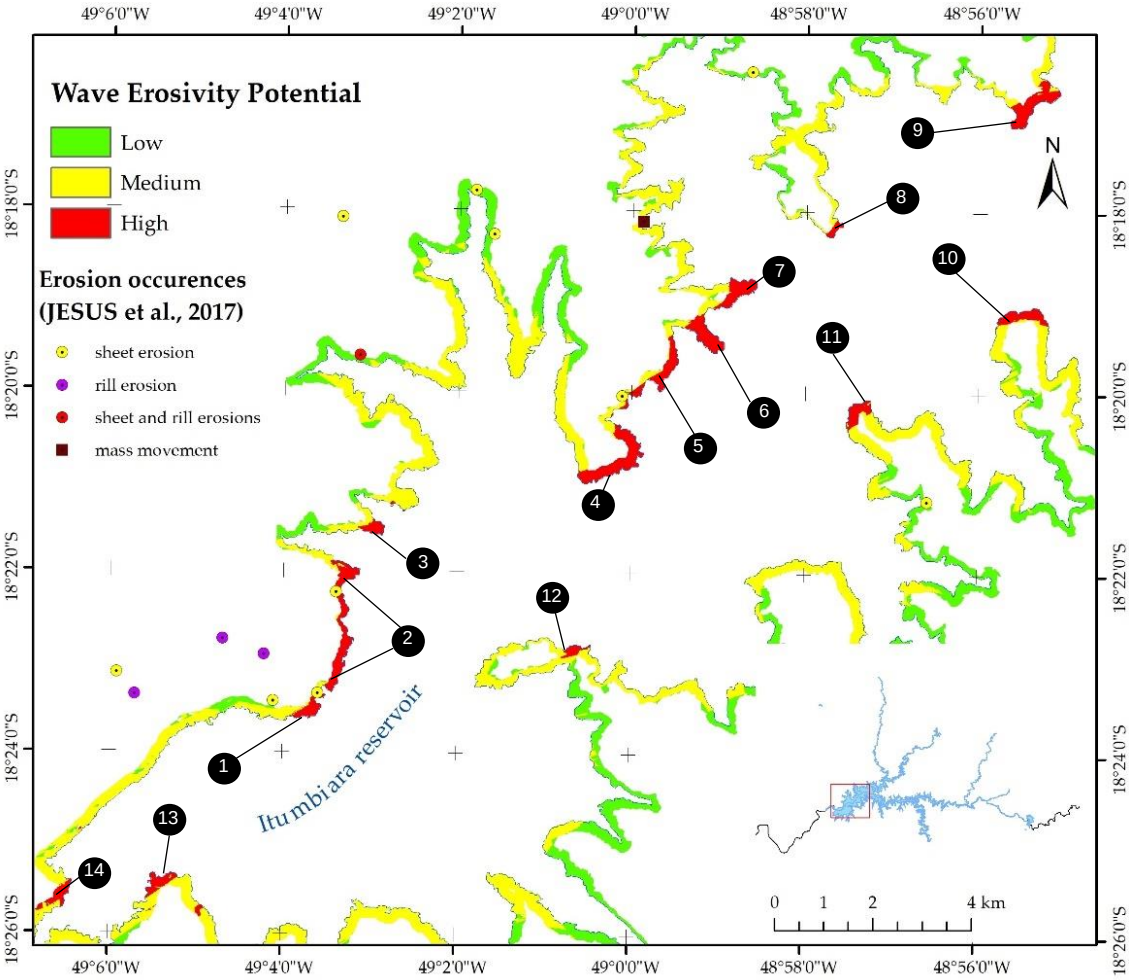

Figure 8. The area at the shoreline with higher wave erosivity potential from the SODAR sensor data.

Remote sensing represents a powerful technique for wave erosion investigations, and it was used to confirm the high potential sites on the wave erosivity potential map. Satellite imagery was acquired in December 2015 at the ESRI/ArcGIS World Imagery platform from the GeoEye satellite owned by Digital Globe. Evidence of semicircular or a half ellipse form of small steep banks and exposed soil was verified on imagery as a shoreline erosion feature. Even the concentration of high wave erosivity values on the small buffer strip of the shoreline reservoir, according to Table 2, was found at large erosion sites from remote sensing analysis. Figure 10 shows four large areas with advanced erosive processes that coincide with higher wave erosive potentials.

These sites were denoted as Area 1 (Figure 10a), Area 2 (Figure 10b), Area 3 (Figure 10c), and Area 4 (Figure 10d). Areas 1 and 2 are located in a more critical position in the reservoir. Due to the most frequent occurrences of the main wind direction of 67.5°, the higher fetch and major erosive potential are on the shores. These areas lie in the buffer strips 1 and 2, as

illustrated in Figure 8. Areas 3 and 4 were not as affected by the main fetch, and they are located in the buffer strips 3 and 4, as shown in Figure 8.

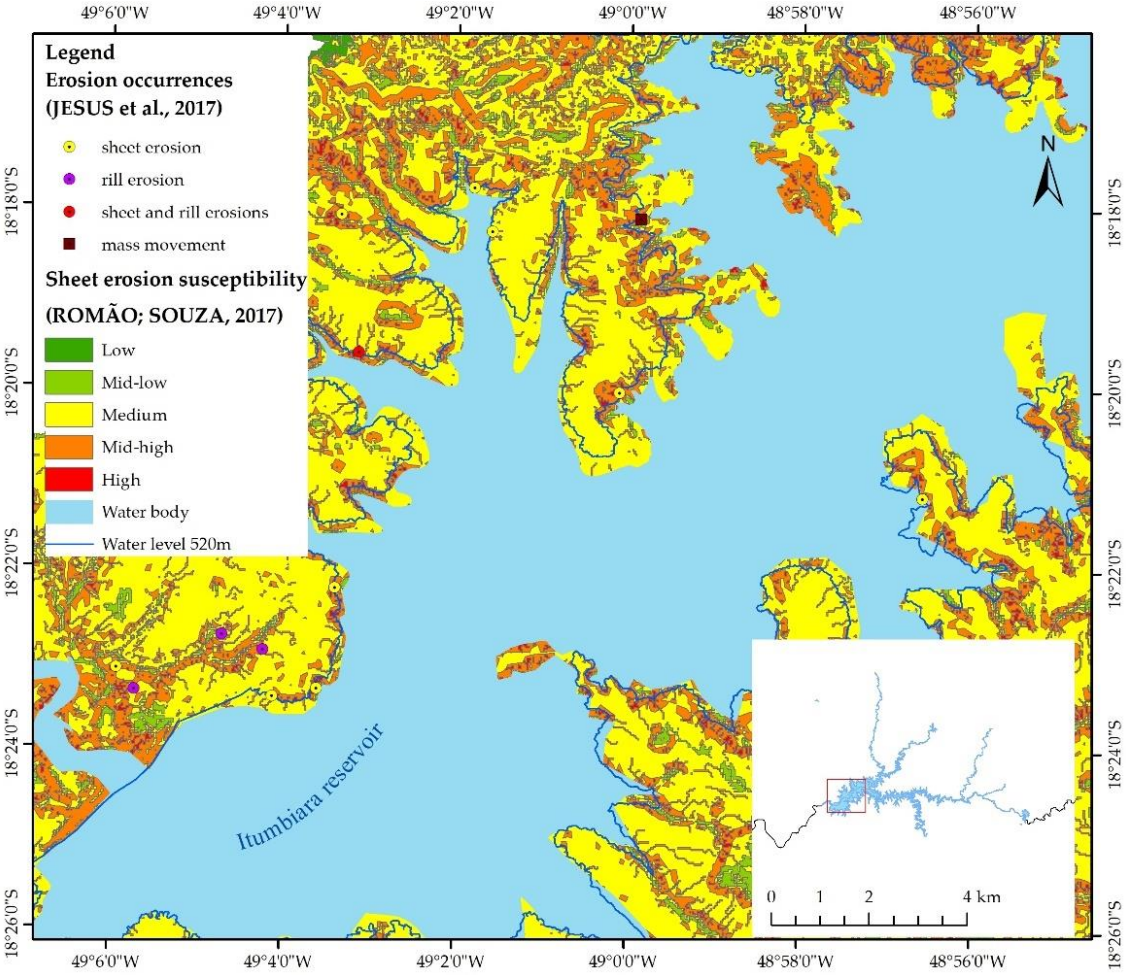

Figure 9. Soil erosion susceptibility of the Itumbiara reservoir with field erosion occurrences.

The management strategy of a shoreline erosion dam reservoir must have awareness of all the main sources of erosive agents, such as wave action [40] and surface runoff [44], which are increased by climate changes [45]. Reservoir managers should also include historical hydrometeorological data in their surveys to evaluate changes in the wind patterns and average precipitation [45]. Shoreline erosions [29] and sediment depositions are a consequence of climate changes [45].

Reservoir managers shall undertake impact assessments to evaluate wave erosivity on the shoreline and the adjacent land, thereby avoiding or reducing environmental problems. This study provides the knowledge with which to choose the effective shoreline erosion control installations, such as nonstructural, structural, bioengineering, and biotechnical [46].

Therefore, this geospatial analysis of shoreline erosion can be used to assist reservoir governance in civil or criminal liabilities for environmental damage.

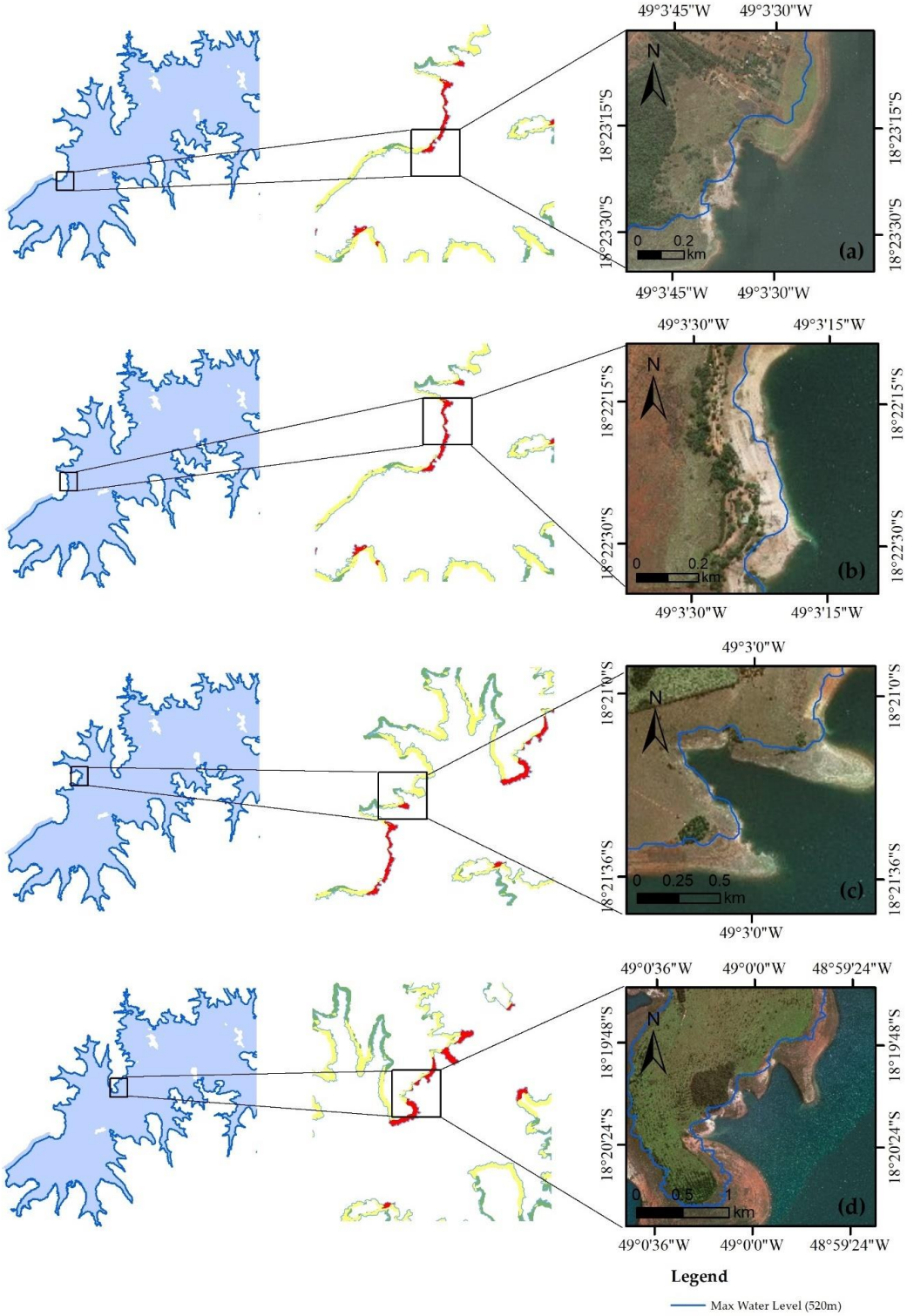

Figure 10. Satellite imagery of the shoreline of erosion sites that have a direct relationship with high values of wave erosivity potential. (a) Area 1. (b) Area 2. (c) Area 3. (d) Area 4.

CONCLUSION

Erosive processes are commonly studied using three different approaches: numerical modeling (GIS-based or non-geospatial analysis), field monitoring and laboratory tests. In this work, a GIS-based model was tested to evaluate the wave erosivity potential due to the wind-generated waves in a Brazilian dam reservoir.

The reservoir of the Itumbiara-GO was the object of this work since previous studies [33,34,37] have verified a high susceptibility to shoreline erosion caused by rainfall. However, it was also necessary to study the influence of the wind.

The conclusions obtained in this paper are as follows:

1. The WAVES tool allows the examination of the reservoir shoreline erosion by wave potential and

guide reservoir research and management.

2. Higher wave erosivity potential areas must be examined with satellite imagery.

3. In general, the wind anemometer and acoustic Doppler sensor are appropriate for estimating the wave erosivity potential.

4. The method presented by Olson and Ventura [29] is applicable to reservoirs used as hydropower systems located in other countries.

The current work has some limitations, such as not including the qualitative erosion rate by wind-generated waves, the lack comparison from rainfall and runoff ratios with soil erosions, the punctual extrapolation of the wind data to analyses a large reservoir and the short period of time (1 year) for statistical analysis from two wind datasets. Besides, the current geospatial method [29] has successfully highlighted some higher erosivity wave potential areas which coincide with large erosions sites detected by satellite imagery. In addition, wave shoreline susceptibility is needed for better correlations. This research project will continue and estimation of the erosion rate will be included in the future.

The analysis of the wind behavior requires several years of the dataset for better understanding; therefore, a long time period of wind data should be included in upcoming work. However, in this paper, the aim was to compare the two sensors, although they did not show significant differences between wind direction data and wind frequency data, any of which is feasible for this method.

Finally, this methodology may support campaigns to collect soil samples for experimental research, to act as a basis for reservoir governance decisions and to promote interventions such as stabilization installations.

AUTHOR CONTRIBUTIONS

R.M.V. wrote the paper and analyzed the data; All authors contributed to manuscript writing; M.M.d.A.M., M.M.S., P.d.A.R. and M.P.d.L. revised the manuscript; M.M.d.A.M. and P.d.A.R. contributed to research development; M.M.S. and M.P.d.L. managed the research and development projects.

FUNDING

This research was funded by Agência Nacional de Energia Elétrica-ANEEL (Brazilian Electricity Regulatory Agency), ANEEL PD.0394-1603/2016.

ACKNOWLEDGMENT

This paper is part of BioEngineering Project (0394-1603/2016) and is financially supported by the Furnas Centrais Elétricas SA, a state-owned company and subsidiary of Eletrobras, and the Agência Nacional de Energia Elétrica-ANEEL (Brazilian Electricity Regulatory Agency). The authors would like to thank the Gerência de Programação Energética e Hidrometeorologia of Eletrobras Furnas for providing the wind data. The authors also greatly appreciate the anonymous reviewers and editors for their constructive and insightful comments in relation to this manuscript.

CONFLICTS OF INTEREST

The authors declare no conflict of interest.

REFERENCES

1. Huang, C.-C.; Lai, J.-S.; Lee, F.-Z.; Tan, Y.-C. Physical Model-Based Investigation of Reservoir Sedimentation Processes. Water 2018, 10, 352. [CrossRef]

2. Edil, T.B. Erosion of Coastal Slopes and Landslides. In Proceedings of the Geo-Congress 2013, San Diego, CA, USA, 3–7 March 2013. [CrossRef]

3. Zhang, Y.; Zhong, P.-A.; Chen, J.; Bing, J.; Xu, D.;Wang, M. Impacts of Climate Change and Human Activities on the Three Gorges Reservoir Inflow. Water 2017, 9, 957. [CrossRef]

4. Enlow, H.K.; Fox, G.A.; Guertault, L. Watershed Variability in Streambank Erodibility and Implications for Erosion Prediction. Water 2017, 9, 605. [CrossRef]

5. Ferreira, V.; Panagopoulos, T.; Andrade, R.; Guerrero, C.; Loures, L. Spatial variability of soil properties and soil erodibility in the Alqueva reservoir watershed. Solid Earth 2015, 6, 383–392. [CrossRef]

6 Su, X.; Nilsson, C.; Pilotto, F.; Liu, S.; Shi, S.; Zenga, B. Soil erosion and deposition in the new shorelines of the Three Gorges Reservoir. Sci. Total Environ. 2017, 599–600, 1485–1492. [CrossRef]

7. Kondolf, G.M.; Gao, Y.; Annandale, G.W.; Morris, G.L.; Jiang, E.; Zhang, J.; Cao, Y.; Carling, P.; Fu, K.; Guo, Q.;et al. Sustainable sediment management in reservoirs and regulated rivers: Experiences from five continents. Earth's Future 2014, 2, 256–280. [CrossRef]

8. Esmaeili, T.; Sumi, T.; Kantoush, S.A.; Kubota, Y.; Haun, S.; Rüther, N. Three-Dimensional Numerical Study of Free-Flow Sediment Flushing to Increase the Flushing Efficiency: A Case-Study Reservoir in Japan. Water 2017, 9, 900. [CrossRef]

9. Shumba, A.; Gumindoga, W.; Togarepi, S.; Masarira, T.P.; Chikuni, E. A remote sensing and GIS based application for monitoring water levels at Kariba dam. In Proceedings of the EAI International Conference for Research, Innovation and Development for Africa (ACRID), Victoria Falls, Zimbabwe, 20–21 June 2017.[CrossRef]

10. Abera, F.F.; Asfaw, D.H.; Engida, A.N.; Melesse, A.M. Optimal Operation of Hydropower Reservoirs under Climate Change: The Case of Tekeze Reservoir, Eastern Nile. Water 2018, 10, 273. [CrossRef]

11. Liu, H.; Deng, B.; Liu, Y.; Jiang, C.;Wu, Z.; Long, Y. Preliminary Numerical Analysis of the Efficiency of a Central Lake Reservoir in Enhancing the Flood and Drought Resistance of Dongting Lake. Water 2018, 10, 225. [CrossRef]

12 Rahmani, V.; Kastens, J.H.; deNoyelles, F.; Jakubauskas, M.E.; Martinko, E.A.; Huggins, D.H.; Gnau, C.;Liechti, P.M.; Campbell, S.W.; Callihan, R.A.; et al. Examining Storage Capacity Loss and Sedimentation Rate of Large Reservoirs in the Central U.S. Great Plains. Water 2018, 10, 190. [CrossRef]

13. Forsythe, K.W.; Schatz, B.; Swales, S.J.; Ferrato, L.J.; Atkinson, D.M. Visualization of Lake Mead Surface Area Changes from 1972 to 2009. ISPRS Int. J. Geo-Inf. 2012, 1, 108–119. [CrossRef]

14. Schleiss, A.J.; Franca, M.J.; Juez, C.; De Cesare, G. Reservoir Sedimentation. J. Hydraul. Res. 2016. [CrossRef]

15. Elçi, S.; Bor, A.; Çalı¸skan, A. Using numerical models and acoustic methods to predict reservoir sedimentation. Lake Reserv. Manag. 2009, 25, 297–306. [CrossRef]

16. Gelagay, H.S. RUSLE and SDR Model Based Sediment Yield Assessment in a GIS and Remote Sensing Environment: A Case Study of Koga Watershed, Upper Blue Nile Basin, Ethiopia. Hydrol. Curr. Res. 2016, 7, 2–10. [CrossRef]

17 Heathcote, A.J.; Filstrup, C.T.; Downing, J.A. Watershed Sediment Losses to Lakes Accelerating Despite Agricultural Soil Conservation Efforts. PLoS ONE 2013, 8, e53554. [CrossRef]

18 Lin, C.Y.; Lin, W.T.; Chouc, W.C. Soil erosion prediction and sediment yield estimation: The Taiwan experience. Soil Tillage Res. 2002, 68, 143–152. [CrossRef]

19. Shen, Z.Y.; Gong, Y.W.; Li, Y.H.; Hong, Q.; Xu, L.; Liu, R.M. A comparison of WEPP and SWAT for modeling soil erosion of the Zhangjiachong Watershed in the Three Gorges Reservoir Area. Agric. Water Manag. 2009, 96, 1435–1442. [CrossRef]

20. Rohweder, J.; Rogala, J.T.; Johnson, B.L.; Anderson, D.; Clark, S.; Chamberlin, F.; Potter, D.; Runyon, K. Application of Wind Fetch and Wave Models for Habitat Rehabilitation and Enhancement Projects—2012 Update; USACE and USGS-UMESC: La Crosse, WI, USA, 2012; pp. 1–52.

21. Menezes, A.V. Proposta Metodológica Para Estudo de Perda de Massa de Solos Situados em Bordas de Reservatório Devido ao Efeito de Ondas Por Meio de um Canal Hidráulico. Masters Thesis, University of Goiás, Goiânia, Brazil, 2018. (In Portuguese)

22. Zheng, J.-W.; Jia, Y.-G.; Liu, X.-L.; Sjan, H.-X.; Zhang, M.-S. Experimental study of the variation of sediment erodibility under wave-loading conditions. Ocean Eng. 2013, 68, 14–26. [CrossRef]

23. Sandford, L.P.; Gao, J. Influences of Wave Climate and Sea Level on Shoreline Erosion Rates in the Maryland Chesapeake Bay. Estuar. Coast. 2018, 41, 19–37. [CrossRef]

24. Marques, M.; Andrade, F.O.; Guetter, A.K. Conceito do Campo de Fetch e sua Aplicação ao Reservatório de Itaipu. RBRH 2013, 18, 243–253. (In Portuguese) [CrossRef]

25. Fonseca, L.A.M.; Lani, J.L.; Fernandes Filho, E.I.; Marques, E.A.G.; Ferreira, W.P.M. Avaliação da erodibilidade de um cambissolo de Juiz de Fora, Minas Gerais. Geotecnia 2016, 136, 143–156. (In Portuguese) [CrossRef]

26 Mattosinho, G.O. Dissipação de Energia de Ondas Geradas por Vento em Reservatórios de Barragens, Devido à Presença de Vegetação. Masters's Thesis, UNESP, Ilha Solteira, Brazil, 2016. (In Portuguese)

27. Kaliraj, S.; Chandrasekar, N.; Magesh, S. Impacts of wave energy and littoral currents on shoreline erosion/accretion along the south-west coast of Kanyakumari, Tamil Nadu using DSAS and geospatial technology. Environ. Earth Sci. 2014, 71, 4523–4542. [CrossRef]

28 Bheeroo, R.A.; Chandrasekar, N.; Kaliraj, S.; Magesh, N.S. Shoreline change rate and erosion risk assessment along the Trou Aux Biches–Mont Choisy beach on the northwest coast of Mauritius using GIS-DSAS technique. Environ. Earth Sci. 2016, 75, 1–12. [CrossRef]

29. Olson, E.R.; Ventura, S.J. Geospatial methods to examine shoreline erosion in the Chippewa Flowage: A case study. Lake Reserv. Manag. 2012, 28, 170–175. [CrossRef]

30. Hernández, J.E.I. Avaliação da Fragilidade das Margens do Reservatório de Ilha Solteira—SP, Utilizando as Geotecnologias como Ferramentas de Análise Ambiental. Masters's Thesis, UNESP, Ilha Solteira, Brazil, 2014. (In Portuguese)

31. Luz, M.P.; Beevers, L.C.; Cuthbertson, A.J.S.; Medero, G.M.; Dias, V.S.; Nascimento, D.T.F. The Mitigation Potential of Buffer Strips for Reservoir Sediment Yields: The Itumbiara Hydroelectric Power Plant in Brazil.Water 2016, 8, 489. [CrossRef]

32. Furnas Centrais Elétricas S/A. Aproveitamento Hidrelétrico de Itumbiara—Relatório Final do Projeto Básico—Volume I—Texto; n°. HE-161-R02-0975; HIDROSERVICE Engenharia Ltda: São Paulo, Brazil, 1974; pp. 1–55. (In Portuguese)

33 Romão, P.A.; Souza, N.M. Aspectos geológicos e hidrogeológicos na deflagração e evolução da erosão hídrica em margens de reservatórios. In Erosão em Bordas de Reservatório, 1st ed.; Sales, M.M., Camapum de Carvalho, J., Mascarenha, M.M., Luz, M.P., Angelim, R.R., Souza, N.M., Eds.; Gráfica UFG: Goiânia, Brazil, 2017; pp. 153–170. ISBN 978-85-495-0118-9. (In Portuguese)

34. Sales, M.M. Monitoramento e Estudo de Técnicas Alternativas na Estabilização de Processos Erosivos em Reservatórios de UHEs, 2nd Work Report; FUNAPE: Goiânia, Brazil, 2014; pp. 1–40. (In Portuguese)

35. Manwell, J.F.; Mcgowan, J.G.; Roges, A.L. Wind Energy Explained: Theory, Design, and Application, 2nd ed.; John Willey and Sons Ltd.: West Sussex, UK, 2010; pp. 46–85. ISBN 978-0-470-01500-1.

36. Topodata. Available online: http://www.dsr.inpe.br/topodata/ (accessed on 10 January 2018).

37. The Beaufort Wind Force Scale. Available online: https://en.wind-turbine-models.com/winds (accessed on 28 August 2018).

38. Jesus, A.S.; Sousa, M.S.; Nascimento, D.T.F.; Romão, P.A.; Camapum de Carvalho, J. A influência de aspectos geomorfológicos, de cobertura do solo e climáticos no surgimento e evolução de processos erosivos no entorno de reservatório. In Erosão em Bordas de Reservatório, 1st ed.; Sales, M.M., Camapum de Carvalho, J., Mascarenha, M.M., Luz, M.P., Angelim, R.R., Souza, N.M., Eds.; Gráfica UFG: Goiânia, Brazil, 2017; pp. 172–192. ISBN 978-85-495-0118-9. (In Portuguese)

39. Kelley, N.D.; Jonkman, B.J.; Scott, G.N.; Pichugina, Y.L. Comparing Pulsed Doppler LIDAR with SODAR and Direct Measurements forWind Assessment. In Proceedings of the AWEA's 2007WindPower Conference, Los Angeles, CA, USA, 3–6 June 2007; pp. 1–21.

40. Lawson, D.E. Erosion of Northern Reservoir Shores, an Analysis et Application of Pertinent Literature; CRREL, Monograph 85-1; USACE: Hanover, NH, USA, 1985; pp. 35–37.

41. Assireu, A.; Pimenta, F.; Souza, V. Assessment of wind power potential of hydroelectric reservoirs. In Energy Resources: Development, Distribution and Exploitation, 1st ed.; Alcantara, E.H., Ed.; INPE: Sao Paulo, Brazil, 2011; pp. 1–28. ISBN 978-1-61324-520-0.

42. Assireu, A.; Pellegrini, C.C.; Pimenta, F. Intensificação do vento devido a influências do relevo: Evidências a partir de modelos numéricos e medidas in situ. Ciência e Natura 2013. (In Portuguese) [CrossRef]

43. Pellegrini, C.C.; Neto, A.V.L.; Assis, J.V.B.; Assireu, A. Um Estudo Numérico da Intensificação do Vento em Reservatórios de Centrais Hidroelétricas da Região Sudeste do Brasil. Ciência e Natura 2016, 38, 197–203. (In Portuguese) [CrossRef]

44 Li, Y.; Huang, T.; Ma,W. Correlation Analysis of Rainstorm Runoff and Density Current in a Canyon-Shaped Source Water Reservoir: Implications for Reservoir Optimal Operation. Water 2018, 10, 447. [CrossRef]

45. De Souza Dias, V.; Pereira da Luz, M.; Medero, G.M.; Tarley Ferreira Nascimento, D. An Overview of Hydropower Reservoirs in Brazil: Current Situation, Future Perspectives and Impacts of Climate Change. Water 2018, 10, 592. [CrossRef]

46. Northwest Regional Planning Commission. Shoreline Stabilization Handbook for Lake Champlain and Other Inland Lakes; Lake Champlain Basin Program and US Environmental Protection Agency: St. Albans, VT, USA, 2004; pp. 1–49. ISBN 0-9754546-0-9.

APPENDIX B

WAVE FLUME TESTS

This appendix presents test sheets containing a schematic of the results and photographs from wave flume tests.

Lateritic Soil Reference Soil / untreated

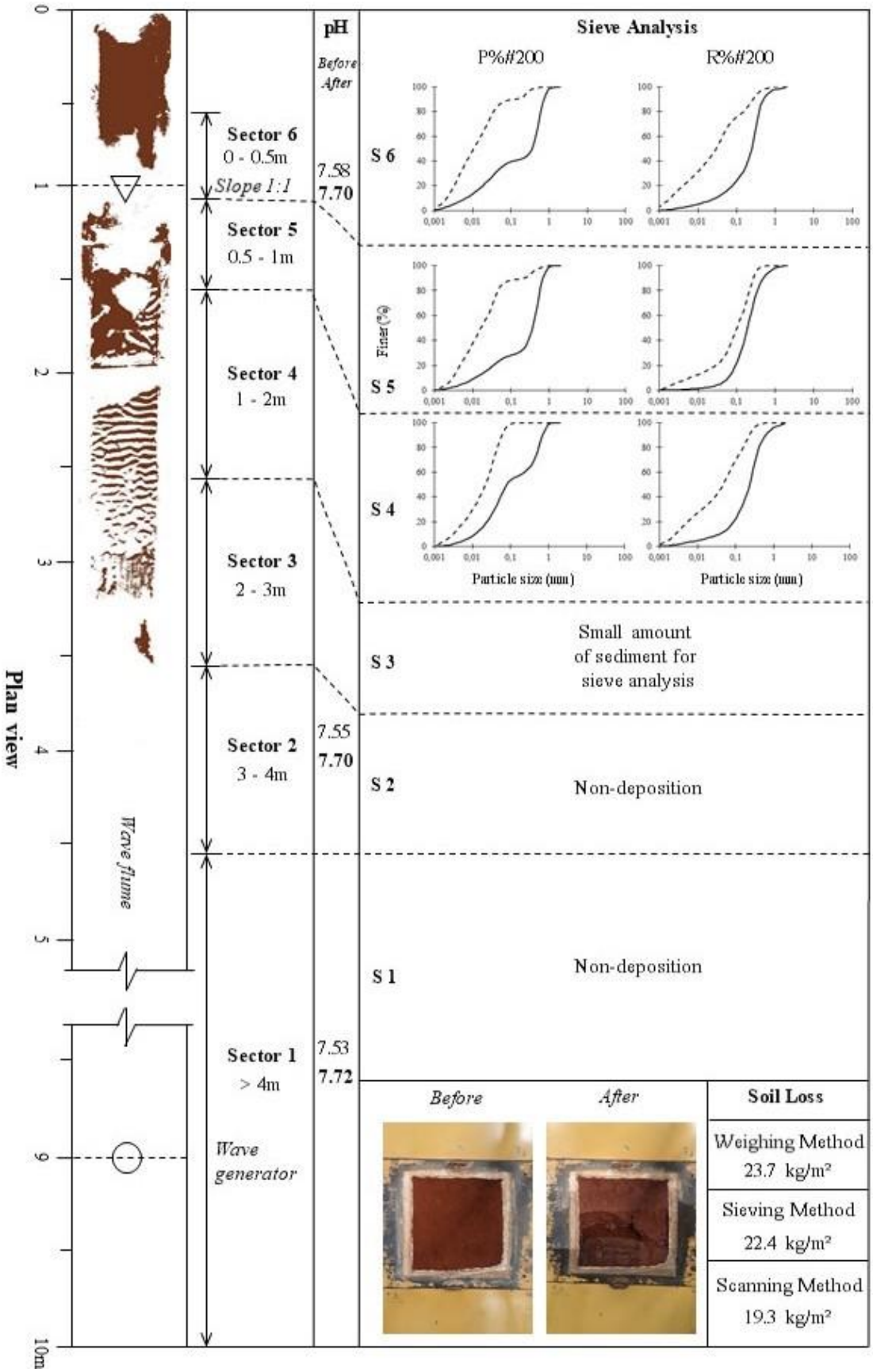

Lateritic Soil with 1 % of solution of lime and 1-day curing time

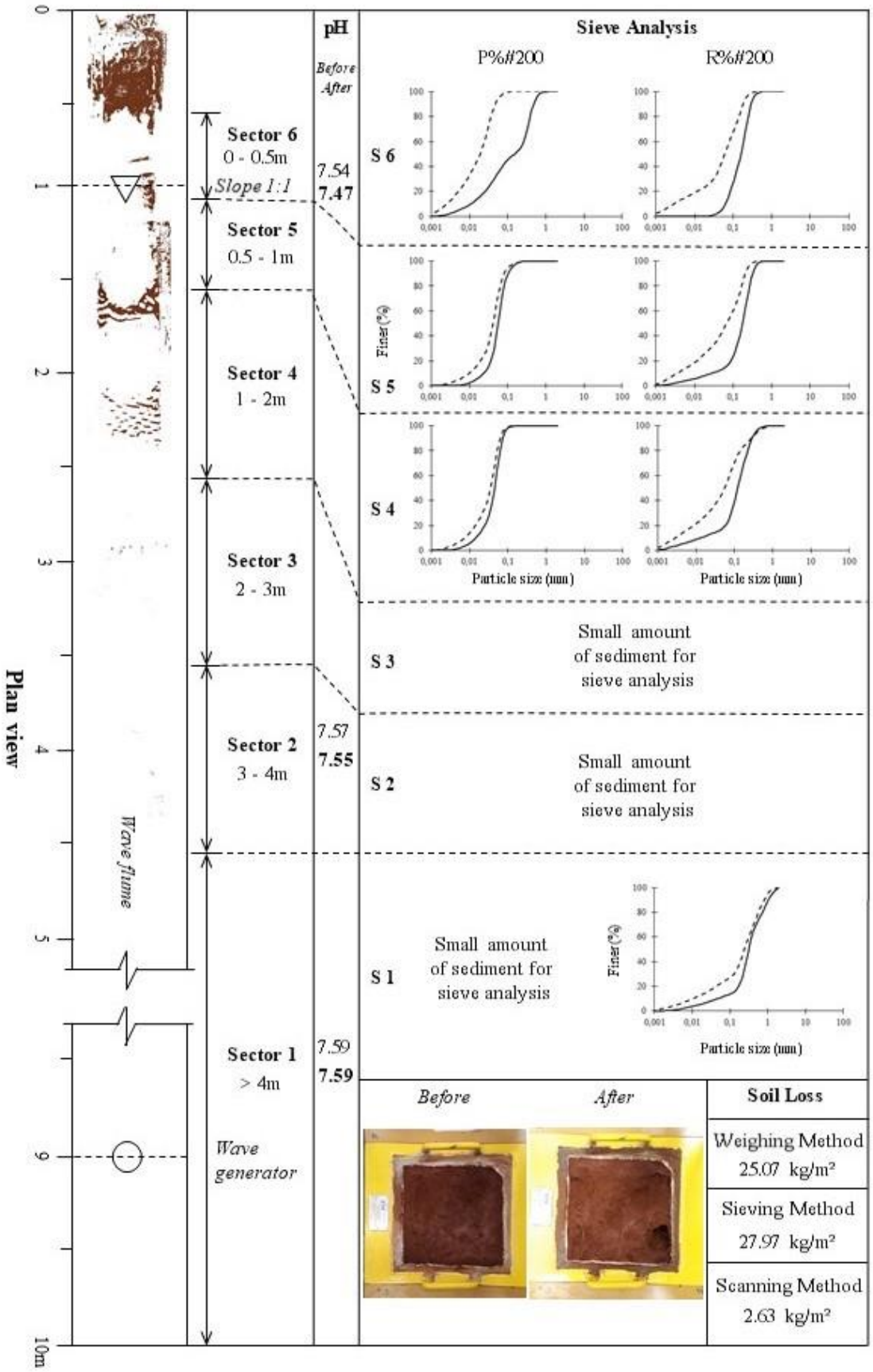

Lateritic Soil with 1 % of lime and 1-day curing time

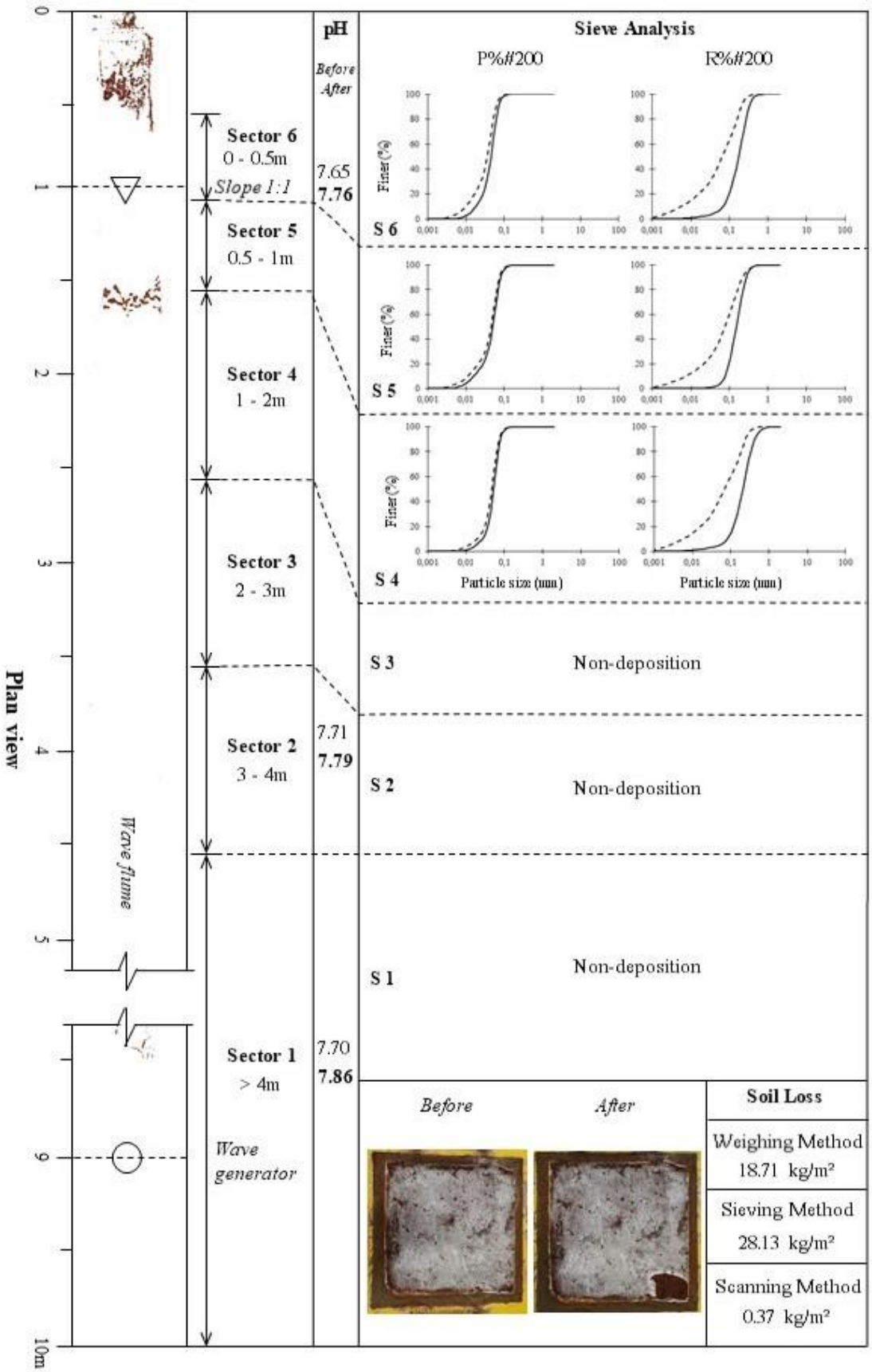

Lateritic Soil with 2 % of lime and 1-day curing time

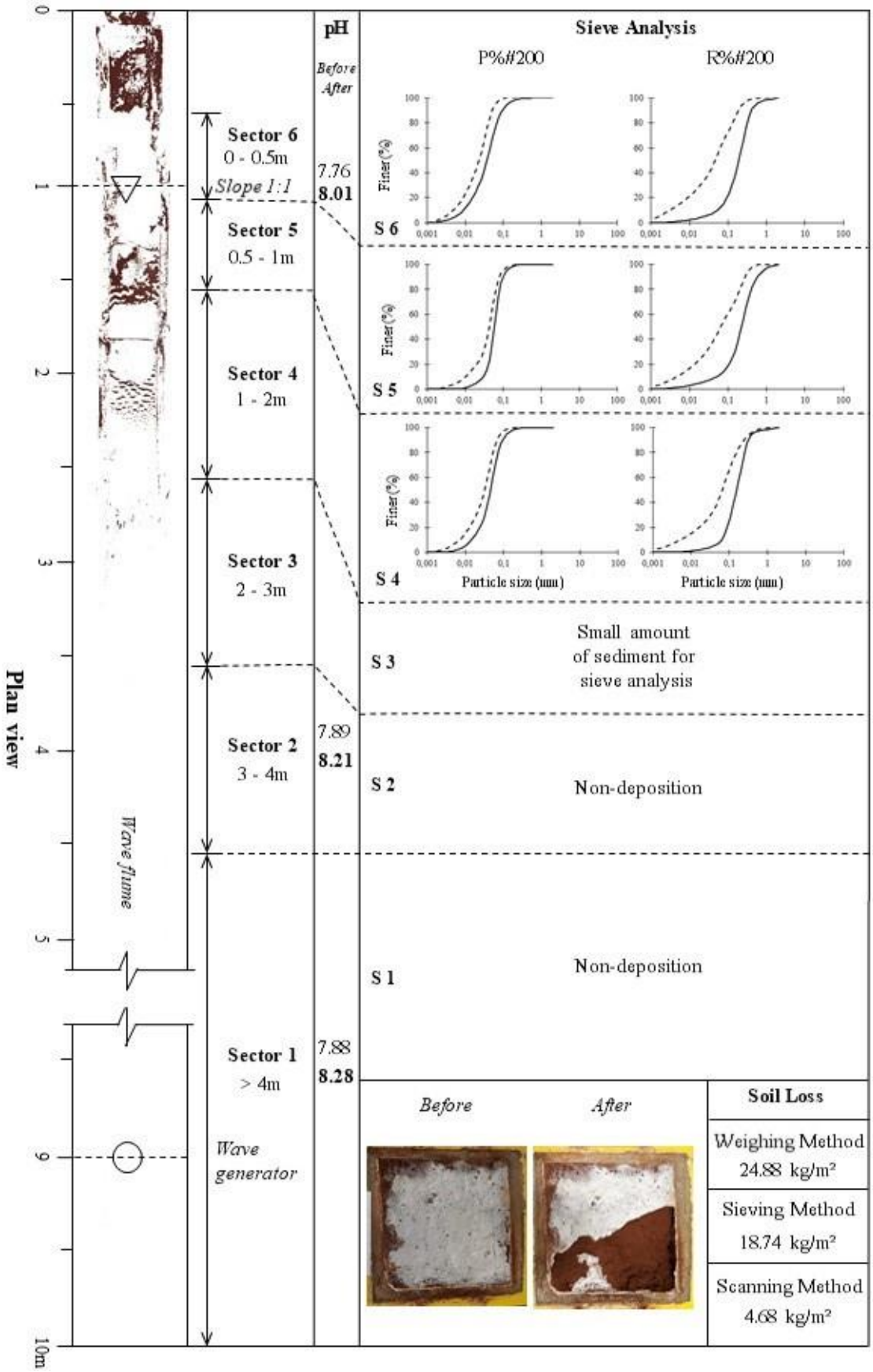

Lateritic Soil with 4 % of lime and 1-day curing time

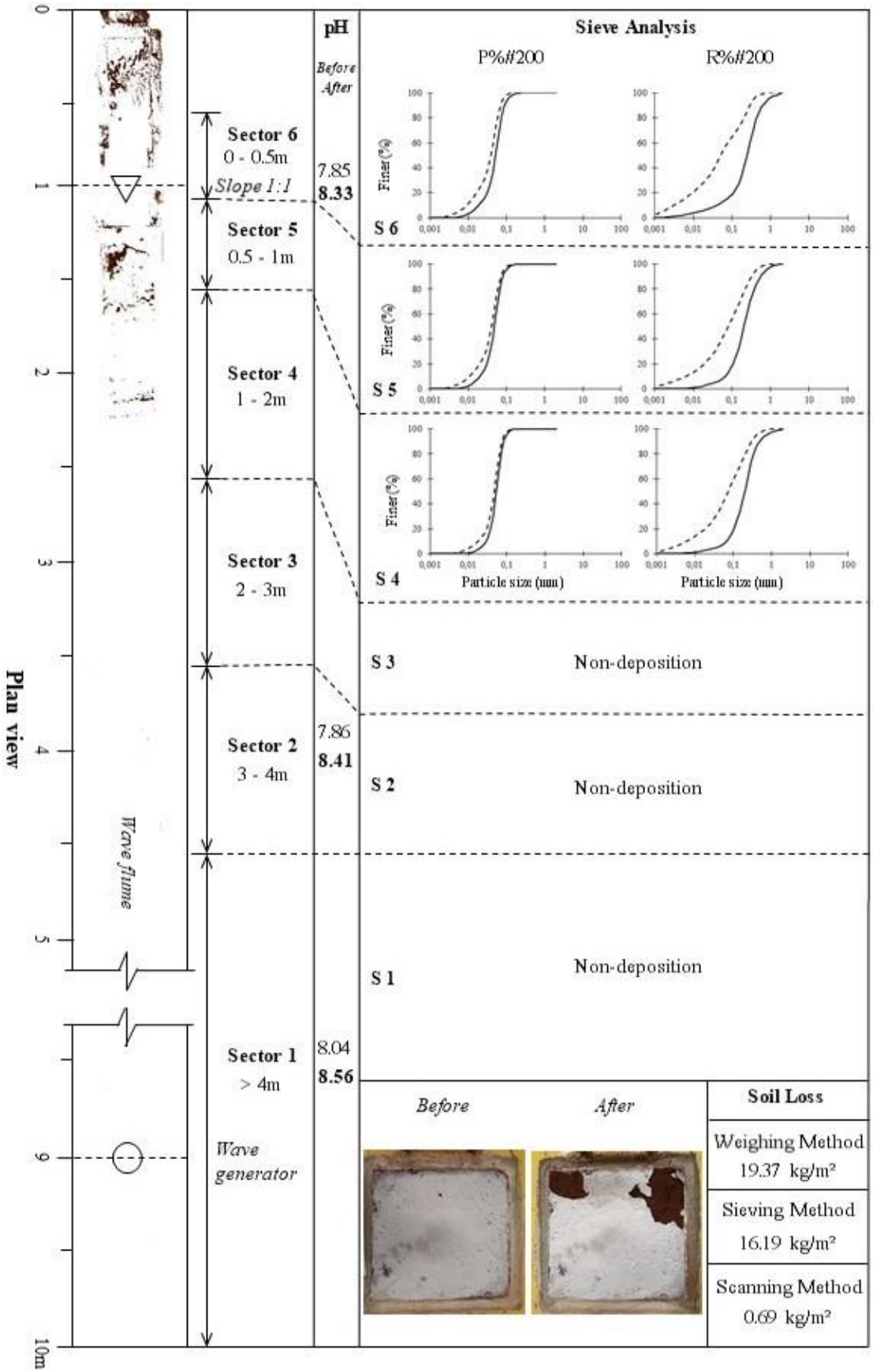

Lateritic Soil with 1 % of lime and 7-days curing time

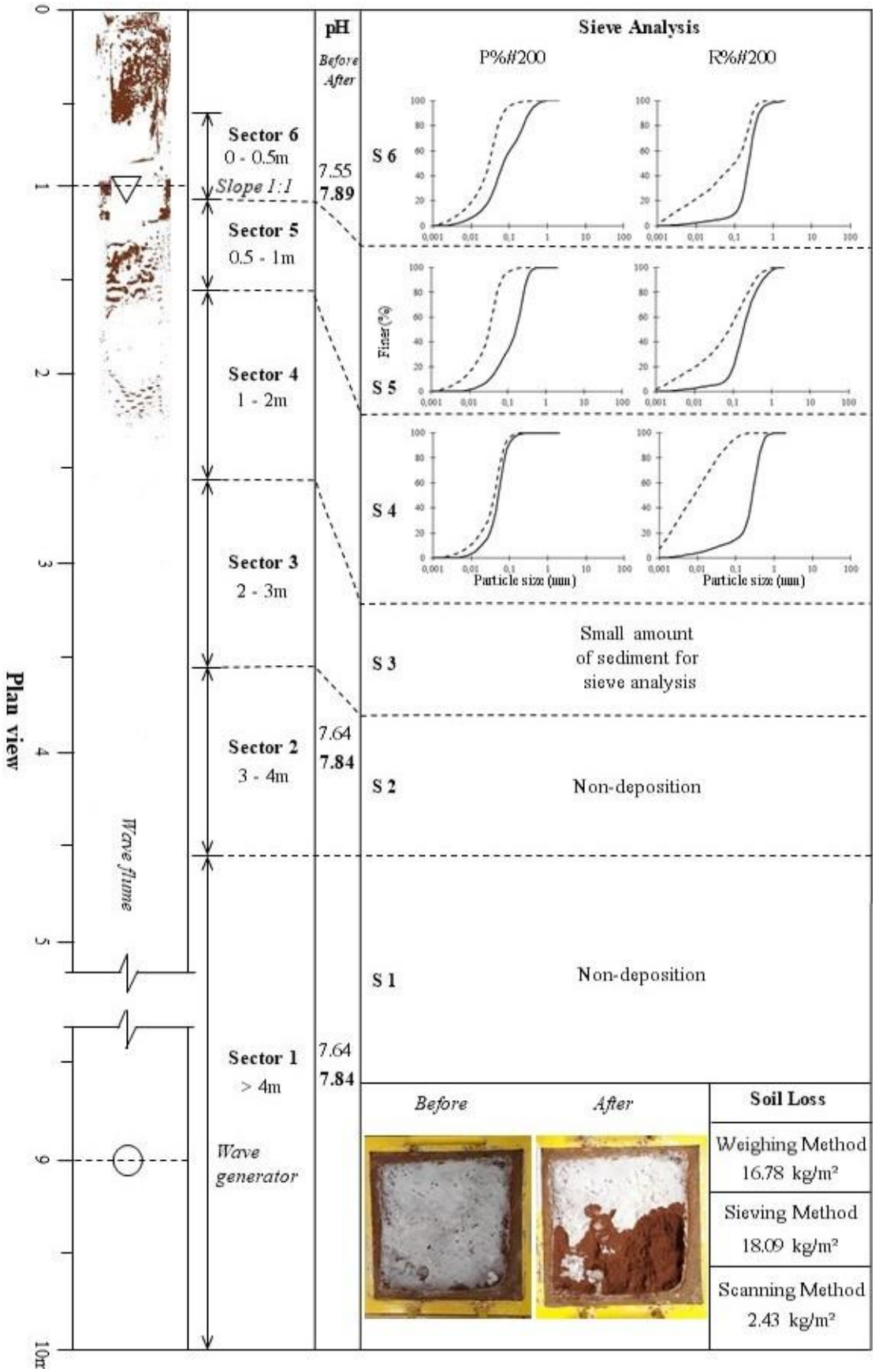

Lateritic Soil with 2 % of lime and 7-days curing time

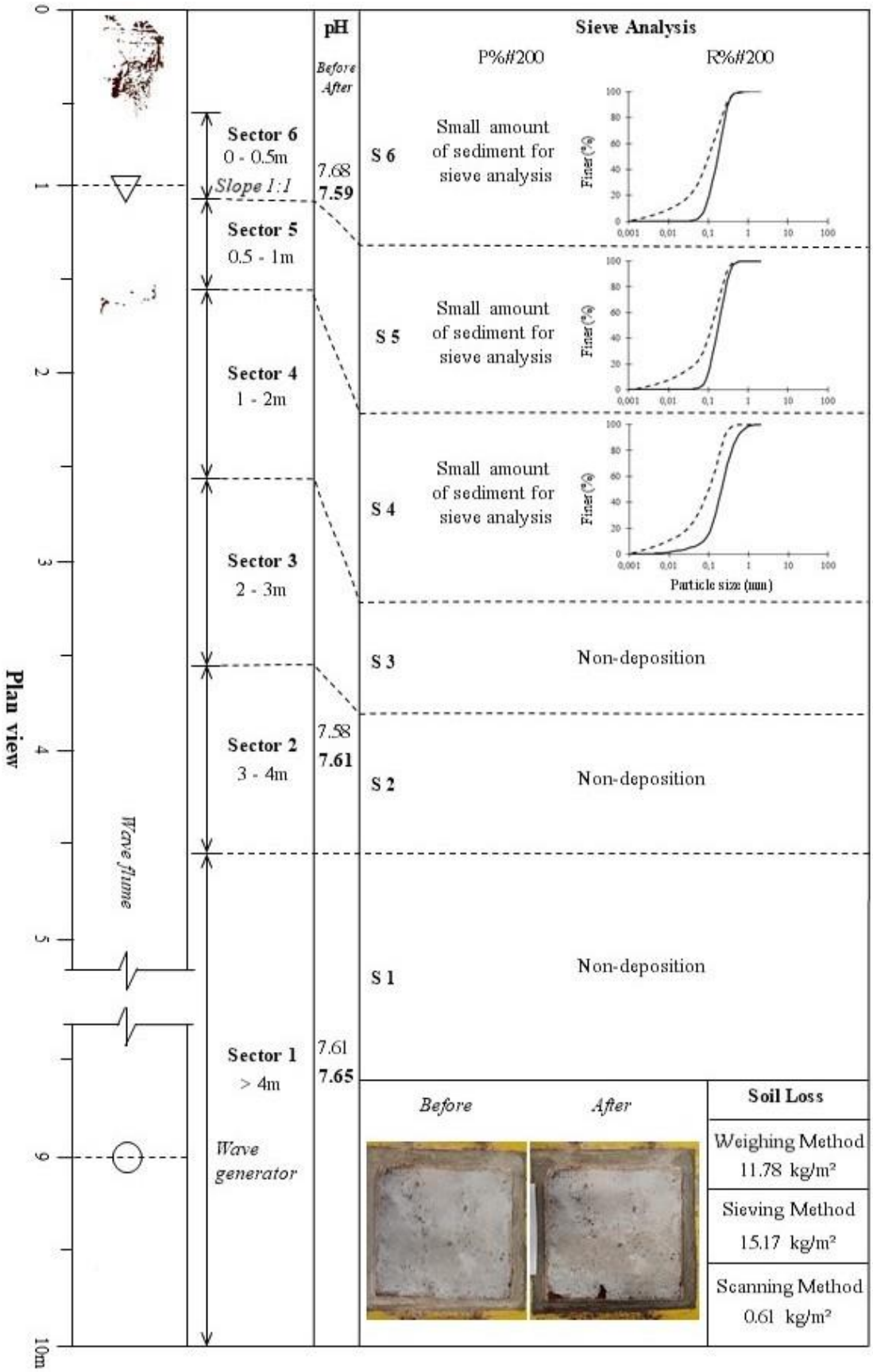

Lateritic Soil with 4 % of lime and 7-days curing time

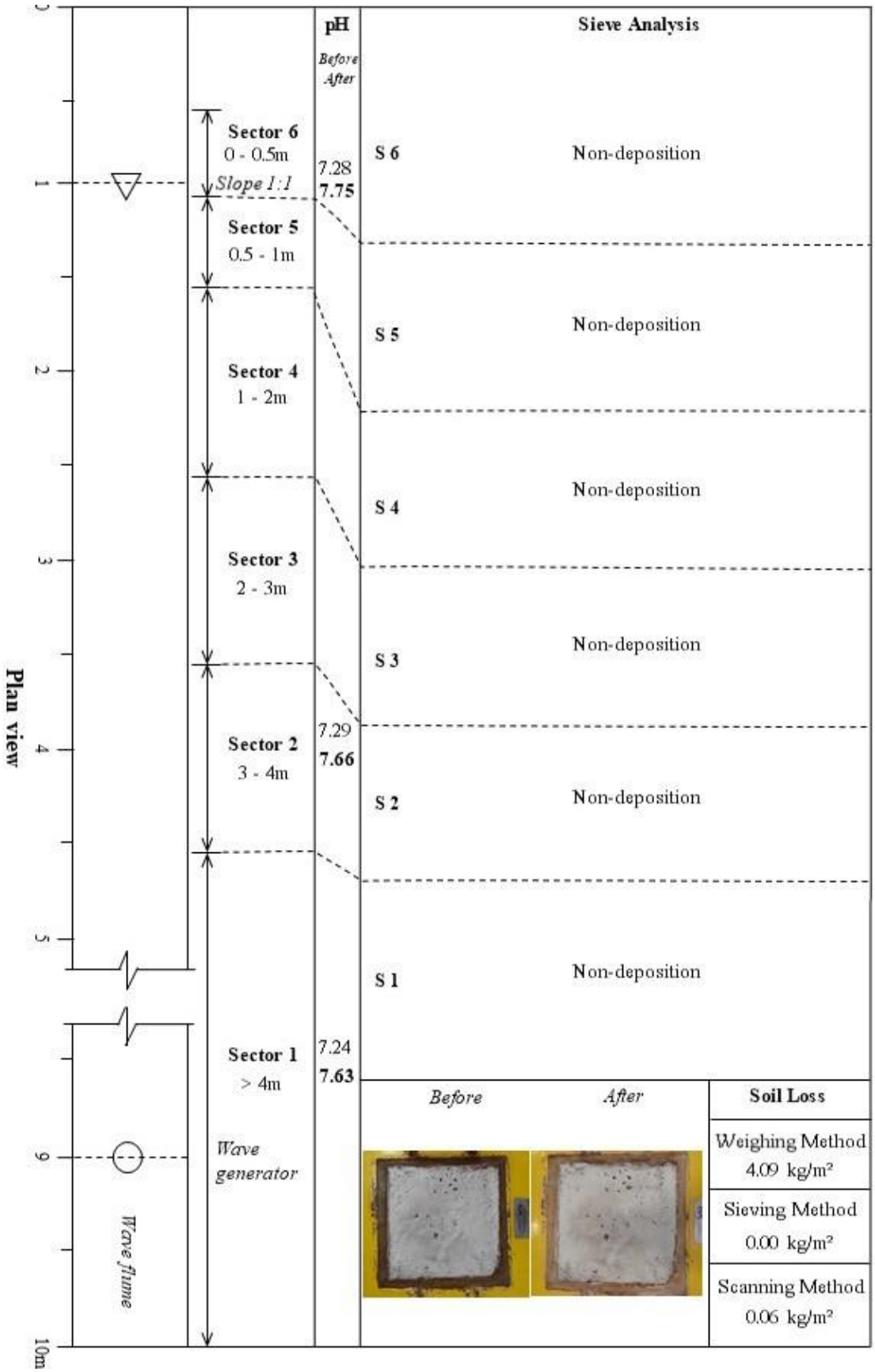

Lateritic Soil with 1 % of lime and 28-days curing time

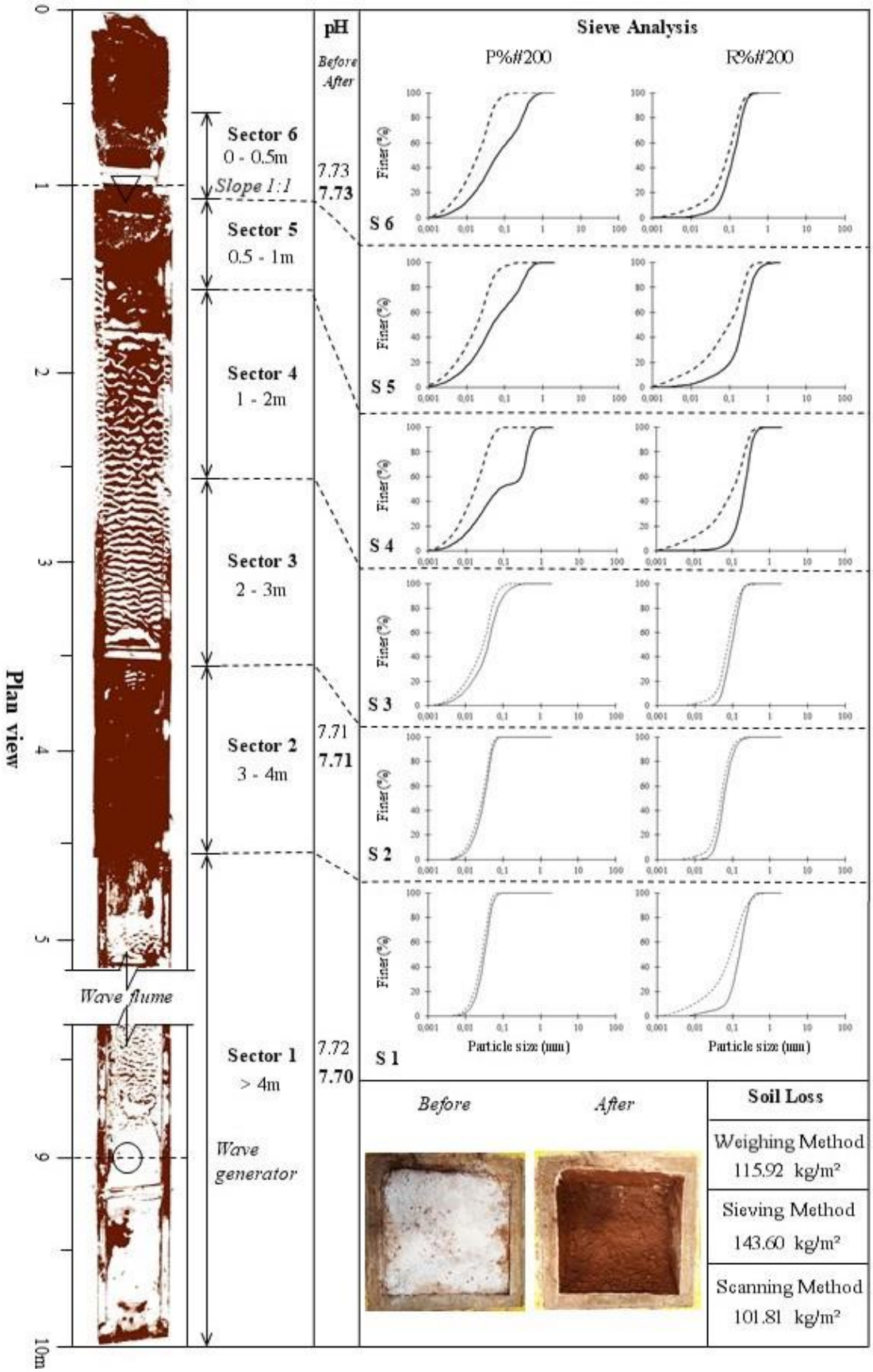

Lateritic Soil with 2 % of lime and 28-days curing time

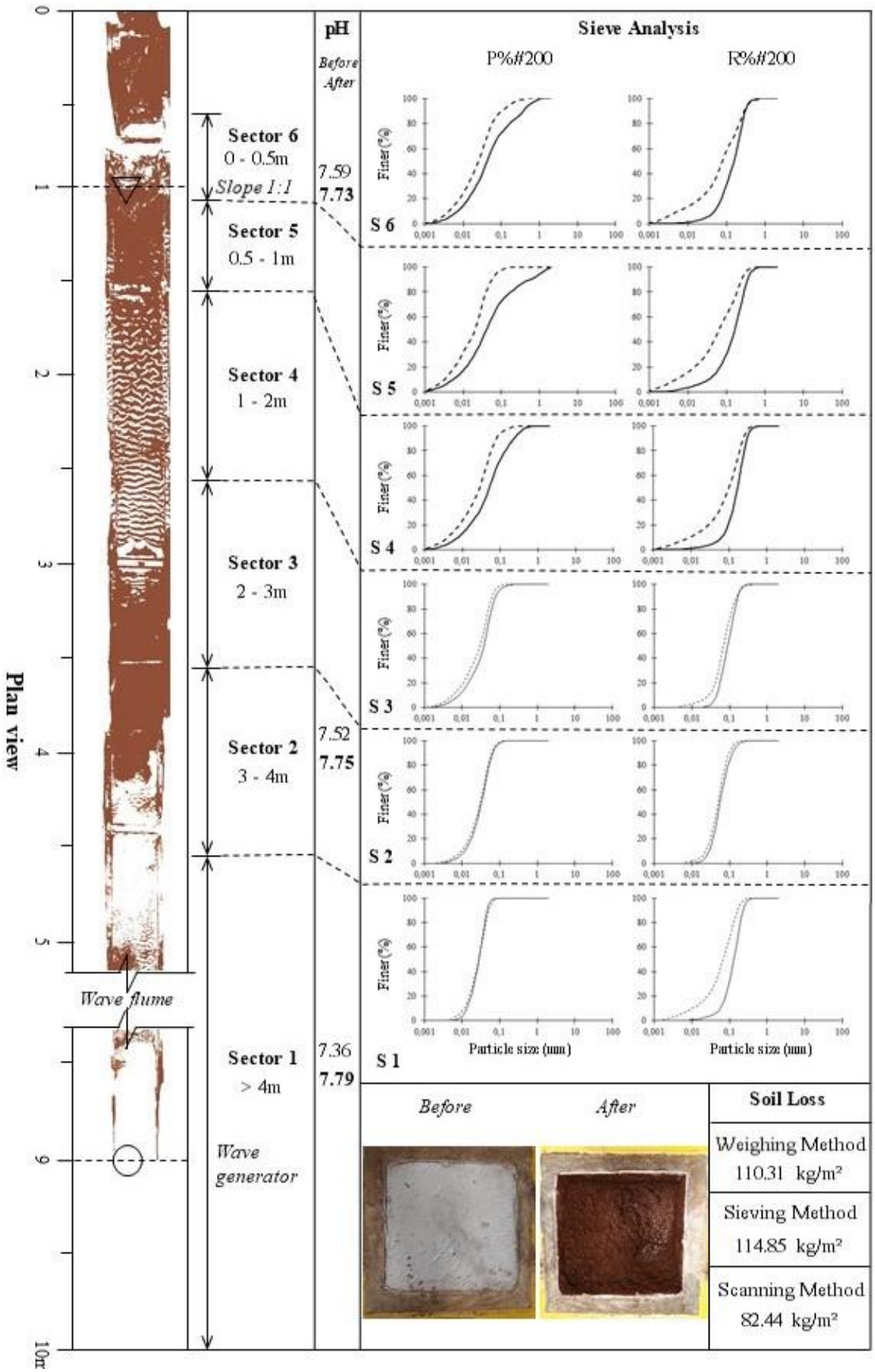

Lateritic Soil with 4 % of lime and 28-days curing time

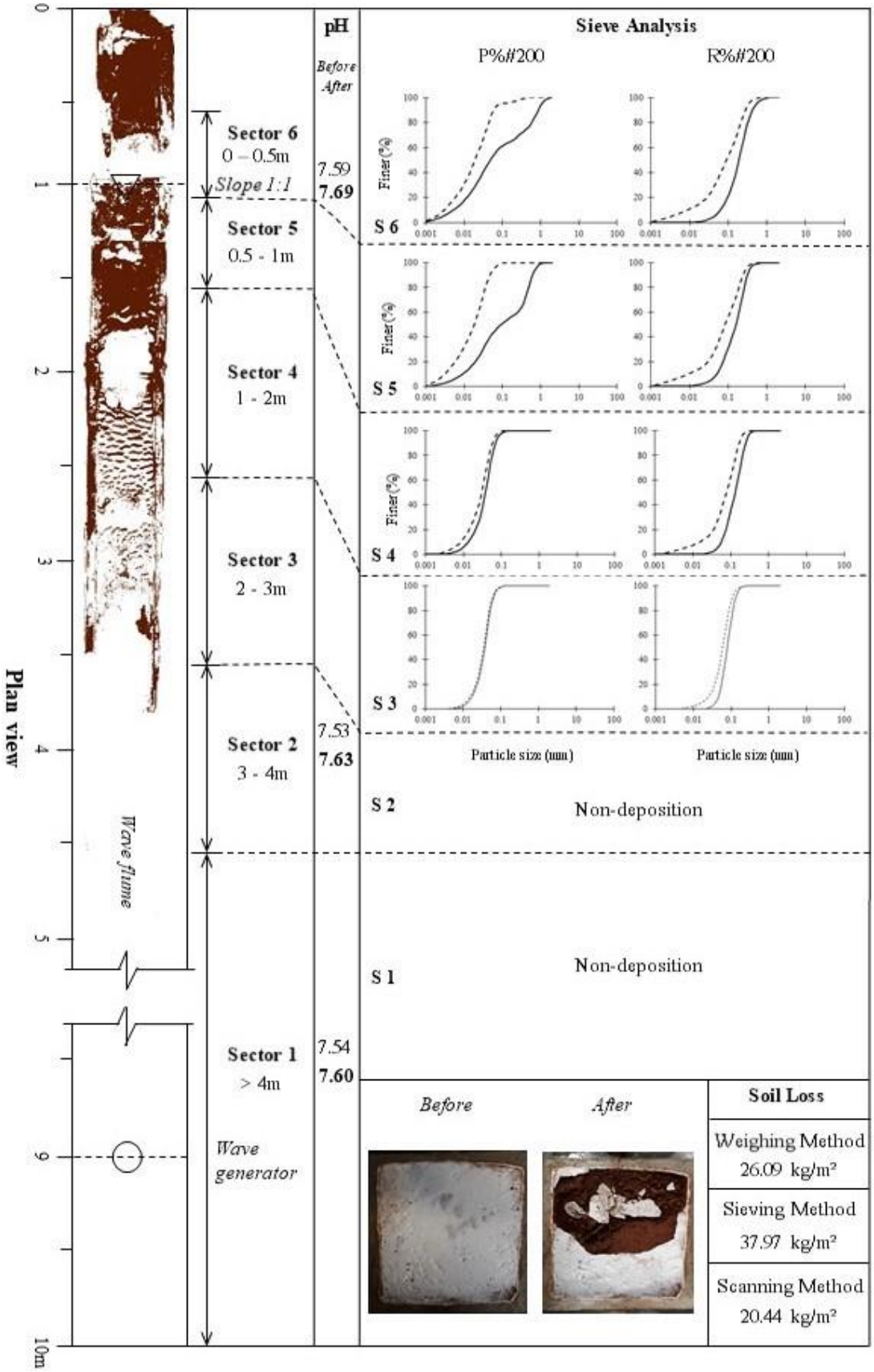

Lateritic Soil with 1 % of lime and 56-days curing time

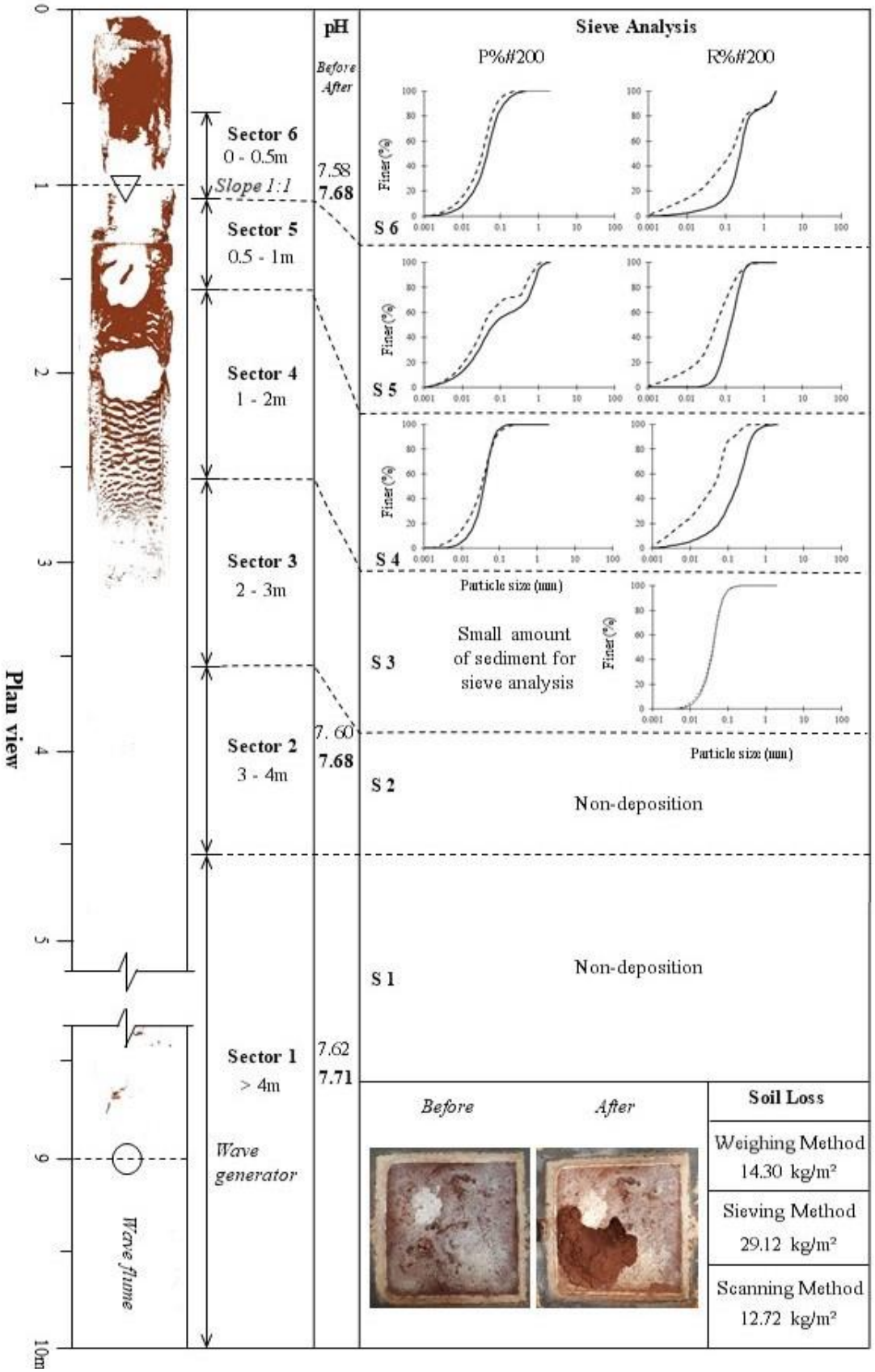

Lateritic Soil with 2 % of lime and 56-days curing time

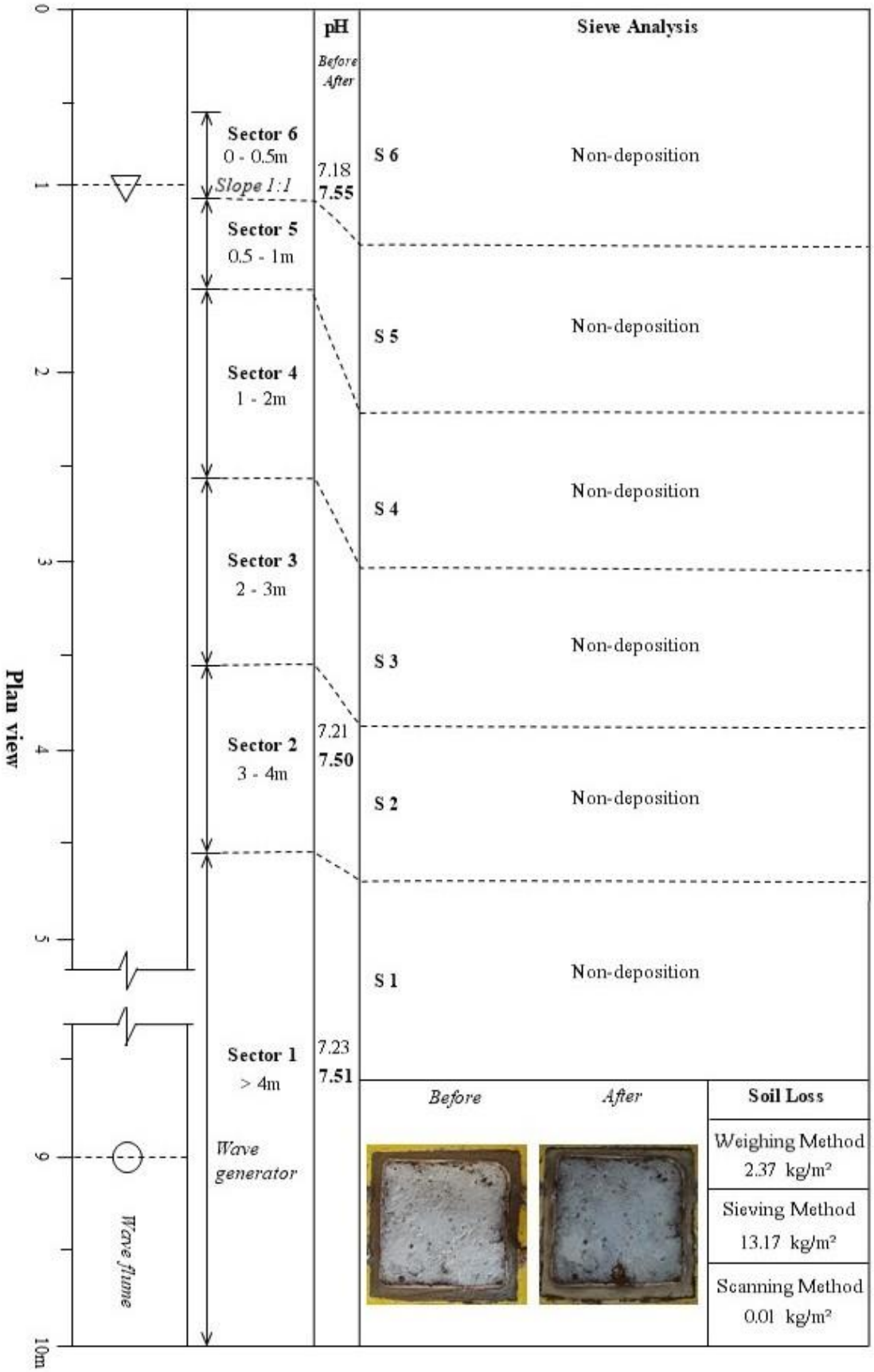

Lateritic Soil with 4 % of lime and 56-days curing time

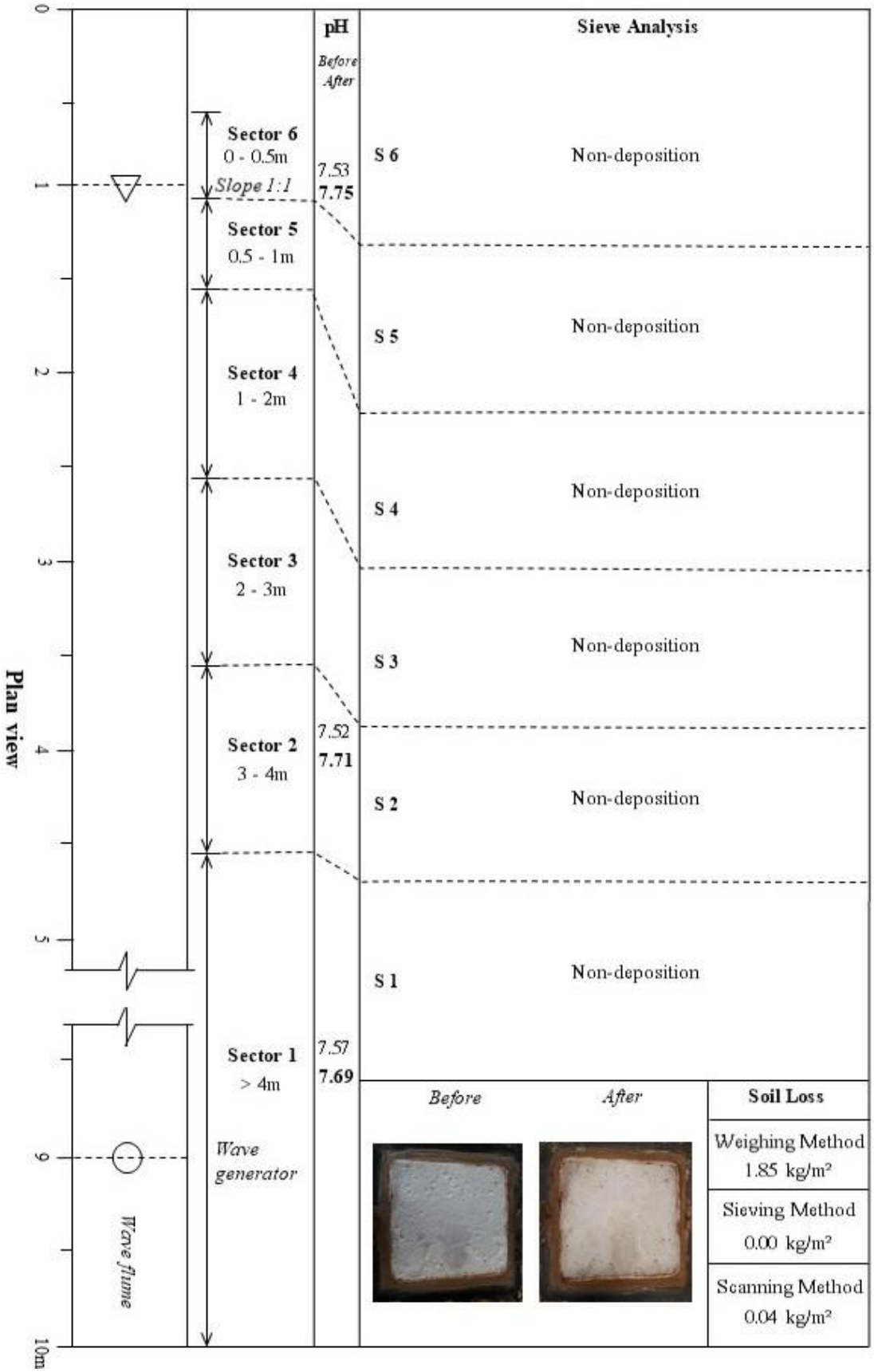

Saprolitic Soil Reference Soil / untreated

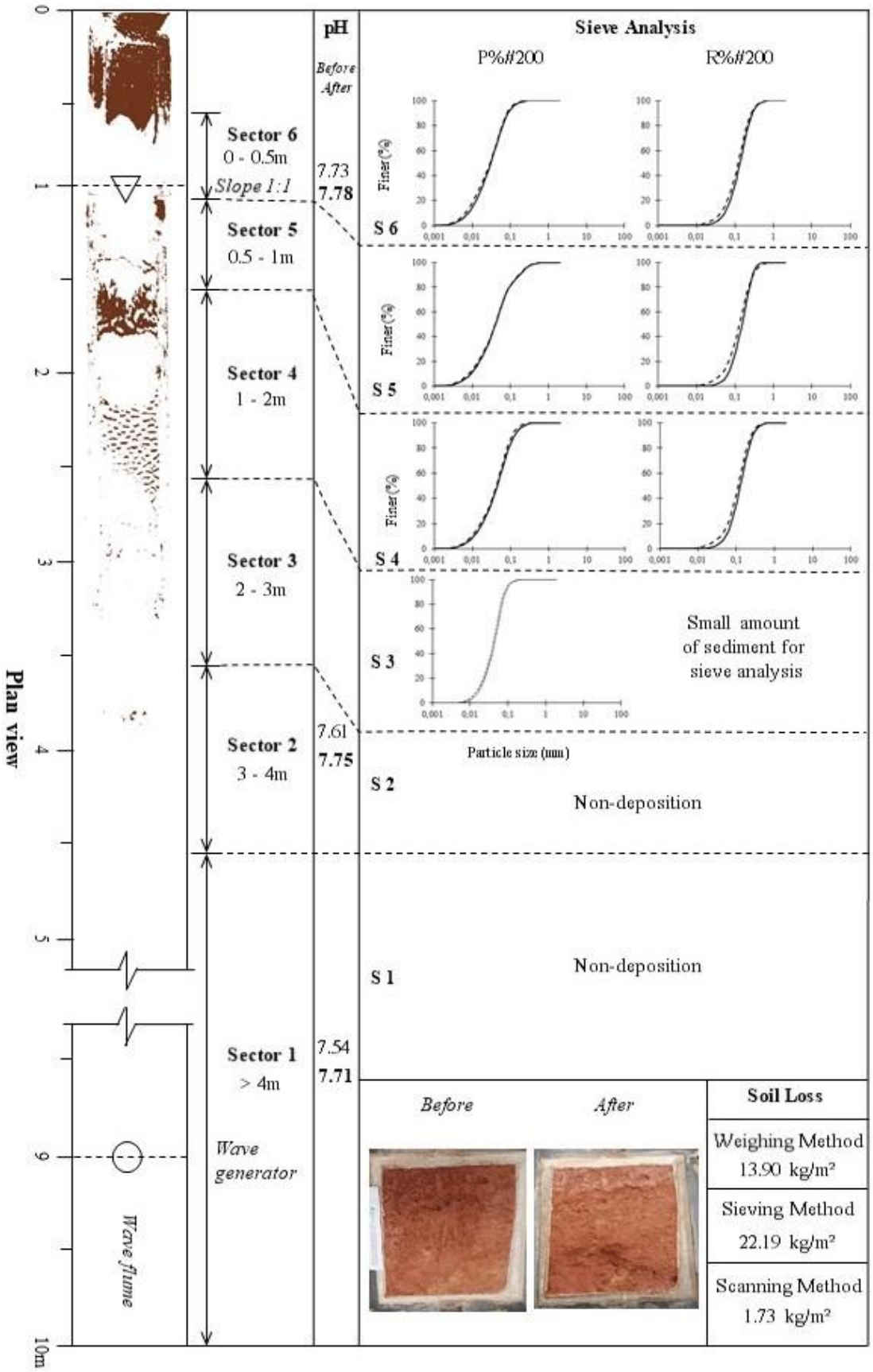

Saprolitic Soil with 1 % of lime and 7-days curing time

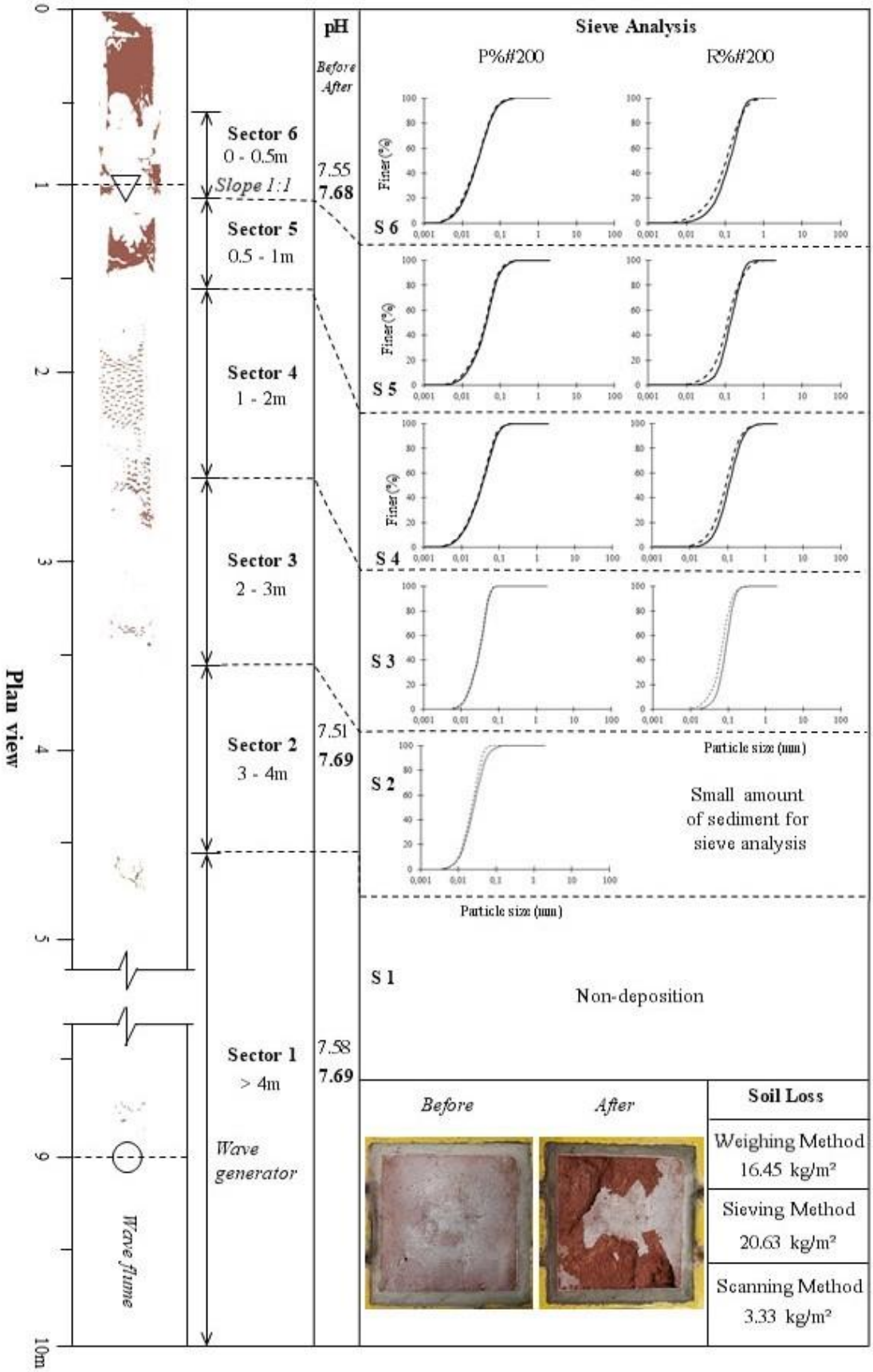

Saprolitic Soil with 2 % of lime and 7-days curing time

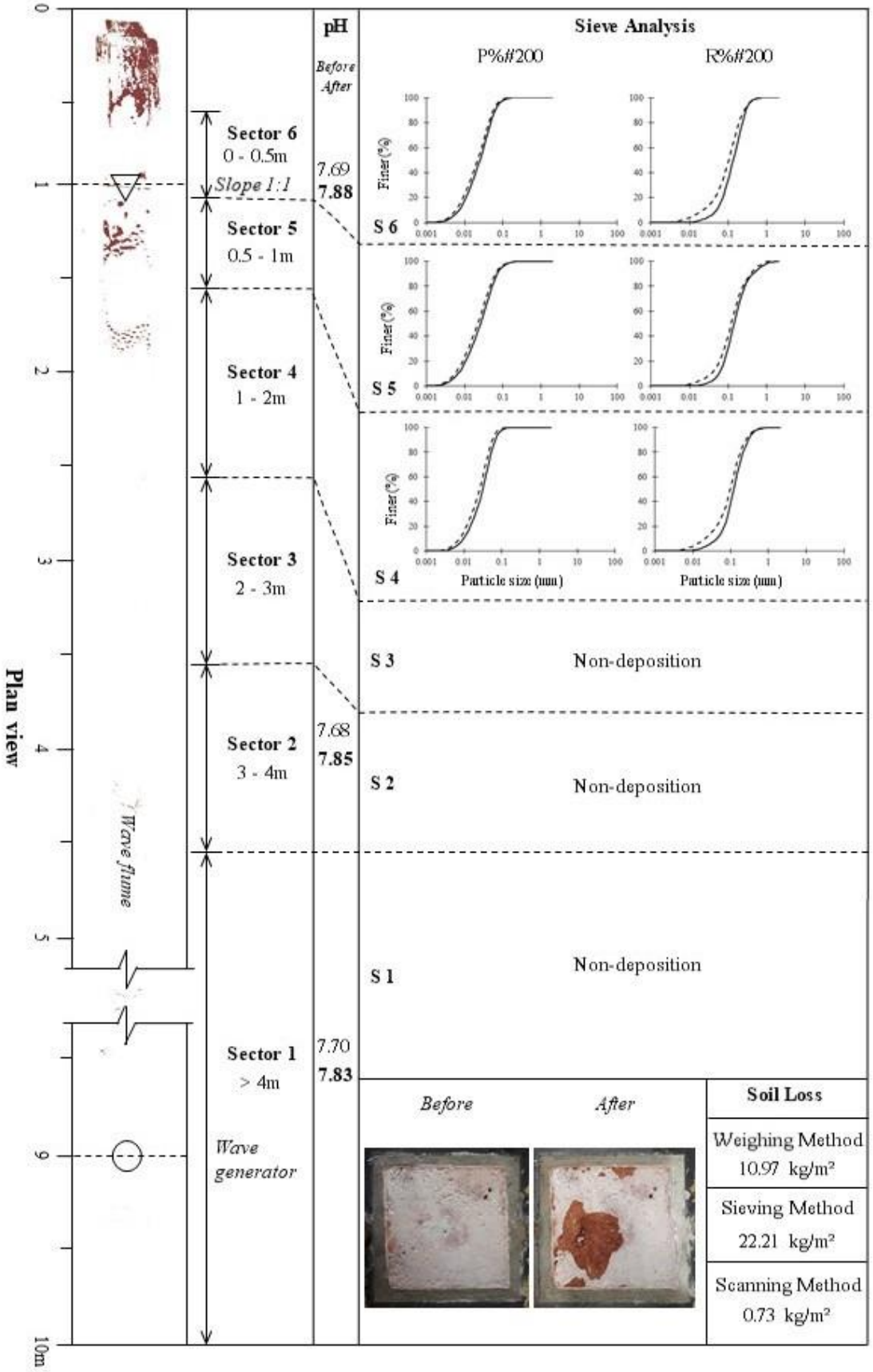

Saprolitic Soil with 4 % of lime and 7-days curing time

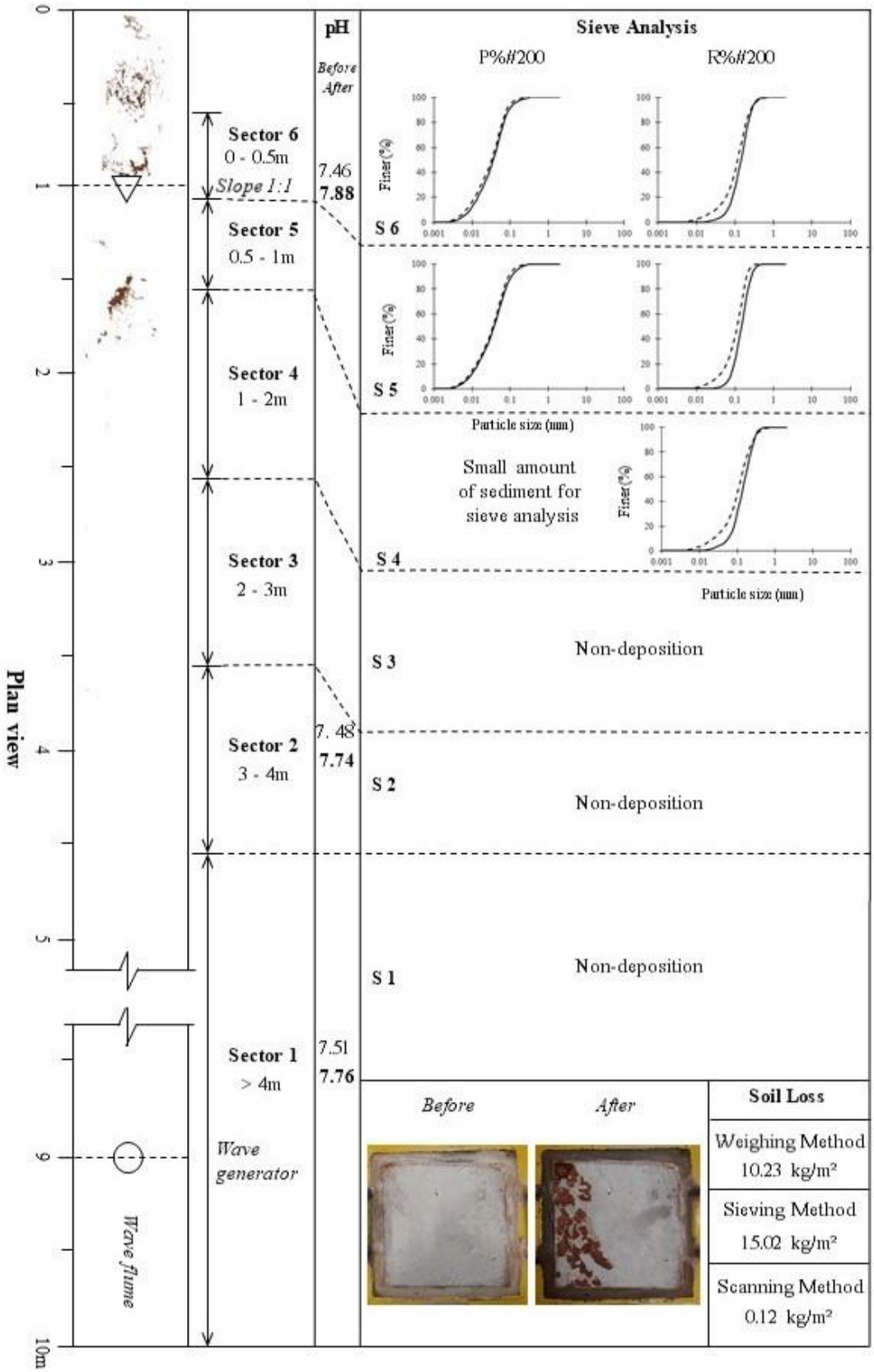

Saprolitic Soil with 1 % of lime and 56-days curing time

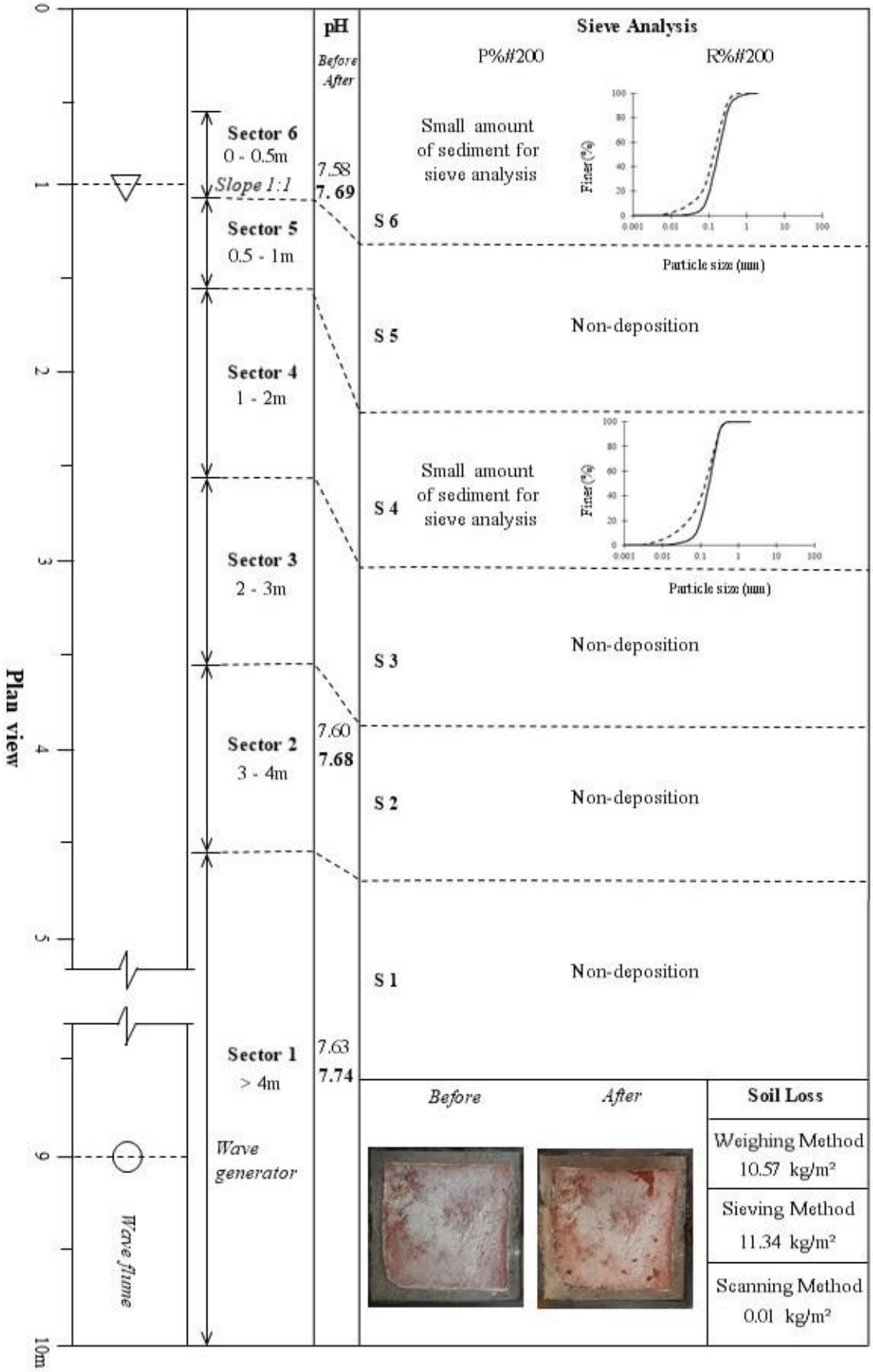

Saprolitic Soil with 4 % of lime and 56-days curing time

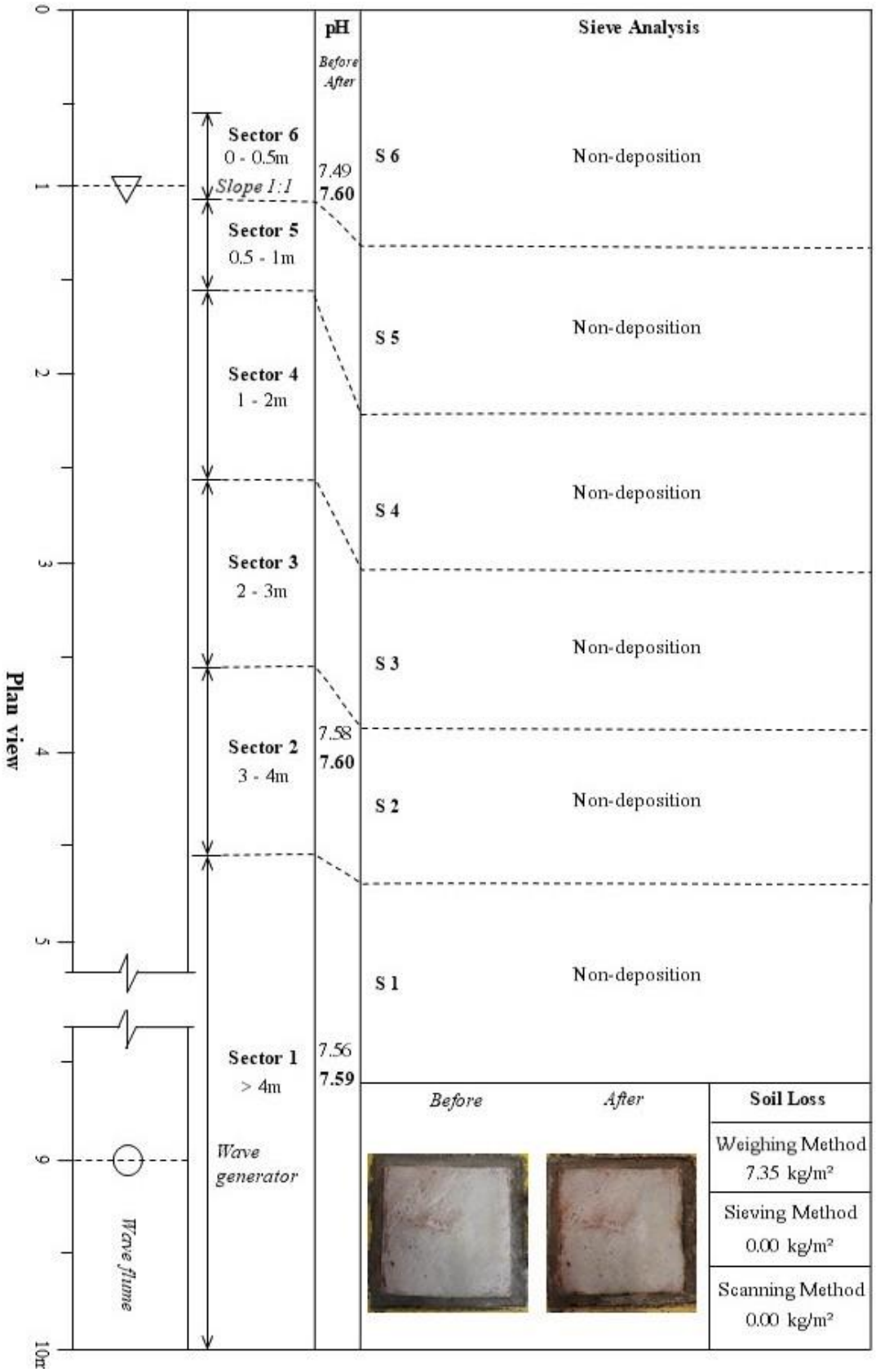

APPENDIX C

INDERBITZEN TESTS

This appendix presents photographs of Inderbitzen test from the sample preparations to the final aspect of soil after the test.

Lateritic Soil

Id.	Pre-treatment	Post-treatment	Removed crust	Post-saturation	Post-test
Lat. Ref.					
1%1dSol.					
1%56dSol.					
1%1d					
2%1d					
4%1d					
1%7d					
2%7d					
4%7d					

Id.	Pre-treatment	Post-treatment	Removed crust	Post-saturation	Post-test
1%28d					
2%28d					
4%28d					
1%56d					
2%56d					
4%56d					

Saprolitic Soil

Id.	Pre-treatment	Post-treatment	Removed crust	Post-saturation	Post-test
Sap. Ref.					
1%1d					
2%1d					
4%1d					

Id.	Pre-treatment	Post-treatment	Removed crust	Post-saturation	Post-test
1%7d					
2%7d					
4%7d					
1%28d					
2%28d					
4%28d					
1%56d					
2%56d					
4%56d